Dual Responsive Hydrogels
Based on ABC Triblock Polymers

A DISSERTATION
SUBMITTED TO THE FACULTY OF
UNIVERSITY OF MINNESOTA
BY

Isha Koonar

IN PARTIAL FULFILLMENT OF THE REQUIREMENTS
FOR THE DEGREE OF
DOCTOR OF PHILOSOPHY

Dr. Ronald A. Siegel

March, 2014

Acknowledgements

I would like to thank my advisor, Dr. Ron Siegel, for his guidance that helped me pursue doctoral research. I thank Marie Gaumet for her help with the PNIPAm-P(NIPAm-co-AA)-PDEAm triblock work. I am grateful to Dr. Dave Giles, at the UMN Polymer Characterization Facility, for his help and guidance with rheology experiments. NMR experiments were performed at the Institute of Therapeutic Discovery and Development (ITDD) at the University of Minnesota.

I am grateful to Prof. Tim Lodge and Prof. Marc Hillmyer for their valuable input and access to lab facilities. I am also thankful to Dr. Tushar Navale and Prof. Theresa Reineke for their help with performing reactivity ratio studies. Thanks to MRSEC program of the National Science Foundation (Award DMR-0819885) at the University of Minnesota for funding my thesis work.

I am grateful to my family and friends for their support and encouragement for my graduate education.

Dedication

Dedicated to my family,

for their inspiration, love and trust.

Abstract

Polymers based on PNIPAm and PDEAm have great utility in injectable biomedical applications as they exhibit inverse phase solubility at transition temperatures between room temperature and physiological temperature. The aim of this study was to design polymers that would lead to physical gels at elevated temperatures.

Two polymer systems were studied, one a triblock poly(ethylene-*alt*-propylene)-*b*-poly(ethyleneoxide)-*b*-poly(N-isopropyl acrylamide-*co*-acrylic acid), PEP-PEO-P(NIPAm-*co*-AA), or PO(N/A) triblock. This construct comprised of a hydrophobic PEP and a hydrophilic PEO mid block. The third block was based on PNIPAm, a thermoresponsive polymer exhibiting inverse phase solubility at a temperature of 32 °C. PNIPAm was substituted with AA to render the block dual temperature and pH responsive. The other triblock PNIPAm-P(NIPAm-*co*-AA)-PDEAm [(PN(N/A)D] comprised thermoresponsive blocks with the midblock being both temperature and pH responsive. PDEAm exhibited an LCST, 30 °C, close to that of PNIPAm.

The triblocks were designed with the intent that on heating, the reduced solubility of the side blocks would cause the polymer to self assemble resulting in polymer aggregation/gelation. The polymers were synthesized by RAFT polymerization and anionic polymerization. Polymer association was studied by DLS, UV spectroscopy and rheology. Greater success was found with the PO(N/A) triblocks in achieving gelation at a critical temperature at low pH, than for the PN(N/A)D system, perhaps due to differences in the self assembly mechanisms.

Table of Contents

List of Tables

List of Figures

List of Schemes

Chapter I

Background

1.1. Block polymers

Block polymers are long chain molecules whose segments are organized into long blocks with distinct chemical compositions. Such polymers are typically formed by a sequence of living polymerizations, with the polymers formed at each stage serving as so called macroinitiators for the next stage, until a final stage is reached. Interest in block polymers is fueled by their ability to assemble into supramolecular structures. Due to differences in their chemical structures, the different polymer blocks may be incompatible with one another and phase separate into microdomains. Due to chain connectivity, these microdomains are on the nanometer size range. Such nanoscale self assembly has made block copolymers of great interest in the bottom-up fabrication of nanomaterials [1-7].

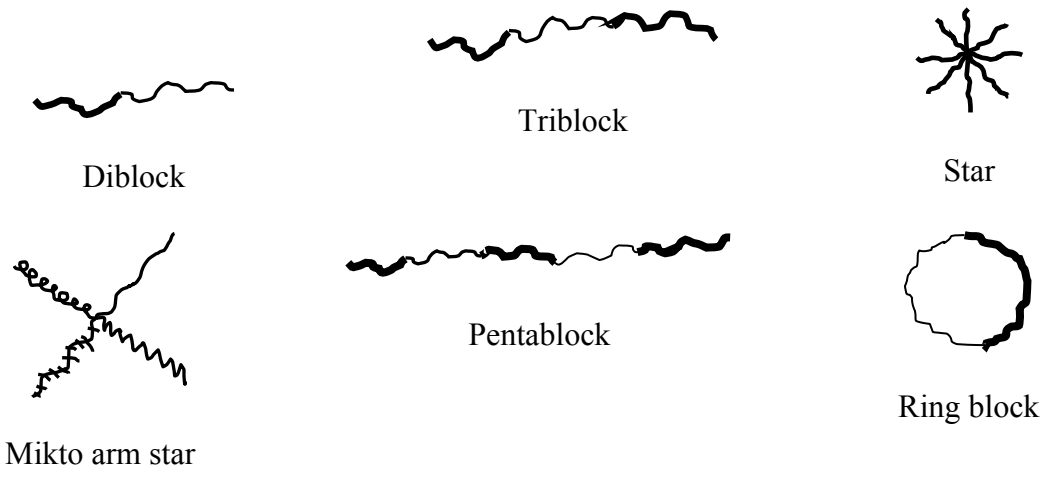

Figure 1.1. Block polymer architectures

Block polymers are classified based on the number and topology of the blocks. Examples include linear diblocks (AB), triblocks (ABA or ABC), and pentablocks (e.g. ABABA), where A, B and C refer to different monomers and nonlinear ring and mikto arm star structures, as illustrated in Figure 1.1.

Block polymers self assemble both in melts and in solutions. In melts, the nature of self assembly depends upon the volume fraction, the degree of polymerization and the Flory interaction parameters between monomers in the different blocks. For example, a linear AB diblock polymer can assemble into various microdomains, such as lamellae, cylinders and spheres, depending on the volume fraction of the two blocks. The pattern of self assembly is selected to minimize the combination of surface energy between the blocks and stretching energy within the blocks [8-10]. In solution, self assembly is also guided by the need to minimize energetically unfavorable interactions between the solvent and the solvophobic blocks. Polymer self assembly in solution can lead to formation of monolayers, micelles, vesicles and three dimensional networks. As with polymer melts, block polymer morphology in solution depends on polymer architecture, molecular weight, solvent-polymer interactions, and volume fraction of the constituent blocks [1, 5, 11, 12].

1.2. Stimuli responsive polymers

Stimuli responsive polymers, as the name suggests, are polymers that self assemble in response to external stimuli. A variety of stimuli can be used to elicit a response. The stimulus may be chemical, such as a change in pH, ionic strength or concentration of specific molecules, or it may be physical, such as a change in

temperature, light, mechanical stress, magnetic or electric field [13, 14]. On application of a stimulus, the polymer can undergo a change in its shape, surface activity, solubility, self assembly or chemical stability [15]. The polymer response manifests itself in different ways, such as polymer collapse and phase separation, micellization, micellar aggregation, hydrogel formation or gel volume transitions.

Stimuli responsive polymers can be classified into various categories based on the stimulus they respond to, for example, thermo- or pH-responsive polymers. They can also be categorized according to polymer conformation, such as free chains, stars, brushes, micelles, vesicles (polymersomes), aggregates or gels [16-18]. Stimuli responsive polymers, by virtue of their ability to self assemble at a molecular level, provide a method for 'engineering' structure at the nanometer level. Also, because of the ability to respond to a change in the environmental conditions, stimuli responsive polymers have sometimes been referred to as 'intelligent' or 'smart' polymers [19, 20]. Because stimuli sensitivity is inherent in biological macromolecules such as proteins, polysaccharides and nucleic acids, stimuli responsive polymers have attracted a great deal of interest in the biomedical field [21, 22].

Much biomedical research focuses on designing therapeutic products that can deliver medicines as required by the body. Achieving controlled drug release is a very important component of pharmaceutical research, and to this end various polymer based delivery systems have been investigated such as polymer micelles, layered tablets and gels. Stimuli responsive polymers have also been also been studied as cell culture substrates, tissue engineering scaffolds, in sensor or actuator devices, and in diagnostics.

They have been used in biocatalysis as well, with enzymatic catalysts coupled to the polymer catalytic activity being mediated by polymer solubility in solution [23-30].

In this thesis, two stimuli will be investigated, namely temperature and pH. Here we provide a brief review of how polymers respond to each of these stimuli.

1.2.1. Thermoresponsive polymers.

Out of the wide variety of stimuli investigated for polymeric response, temperature is the most commonly used. It is the variable of choice because of its facile regulation and convenient application, both *in vitro* and *in vivo* [14]. Polymers that exhibit a change in solubility or conformation as a function of temperature are termed 'thermoresponsive'. The thermoresponsive polymers of most interest to us undergo a rapid physical transition over a relatively small temperature range. The transition is either a collapse from an extended coil to a more compact globular configuration when the polymer solution is very dilute, or separation of polymer chains into concentrated and dilute phases in more highly concentrated solutions.

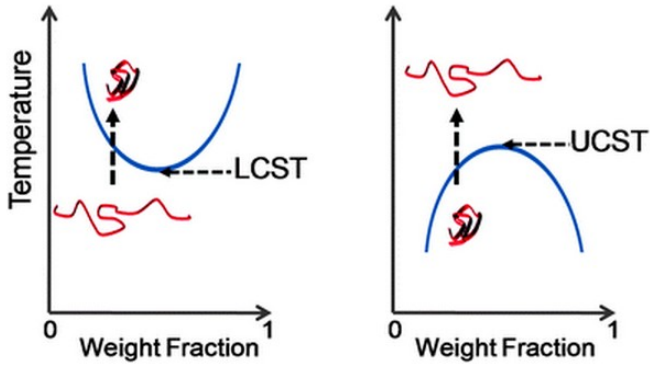

Figure 1.2. Schematic showing temperature-composition phase diagrams for LCST (lower critical solution temperature) and UCST systems (upper critical solution temperature) systems (Figure from ref. [31])

As shown in Figure 1.2, if the polymer-solvent miscibility increases on heating, then the temperature above which the polymer is miscible with the solvent in all proportions is called the Upper Critical Solution Temperature (UCST) and the polymer is said to exhibit UCST behavior. An example of such behavior is poly(methylmethacrylate) (PMMA) in ethanol which exhibits UCST at ~ 70°C [32]. There are few polymer systems that exhibit UCST behavior in water. One example is poly(N-acryloylasparaginamide) with a UCST at ~22 °C [33]. Poly(6-(acryloyloxymethyl)uracil) is another polymer that exhibits a UCST in water at ~60 °C [34].

When polymer-solvent miscibility increases on cooling, then the temperature below which the polymer and solvent are miscible in all proportions is called the Lower Critical Solution Temperature (LCST) and the polymer is said to exhibit LCST behavior [35]. From a biomedical perspective, LCST polymers are of greater interest as they can undergo a sol-gel transition, in aqueous media, when heated from room temperature to body temperature.

Two molecular interactions that can lead to LCST behavior are hydrogen bonding and hydrophobic interactions [14]. Polymers containing polar groups such as carboxylic acids, amides, etc. with a H atom bound to an electronegative atom such as O or N, can have significant H-bonding interactions with water. The electronegative atoms can themselves interact with water by acting as H-bond acceptors. Water molecules that are H-bonded with the polymer are called ‘bound’ water and contribute strongly to polymer-water miscibility. On heating, there is a specific temperature (LCST) above which release

of bound water from the polymer chain becomes favorable. Release of bound water is an endothermic process that leads to a gain in entropy of water molecules, thus making the transition favorable. When this occurs, H-bonds between the polymer and water molecules are broken and the polymer rearranges its conformation in order to become more energetically stable. Energetic stability is usually acquired by replacing the polymer-solvent interactions with polymer-polymer interactions, leading to polymer phase separation.

Hydrophobic interactions are somewhat more complex. Hydrophobic groups in the polymer typically do not have H-bond donor or receptor capacity, which forces neighboring water molecules to rearrange into so called "clathrate" structures [36, 37]. These structures have reduced entropy compared to bulk water. Upon heating, the clathrates break up and join to bulk water, and the hydrophobic groups on the polymer chains coalesce. In addition to hydrophobic interactions, intra- and intermolecular H-bonding between the various polymer functional groups can also drive phase separation above the phase transition temperature [38-40].

LCST behavior is most common in nonionic polymers such as N-alkyl substituted polyacrylamides (e.g.: poly(N-isopropylacrylamide) (PNIPAm), poly(N,N'-diethylacrylamide) (PDEAm), poly(2-carboxyisopropylacrylamide) and poly(N-(L)-(1-hydroxymethyl)propylmethacrylamide) [14], polyvinylamides (e.g. poly(vinylcaprolactone) (PVCL) and poly(N-vinyl propylacetamide), alkyl modified poly(vinylpyrrolidone) (PVP), poly(methyl vinyl ether) and Pluronics (PEO-PPO block

copolymers) [15, 41]. The LCST of a thermoresponsive polymer can be modulated by substituent groups, molecular weight, pH and added electrolytes.

1.2.2. pH responsive polymers

Polymers that contain ionizable groups are capable of undergoing changes in solubility and conformation in response to changes in the environmental pH. When ionized, these polymers are called 'polyelectrolytes'. When the ionizable groups are weakly acidic, the polymers are called 'polyacids', whereas when the ionizable groups are weak bases the polymers are called 'polybases'. Polyacids usually comprise free carboxylic groups that are uncharged at low pH values and ionize at higher pH. Well known examples are poly(acrylic acid) and poly(methacrylic acid) [21]. Polybases, on the other hand, usually contain amino groups. The amine moiety is uncharged at higher pH values and ionizes to the protonated form at low pH. Examples include poly(N,N-diethylamino methacrylate) and poly(4-vinylpyridine).

pH responsive polymers are used clinically as coatings on enteric drug delivery systems. In such systems, the polymers are hydrophobic at acidic pH (stomach) and thereby prevent drug dissolution. On reaching the intestine, the alkaline intestinal pH leads to polymer ionization and hydration, causing release of the encapsulated drug. Such coatings help in oral administration of drugs that are degraded in the stomach, or that cause irritation upon release in the stomach [42, 43].

1.2.3. Dual responsive polymers

Polymers can exhibit dual response by copolymerizing monomers that respond to different stimuli. This helps achieve greater control of polymer solution behavior under a

given set of environmental conditions. For example, copolymerizing a pH responsive monomer with a LCST monomer will result in dual temperature/pH response. The advantage of incorporating an ionic monomer into an otherwise thermoresponsive polymer is that the added pH response due to monomer ionization can provide a means of adjusting polymer LCST within a desired temperature range. For example, Feil and coworkers studied the effect of charge on PNIPAm-co-butylmethacrylate-co-acrylic acid and PNIPAm-co-butylmethacrylate-co-(diethylamino)ethyl methacryalte polymers. They found the LCST to increase linearly with charge [39]. Stayton et al. investigated a copolymer of PNIPAm and propylacrylic acid, and found the LCST to be modulated by pH and polymer composition. They showed that the LCST could be made to undergo large shifts (from 30-55°C) with relatively small changes in pH, i.e. pH 5.0 to 7.0 [44, 45]. Maeda and coworkers studied the effect of ionization on the phase transition temperatures of polymers containing N-vinylimidazole (VIm) copolymerized with NIPAm, DEAm and NVCL. They found the transition temperature to be a direct function of VIm ionization, and thus pH [46]. In a later study, the same group discussed the effect of pH on phase transition temperature, T_p, of P(NIPAm-co-AA) and P(DEAm-co-AA) polymers. pH, and thus AA ionization, was found to cause a linear increase in T_p [47].

1.3. Block polymer assemblies

1.3.1. Self assembled monolayers

Polymers can be covalently or physically bound by hydrophobic or H-bonding interactions to surfaces. They can also be covalently grafted on solid surfaces such as

silicon or metals to prepare specialized interfaces. Hydrophilic polymer grafts are useful in preventing protein and cell adhesion on otherwise hydrophobic surfaces.

Proteins and cells are known to attach to solid surfaces without specific recognition. This process is known as nonspecific adsorption. Many solid surfaces have hydrophobic groups on the surface, as can be observed by a large contact angle. When proteins in solution come in contact with a hydrophobic surface, they unfold and present their normally tightly packed hydrophobic core amino acids to the surface. At the same time, water of hydrophobic hydration is released from the hydrophobic surface. These two processes, working in combination, make the protein adsorption process entropically favorable. In biological contexts, protein adsorption leads to cell adhesion and, when the adhering cells are microbes, biofilm formation. This is a major problem in the shipping industry, where biofilm formation on marine vessels, termed as ship 'fouling', leads to a drastic increase in hydrodynamic drag and increases fuel consumption, in addition to making vessel cleanup difficult. The same process of biofilm formation also occurs on implantable biomedical devices and can lead to bacterial infection and inflammation. Finally, implants are normally greeted with a foreign body reaction, which proceeds by a protein adsorption-cell attachment-fibrous network formation process.

Self assembled polymer monolayers and polymer brushes have been successfully used in preventing nonspecific protein adsorption. Self assembled monolayers of PEG render surfaces resistant to protein and cell adsorption [48, 49]. PEG and 2-methacryloyloxyethyl phosphorylcholine-based polymer brushes, grafted off silicon oxide coated surfaces, are also used for protein and cell proof surfaces [50-52]. The

hydrophilic/hydrophobic balance of the surface can be further controlled by employing stimuli responsive polymers. Such surfaces with modulated wettability have been employed in cell culturing and transplantation, and in protein and enzyme isolation [24]. PNIPAm has been used to design thermoresponsive cell culture surfaces that allow for cell growth to a confluent cell sheet above polymer LCST, and facile cell sheet detachment below LCST. Such surfaces were investigated as a method for layer by layer myocardial tissue regeneration [53]. PNIPAm grafted surfaces are also used for cell coculturing.

1.3.2. Polymer Micelles

When amphiphilic polymers comprising hydrophilic and hydrophobic segments are placed in aqueous solution, the incompatibility of the hydrophobic block with water causes it to segregate away from the water, "coated" by the hydrophilic blocks. Segregation occurs due to hydrophobic interactions, electrostatic interactions or hydrogen bonding. Hydrophobic blocks belonging to different polymer chains segregate into common domains leading to micellization [54]. Micellar morphology can vary from spherical to cylindrical to lamellar. Spherical micelles may be simple core-shell micelles, or cross-linked versions of the same. Cross linking has been reported in both the core and the shell. Core or shell crosslinked micelles possess greater stability to their un-cross linked counterparts. In spherical micelles different chemical domains can segregate in different ways. If the micelle contains two chemically distinct hemispheres, they are termed as 'Janus' micelles. Similarly, multi compartment micelles are observed where there are multiple segregation domains. Cylindrical or 'worm like' micelles have also

been reported. These can be utilized as nanotubes with the interior providing high drug loading capacity [55]. Micellar structure may be influenced by environmental conditions such as temperature and pH. Micellar morphology is also influenced by polymer architecture. For example, while diblock polymers usually form core-shell micelles, other architectures such as triblocks, dendrimers and star polymers show specialized morphologies such as toroids or multicompartment micelles.

Polymer micelles have been widely investigated in drug delivery, including delivery of genes and proteins. Core-shell micelles formed from amphiphilic block polymers can be used as vehicles for hydrophobic drugs, wherein the active is loaded physically into the core or through favorable interactions with the core, thus resulting in controlled drug release. This strategy also helps formulate poorly soluble drugs in aqueous solution via stabilization of the hydrophobic drug loaded core by the outer hydrophilic corona [1]. For example, Kataoka and coworkers loaded PEG-PAsp micelles with doxorubicin (DOX), a cytotoxic agent [54]. In this study, DOX was covalently linked to PAsp via condensation between carboxylic groups of PAsp and the primary glycosidic amino group of DOX. Binding of DOX, a hydrophobic drug, to PAsp increased the hydrophobicity of PAsp segment causing PEG-PAsp-DOX to form core-shell micelles. The micelles were further loaded with DOX, which became physically entrapped in the core through $\pi-\pi$ interactions with the covalently tethered DOX molecules. The PEG-PAsp-DOX micelles exhibited prolonged circulation time in the blood. The presence of PEG helped prevent nonspecific uptake of micelles by the

reticuloendothelial system (RES), one of the major obstacles to colloidal carrier mediated drug delivery.

As polymeric micelles are being widely used for drug delivery, for further advancement in the field of micellar drug carriers, it is important to be able to control the kinetics and site of drug release. Cell specific ligands conjugated to the coronal PEG end of the micelles can be employed for targeted drug delivery. PEG-polycation block polymers or PEG-liposome complexes have been tested as a means to deliver nucleic acids [56-59]. Pharmaceutical companies, including Alnylam, Roche, Merck and Calando have performed clinical tests on these systems for siRNA delivery [60].

The timing of drug release can be controlled using polymers that exhibit stimuli responsive phase behavior. For example, LCST polymers incorporated in block polymers can cause micelle stabilization/destabilization, depending on temperature. This can help in initiating burst release of encapsulated drugs. Release kinetics can be further modulated by core or shell crosslinking.

Polymeric micelles, by virtue of their nano size, offer distribution control as they preferentially accumulate in tumor tissue due to the enhanced permeation and retention (EPR) effect, in which nanometer sized particles penetrate into the tumor through the leaky tumor vasculature. Micelles can thus be used as carriers for anticancer drugs. Micelles can further be actively targeted to the desired site of action by functionalizing the polymer chains with ligands. The ligands used should have affinity for receptors at the site of action. This would help in increasing drug efficacy and at the same time

minimize undesirable side effects [61]. Alternatively, release of drugs can be modulated by local changes in pH, such as occur in solid tumors.

Polymer micelles can be employed in diagnostics. The micelle core can be loaded with magnetic nanoparticles/quantum dots and used as an imaging agent [1]. Block polymer micelles can also be transformed into nanocontainers through selective etching of the core forming block in a shell-crosslinked micelle. The core can be removed by ozone treatment, UV-mediated photolysis, hydrolysis and thermolysis. This would allow higher amount of drugs to be loaded inside the micelle [61].

1.3.3. Vesicles

Block polymers can self assemble to form bilayer structures known as vesicles or polymersomes [62, 63]. Polymer vesicles were first reported by Eisenberg and coworkers in 1995, who studied the self assembly of polystyrene (PS)-PAA block copolymers. Subsequently, vesicle formation has been reported for a variety of AB diblock and ABC triblock copolymers. Polymer vesicles are superior to lipid vesicles in terms of mechanical strength. Moreover the membrane permeability can be tuned by controlling polymer molecular weight and membrane polarity, and by addition of molecules such as channel proteins and membrane plasticizers. Polymer vesicles can be employed for targeted drug delivery as well as nanoreactors [64-66]. The vesicle membrane permeability can be made responsive to external stimuli by incorporating monomers such as NIPAm which makes the vesicle temperature responsive. pH sensitivity can also be introduced by using acid or amine based monomers [1, 67, 68].

In addition to stimuli responsiveness, biologically motivated polymer systems also require the constituent blocks to be biocompatible. For example, an amphiphilic diblock polymer composed of poly (2-(diisopropylamino)ethyl methacrylate) PDPA (pH responsive, pKa ~ 6.3) and the biomimetic polymer poly(2-methacryloyloxyethyl phosphorylcholine) PMPC (hydrophilic) was used to develop biocompatible vesicles [69]. The PDPA-PMPC vesicles were used for *in vitro* delivery of DNA or dye molecules to living cells. The block copolymer micelles were endocytosed, and the relatively acidic conditions inside the organelle (pH 5-6) caused protonation of PDPA. This led to dissociation of the vesicles, resulting in burst release of the encapsulated contents.

To ensure biocompatibility and reduced antigenicity, while maintaining pH response, polypeptide copolymers have also been used to develop vesicles called 'peptosomes'. These can be formed from copolymers comprised of hydrophilic and hydrophobic polypeptides. For example, Lecommandoux and coworkers developed poly(glutamic acid)-polylysine vesicles that were pH responsive in surface chemistry [70]. Other biocompatible polymers such as poly(ethylene oxide) (PEO), polylactide (PLA) and poly(ε-caprolactone) (PCL) have also been studied for vesicle-mediated drug delivery [71-73]. PEO is commonly used to form the outer block in polymer micelles and vesicles because of its hydrophilic nature and stealth properties. When copolymerized with a hydrophobic polymer such as PLA or PCL, it can form vesicles, which have been used for controlled release of anti cancer drugs.

Ahmed et al studied PEO-PLA vesicles for anticancer drug delivery [64]. Hydrophilic doxorubicin was loaded in the interior aqueous cavity of the vesicle and

hydrophobic paclitaxel was introduced into the membrane. *In vivo* mouse studies showed a three-fold increase in tumor apoptosis on treatment with multiple drug-loaded vesicles as compared to free drug. PEO-PCL vesicles were also investigated by Pang et al. for *in vivo* brain delivery of peptides in rats. PEO-PCL or PEO-PLA vesicles loaded with the oxygen carrying molecule haemoglobin have been developed as a potential treatment for ischemia. [55]

1.3.4. Hydrogels

Hydrogels, a class of 'soft matter,' are three-dimensional networks of polymer chains dispersed in water. These networks possess high water holding capacity and at the same time the ability to maintain shape. The network is held in place by crosslinks that may be chemical or physical in nature. Depending on the nature of crosslinks, hydrogels are described as being either chemical or physical. Chemical gels are held together by permanent covalent crosslinks. Once formed, they cannot revert back to the sol state except by chemical degradation. Retention of unreacted monomer in a chemically crosslinked gel matrix may lead to toxicity. The utility of chemically crosslinked hydrogels is further limited because of problems encountered with administration of pre-formed gels.

Physically associating polymers can also form hydrogels. In physical hydrogels, polymer chains are linked to one another by aggregated domains formed by physical interactions. The physical domains act as crosslinks and may be formed due to H-bonding, hydrophobic or electrostatic interactions, crystalline regions or ionic clusters. Because of the non-permanent nature of these interactions, physical gels can undergo

reversible sol-gel transitions. Physical gels are often based on stimuli responsive polymers.

Stimuli responsive polymer networks can respond to an external stimulus in two ways. First, they can swell or shrink, and when this is dramatic it is often called a volume transition. In case of a volume transition the network will swell or shrink in response to stimulus. Second, a polymer system can transform from a gel to a sol state and *vice versa*. The latter will occur with physical hydrogels. Both kinds of transitions can be reversible. The ability to undergo a change in shape/volume in response to an external stimulus has brought attention to stimuli responsive polymer gels [45]. If responsive to physiological stimuli, they can be used in biomedical applications such as controlled drug release, biosensors, diagnostics and tissue regeneration. They are also useful in designing microfluidic channels that can be used for separation, catalysis, sensing and actuation. For these applications, it is required that the gels have good mechanical strength and response time. For biomedical applications, additional attributes of biocompatibility and biodegradability are desired [74].

1.4. Stimuli responsive gels based on triblock polymers

By incorporating stimuli sensitive domains into a multiblock polymer, it is possible to control both sol-gel and volume transitions. Zhao et al. [75] synthesized dual temperature- and pH-responsive ABA triblock polymers. The polymers were comprised of a hydrophilic poly(ethyleneoxide) (PEO) midblock and thermosensitive poly(methoxydi(ethylene glycol) methacrylate-co-ethoxydi(ethylene glycol) methacrylate), P(DEGMMA-co-DEGEMA) outer blocks. The outer blocks contained ~5

mol% tertiary amines such as N,N-diethylaminoethyl methacrylate, N,N-diisoproplyaminoethyl methacrylate or N,N-di(*n*-butyl)aminoethyl methacrylate. It was found that 10 wt% solutions of these triblocks underwent sol-gel transitions with the transition temperature ($T_{sol-gel}$) dictated by the LCST of the thermosensitive outer blocks. The presence of tertiary amines caused the LCST of P(DEGMMA-co-DEGEMA), and hence $T_{sol-gel}$, to depend on pH.

Schmalz et al. [76] prepared dual temperature and pH responsive ABC triblock polymers with a pH-sensitive poly(2-vinylpyridine) (P2VP) A block, a water soluble PEO B block, and a thermosensitive poly(glycidyl methyl ether-co-ethyl glycidyl ether) (P(GME-co-EGE)) C block. The polymer could be made to arrange into core-shell-corona micelles by making one of the outer blocks hydrophobic. At room temperature and pH<5, the polymer was in solution. At room temperature and higher pH (pH=7), the polymer formed core-shell-corona micelles with the pH responsive P2VP block forming the core. Increasing the temperature at low pH (pH=3) led to an inversion of the micellar structure with the thermoresponsive p(GME-co-EGE)) block forming the core. At high pH and high temperature, a sol-gel transition was observed due to hydrophobic domains formed by P2VP and (P(GME-co-EGE)) blocks.

Armes and coworkers [77, 78] studied ABA triblock polymers comprised of hydrophilic midbocks such as poly(glycerol monomethacrylate) (PGMA) and PMPC. The outer blocks were pH responsive and were composed of either PDPA or poly(diethylaminoethylmethacrylate) (PDEA). At low pH values, the polymers were molecularly dissolved in solution. At high pH, pH>7, the outer PDPA/PDEA blocks

became deprotonated and collapsed into hydrophobic domains leading to the formation of gels. Gelation was said to be preceded by formation of 'flower' micelles in dilute solutions. At high concentrations, the probability of polymer chains bridging between adjacent micelles, rather than looping back into the same micelle, increases. This leads to formation of a three dimensional polymer network. The PDPA-PMPC-PDPA polymer gels were further investigated as matrices for release of a model hydrophobic drug, dipyridamole. Drug was released at a slow, sustained rate from the gel matrix at pH 7.4 in phosphate buffer. At pH 3, the gels exhibited immediate drug release due to gel dissolution.

Butun and Taktak [79] performed a similar release study with gels based on ABA triblock polymers containing PDPA side blocks and a poly(dimethylamino ethyl methacrylate) (PDMA) mid block. The polymer solution remained fluid at acidic pH and formed a gel under alkaline conditions. Thus the model drug, dipyridamole, could undergo either a burst or a controlled release depending on pH. The midblock, PDMA, was thermoresponsive with LCST ~35 °C. Thus, dipyridamole release in this case was affected by both pH as well as temperature.

Thermoresponsive polymers with LCST below the physiological temperature have been shown to form gels when injected intramuscularly or subcutaneously. These polymer gels have further been investigated as depot drug delivery systems. ABA triblock polymer composed of hydrophobic PLGA A blocks and hydrophilic PEG B blocks is being tested as a carrier for paclitaxel for the treatment of esophageal cancer, and is currently in Phase II clinical trials [42].

1.5. Polymer Synthesis: RAFT polymerization

Block polymers have been synthesized by a variety of polymerization techniques such as ring opening, cationic and anionic polymerization. Controlled radical polymerizations such as nitroxide mediated polymerization, and metal catalyzed atom transfer radical polymerization have also been widely used for block polymer synthesis [80]. One relatively new free radical controlled polymerization technique widely used for synthesizing block polymers is Reversible Addition-Fragmentation Chain Transfer, or RAFT polymerization. RAFT falls into the category of reversible deactivation radical polymerizations (RDRP). RAFT is similar to conventional free radical polymerization in terms of having an initiator, but in addition it utilizes a chain transfer agent (CTA) that helps in controlling polymerization kinetics.

In RAFT polymerization, as shown in Scheme 1.1, initiation takes place as in conventional free radical polymerization. The decomposed initiator free radical, I•, interacts with a monomer M to form a free radical, which propagates as a polymeric growing chain, P_n•. In the second step, the propagating radical $P_n^{\bullet}$ adds to the CTA, a thiocarbonyl thio compound (**1**), to form an intermediate radical (**2**), which fragments to form a polymeric CTA (**3**) and an initiating radical $R^{\bullet}$. The radical $R^{\bullet}$ starts a new polymer chain $P_m^{\bullet}$, in the same way as the primary initiating radical $I^{\bullet}$. The thiocarbonyl thio compound maintains the propagating chains $P_n^{\bullet}$ and $P_m^{\bullet}$ in equilibrium by shuttling between the two polymeric radicals.

Scheme 1.1. Mechanism of RAFT polymerization (adapted from Ref [81])

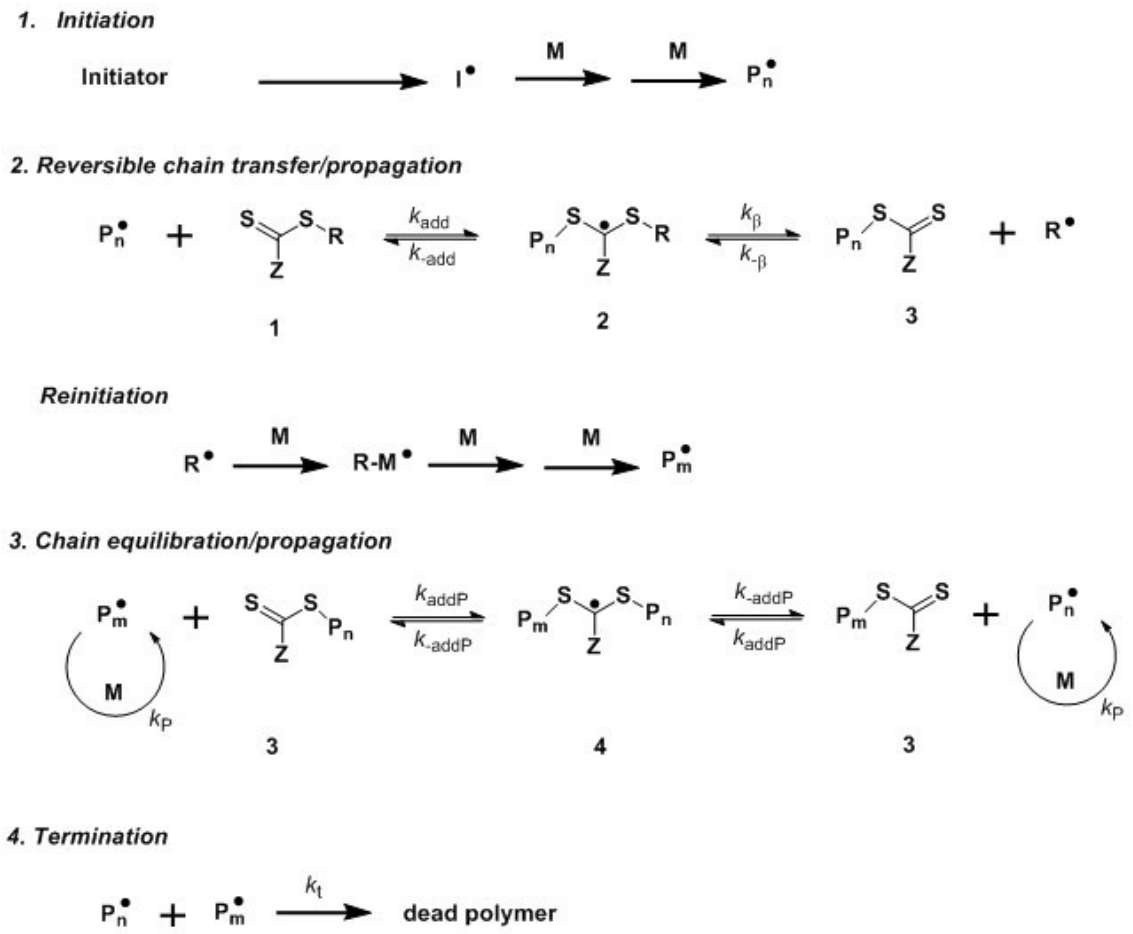

The CTA thus serves as a stabilizing moiety that regulates the rate of propagation of the polymer chains. It also severely reduces the rate of termination, which is bimolecular in the propagating chain concentration. With respect to the total polymerization time, all chains are initiated at about the same time, and they remain "living" throughout the polymerization. As a result, the molecular weight distribution is very narrow [81].

RAFT polymerization can be used to prepare a wide variety of polymeric structures such as linear block polymers as well as more complex architectures such as

branched and hyperbranched polymers. It is also compatible with a wide range of functional monomers and is easy to carry out [82-84].

1.6. Motivation

Hydrogels hold great potential in controlled drug release as well as topical coatings for treatment of inflammation and burn wounds. Conventionally, hydrogels are formed by chemical crosslinking of polymer chains. Following gelation, there is often a fraction of unreacted monomer/crosslinker retained in the gel. This residue is undesirable in the finished product and must be removed before the gel can be used for its intended application. Also, chemical gelation is a non-reversible process and this makes the gels difficult to process once formed.

Phsyical gels overcome the need for a chemical crosslinker. Gelation in this case arises due to physical interactions rather than a chemical reaction. This makes the gelation process simpler and also safer for use *in vivo*. Injectable gels, i.e. polymer solutions that are liquids at the time of administration, and become gels after reaching the site of deposition, have attracted widespread interest. They are expected to increase the applicability of polymer matrices due to ease of administration. Such gels can be used to form drug depots at topical or internal sites, while being minimally invasive in their placement. Also, injectable gels provide a convenient means of drug loading. The drug can be loaded in the polymer matrix simply by mixing the drug with the aqueous polymer solution before administration.

The aim of this dissertation has been to design a polymer that will undergo a sol-gel transition when heated from room temperature (25 °C) to body temperature (37 °C).

This was intended to serve as a model for developing injectable gels that could be used as matrices for controlled drug release. The gelation was desired to be physical i.e. without the need for any chemical crosslinker. Physical gels can be easily prepared using block polymers.

Diblock, triblock and higher order multiblock polymers have been reported to form physical hydrogels. Diblock polymers, if comprised of blocks with different solvent affinities, phase separate to form micelles. The solvophobic blocks internalize in the core and the solvophilic block screens it from the solvent by arranging on the outside as a shell. At high polymer concentrations, shells of adjacent polymers come in contact with one another. At this point, micellar packing and chain entanglements lead to the formation of a three dimensional polymer network/gel.

Triblock gelators usually comprise of solvophobic end blocks and a solvophilic mid block. When dispersed in a solvent, the solvophobic end blocks collapse into aggregated domains. The solvophilic mid block, due to higher solubility, still maintains its extended conformation. This results in a sol-gel transition in which the compact polymer rich domains serve as physical crosslinks in the formed polymer network. In the current study, the solvent was water, the most widely used solvent for biomedical solutions. The triblock comprised hydrophobic end blocks and a relatively hydrophilic midblock. Gelation was expected to occur due to physical association of the hydrophobic end blocks. On phase separation, the polymer end blocks were expected to collapse into hydrophobic domains serving as crosslinks in a network of the hydrophilic mid block

chains. The sol-gel transition can also be designed to occur in response to an environmental stimulus by using stimuli responsive polymers.

For a system to undergo a sol-gel transition on heating from room temperature to body temperature, it was required that the side blocks be temperature responsive and undergo a phase transition at an intermediate temperature, between 25 and 37 °C. Thus, polymers exhibiting inverse phase behavior i.e. reduced solubility on heating, were ideal candidates for the end blocks. Poly(N-alkylacrylamides) are a well known class of LCST polymers. Poly(N-isopropylacrylamide) (PNIPAm) and poly(N,N-diethylacrylamide) (PDEAm) were chosen as the end blocks as they exhibit LCST transition at 32 and 30 °C, respectively.

The midblock was required to remain hydrophilic during gelation. It was further designed to be responsive to pH, as pH is another important stimulus from a biological perspective. Physiological pH varies widely depending on the tissue/cellular compartment. Blood has a slightly alkaline pH between 7.35-7.45 while the pH in the extracellular matrix of a tumor can be as low as 6.5. In the gastrointestinal tract, pH changes from acidic (pH 1-3) in the stomach, to basic (pH 8.2) in the duodenum. These pH variations can be exploited for site specific drug delivery by employing pH responsive polymers.

There are many biomedical applications that utilize fluctuations in pH of physiological tissues. For example, enteric drug delivery systems resist dissolution at acidic pH (in the stomach) and dissolve under alkaline conditions (in the small intestine). Enteric drug delivery systems are used for administering drugs that may degrade in the

stomach under acidic conditions or could cause gastric irritation when released in the stomach. A pH-responsive hydrogel could serve as an enteric coated system if it exhibited a shrinking-swelling transition on going from acidic to alkaline environment.

An acidic/basic comonomer can be used to impart pH sensitivity. pH responsive polymers undergo changes in solubility and chain conformation in response to change in environmental pH. Depending on pH, the acidic or basic comonomer is ionized to varying degrees. At high degrees of ionization, the positive or negative charges along the polymer chain experience electrostatic repulsion from adjacent charged moieties. The intrachain repulsion causes the polymer chains to adopt an extended conformation in solution, leading to an increase in polymer solubility. Moreover, a polymer chain with ionized groups also attracts counter ions to screen intrapolymer electrostatic repulsions. The movement of counter ions into the network also draws in water, acting as an osmotic force leading to increased polymer solubility.

A copolymer of NIPAm and acrylic acid (AA) was chosen as the model mid B block for the ABC triblock. Acrylic acid with a pKa of ~ 4.25 would cause the NIPAm-AA copolymer to exhibit limited solubility under acidic conditions. At high pH, when the acrylic acid units are predominantly ionized, P(NIPAm-co-AA) would become more soluble thus leading to increased solubility. It can serve as a model system for developing enteric coated matrices.

We also wanted to see how the ABC triblock compares with an ABA triblock, namely, poly(NIPAm)-poly(NIPAm-co-AA)-poly(NIPAm). Some studies have shown that the ABC triblock architecture leads to more efficient gelation as compared to an

ABA structure.[85] ABA polymers can lead to formation of 'flower-like' micelles[86], in which the A blocks on a polymer chain can collapse into the same hydrophobic domain rather than aggregating in different domains. This leads to looping back of the mid block and reduces the number of interdomain linkages or 'bridging' chains. In such cases, higher polymer concentration is required to achieve gelation. Thus we also wanted to study the solution behavior of ABA vs ABC triblock polymers.

The triblock polymers were to be synthesized by RAFT polymerization because of its versatility and applicability to a wide variety of monomers such as acrylates, acrylamides, acrylonitrile, styrene- and pyridine- derivatives. It can also be used to attain a variety of complex polymer architectures starting from simple linear end-functionalized polymers to block, graft, star, and dendritic polymers. The RAFT process is known to provide good control over the molecular weight and by substantially reducing termination, leads to a low polydispersity, *Đ*.

1.7. Thesis Outline

In this work, polymer systems exhibiting dual temperature and pH sensitivity are studied for aggregation and gelation under different environmental conditions.

Chapter II is based on work done in collaboration with Can Zhou, a fellow student in the Department of Chemistry, under the joint supervision of Prof. Tim Lodge, Marc Hillmyer and Ronald A. Siegel. A poly(ethylene-*alt*-propylene)-*b*-poly(ethyleneoxide)-*b*-poly(N-isopropylacrylamide-*co*-acrylic acid), PEP-PEO-P(NIPAm-*co*-AA), triblock was synthesized by sequential use of anionic and RAFT polymerization. The triblock

exhibited micelle-to-gel transition on heating under acidic conditions. On increasing pH, the gel reverted back to the micellar state.

Chapter III discusses an ABC triblock PNIPAm-P(NIPAm-*co*-AA)-PDEAm. This polymer is comprised of thermo-responsive side blocks formed by PNIPAm and PDEAm and a dual temperature- and pH- responsive mid block P(NIPAm-*co*-AA). The solution behavior of the triblock is studied as a function of pH and temperature. The effect of AA incorporation on the LCST of P(NIPAm-*co*-AA) was investigated. In addition to the ABC triblock, AB, BA and BC diblocks have also been studied for differences in cloud points. This chapter provides some understanding of the effect of block sequence on polymer solution behavior. A preliminary study has also been carried out to look for gelation in ABC 10 wt% solutions under acidic and alkaline conditions.

Chapter IV is an extension of Chapter III in which the ABC triblock is tested for gelation and is compared with the corresponding ABA triblock PNIPAm-P(NIPAm-*co*-AA)-PNIPAm. The triblock exists as free chains in solution at room temperature. On heating, the polymer phase separates from aqueous solution, leading to formation of aggregates or a viscoelastic structured material, depending on pH. The ABA and ABC triblocks exhibit similar phase behaviors at the tested temperature and pH conditions.

Chapter V provides a summary of the various studies along with suggestions for future design of triblock gelators.

Chapter II

ABC Triblock Terpolymers Exhibiting Both Temperature- and pH-Sensitive Micellar Aggregation and Gelation in Aqueous Solution*

2.1. Extract

Two poly(ethylene-*alt*-propylene)-*b*-poly(ethylene oxide)-*b*-poly(*N*-isopropylacrylamide- *co*-acrylic acid) (PEP-PEO-P(NIPAm-*co*-AA)) triblock terpolymers were synthesized by a combination of anionic and RAFT polymerizations, followed by acid hydrolysis. Micellar aggregation and gelation behavior in aqueous solutions were studied by dynamic light scattering (DLS) and rheology, respectively. DLS measurements on dilute solutions revealed that the triblock terpolymers form micelles with PEP cores and PEO-P(NIPAm-*co*-AA) coronae at room temperature, and undergo a micelle to micellar aggregate transition upon heating. Rheological measurements showed that micellar aggregation manifests itself as gelation at higher concentrations (~4 wt%). The observed thermoresponsive aggregation and gelation is due to the intermicellar association of P(NIPAm-*co*-AA) blocks in the coronae above the lower critical solution temperature of the P(NIPAm-*co*-AA) block.

---

* This chapter describes results obtained from a collaborative research project performed in conjunction with Can Zhou, under the direction of Ronald A. Siegel, Marc A. Hillmyer and Timothy P. Lodge. A report on this project has been published (Koonar, I.; Zhou, C.; Hillmyer, M. A.; Lodge, T. P.; Siegel, R. A. *Langmuir* **2012**, 28, 17785-17794).

The critical micellar aggregation and gelation temperatures are controlled by the mole fraction and degree of acrylic acid (AA) ionization in the P(NIPAm-*co*-AA) block, and therefore they can be modulated as functions of both pH and AA content in the polymer.

2.2. Introduction

Stimuli responsive polymers, which can alter their solubility and conformations according to temperature, pH, ionic strength, light, electric or magnetic fields, are of great interest for biomedical and other applications [14, 21, 22, 87-91]. For example, such polymers can form surfaces whose adhesion or wetting properties are modulated by change in the environment, and therefore can be used in the design of novel chromatographic stationary phases [23, 92-95], substrates for reversible protein and cell attachment [96-99], and tissue engineering scaffolds [100, 101]. They are also useful in designing self assembling and stimulus triggered controlled drug release systems [15, 102].

Temperature is a commonly exploited environmental stimulus, and polymers whose conformations and phase behaviors are significantly altered between room temperature (25 °C) and human physiological temperature (37 °C) have received considerable attention. Of these, poly(*N*-isopropyl acrylamide) (PNIPAm) is one of the most widely studied [15, 103-105]. In aqueous solutions, PNIPAm exhibits a convenient lower critical solution temperature (LCST) at 32 °C. The transition is particularly sharp and nearly independent of polymer concentration [106]. In very dilute solutions, PNIPAm collapses into globules upon heating, while at higher concentrations a rather sharp precipitation

occurs, as observed by a rapid onset of turbidity. These phenomena stem from segregation of PNIPAm from water as temperature increases, an entropically driven process manifesting liberation of hydrophobically structured water and association of PNIPAm side chains [104, 107-110]. This sharp temperature driven transition, along with supposed biocompatibility, have driven substantial interest in using PNIPAm and its derivatives for biomedical applications [14, 21, 39, 103, 106, 111].

When PNIPAm is combined with other monomers or polymers, temperature-driven self assembly into a variety of structures is possible. For example, thermoresponsive ABA triblocks with PNIPAm end blocks have been shown to associate in aqueous solutions above the LCST [112, 113]. For example, Li et al.[114] observed micellization in dilute (0.025 wt%) aqueous solutions of PNIPAm-*b*-poly(2-methacryloyloxyethyl phosphorylcholine)-*b*-PNIPAm with increase in temperature above 33 °C. The micelles were of the "flower" type with the PNIPAm "A" groups localized in the core, surrounded by a corona of poly(2-methacryloyloxyethyl phosphorylcholine) "B" groups. In more concentrated solutions (>6.5 wt%), intermicellar association of PNIPAm chains led to reversible, physical gelation [115-117].

Recently, ABC triblock polymers have been investigated as stimuli responsive gelators [76, 118, 119]. Because of the distinct end domains, the ABC architecture may have an advantage over the ABA architecture due to greater efficiency of inter-micelle interactions, especially at low concentrations [120]. The ABC architecture can suppress elastically ineffective looping conformations of the midblock and formation of flower-like micelles. For example, we recently compared the gelation behavior of an ABC

triblock terpolymer, poly(ethylene-*alt*-propylene)-*b*-poly(ethylene oxide)-*b*-poly(*N*-isopropylacrylamide) (PEP-PEO-PNIPAm, or PON) with the corresponding ABA triblock copolymer PNIPAM-PEO-PNIPAM (NON), and found that the ABC triblock polymer undergoes a much sharper sol-gel transition, at significantly lower concentrations [85]. We also investigated the micellization and micellar aggregation behavior of PON terpolymers in dilute aqueous solutions. These polymers self assembled into micelles with PEP cores and PEO-*b*-PNIPAm shells/coronae. When heated above LCST of PNIPAm, the micelles aggregated, and the critical aggregation temperature was studied as a function of PNIPAm molecular weight and polymer concentration [121]. The micellar aggregates formed were elastic but well hydrated. Thus, the PEP core serves as a small, dry, physical crosslinking point inside a hydrated PEO shell. The PNIPAm corona dictates whether the micelles are suspended in solution or aggregated into viscoelastic quasinetwork structures.

It is desirable to have other variables besides temperature to control the polymer assembly process. In many biomedical applications, for example, the transition may be required to occur at a prescribed temperature. Interestingly, thermal transitions can be converted to transitions based on other stimuli if suitable monomers are incorporated into a thermally responsive polymer [122]. Changes in the charge or conformational state of these stimuli-responsive monomers can tune the LCST above or below the temperature set point [39, 123]. In the present work, we are interested in converting the temperature sensitivity of PNIPAm-containing triblocks into pH-sensitivity, due to changes in monomer polarity[39] and the contribution of counterion entropy to the free energy

balance when the polymer is charged [124]. Joint temperature and pH-mediated self assembly can be investigated either by fixing temperature and varying pH or by fixing pH and varying temperature [125].

Acrylic acid (AA) is frequently used to render polymers pH-sensitive [126]. It is well known that pH and temperature effects can be played off one another by copolymerizing NIPAm and AA, with the LCST increasing with increasing ionization of AA [127-130]. These monomers have been combined to form block, graft and statistical copolymers, the last being the most widely investigated. For example, Wu et al.[131] reported that P(NIPAm-*co*-AA) random copolymers aggregate to form colloidal nanoparticles when heated to a temperature higher than the LCST of PNIPAm, with the aggregation temperature increasing with increasing AA fraction. Bokias et al.[132, 133] studied the solution properties of P(NIPAm-*co*-AA) random copolymers and showed that the cloud point of PNIPAm increased even with low amounts of AA substitution (5 mol%), and with increasing neutralization of AA groups by NaOH.

Microgels of P(NIPAm-*co*-AA) were studied by Snowden and coworkers [134], who observed increased transition temperature and hydrodynamic diameter with increasing pH. This work corroborated results obtained earlier in hydrogels of more macroscopic dimensions [135, 136]. P(NIPAm-*co*-AA) hydrogels, in which the LCST and gel swelling are affected by the AA fraction in the copolymer, have been studied as controlled release systems for enteric drug delivery[137] and as artificial matrices for tissue engineering [101]. P(NIPAm-*co*-AA) random copolymer shells have been

employed as pH-responsive gates to control reaction rate of microencapsulated enzymes [138].

In the present work, we study the dual pH- and temperature sensitive self assembly of PON triblocks in which the N block contains a fraction of AA monomers. Poly(ethylene-*alt*-propylene)-*b*-poly(ethylene oxide)-*b*-poly(*N*-isopropylacrylamide-*ran*-acrylic acid) (PO(N/A)) triblock terpolymers self assemble into micelles with a small PEP core, a large PEO shell, and a P(NIPAm-*co*-AA) corona. Aggregation of these micelles is modulated by coronal solubility, which in turn is affected by both temperature and pH. Micellar aggregation at higher polymer concentrations leads to gelation and solid-like rheological properties. This work may be regarded as a natural extension of our previous investigations with PON, since we now augment the latter's thermosensitivity with pH-sensitivity.

2.3. Experimental Section

2.3.1. Materials

All chemicals were purchased from Sigma Aldrich and used as received unless otherwise noted. 2,2'-Azobisisobutyronitrile (AIBN) was purified by recrystallization from methanol; *N*-isopropylacrylamide (NIPAm) was recrystallized from benzene/n-hexane (65/35 v/v); *tert*-butyl acrylate (*t*BA) was washed with 5% aqueous sodium hydroxide solution and then with water, 3 times each. After drying with anhydrous sodium sulfate for 24 hours, *t*BA was distilled under reduced pressure.[139] Methyl acrylate was passed through a basic alumina column prior to use. The chain transfer agent (CTA), *S*-1-dococyl-*S'*-(α,α'-dimethyl-α''-acetic acid) trithiocarbonate (DMAT) was

synthesized according to procedure reported by Lai, et al [140]. Toluene was passed through two columns of activated alumina and a supported copper catalyst. Tetrahydrofuran (THF) was purified by passage through two columns packed with activated alumina and molecular sieves. Dichloromethane (CH_2Cl_2) was purified on an MBraun solvent purification system.

2.3.2. Synthesis of PO(N/A) Triblock Terpolymers

Two PEP-PEO-P(NIPAm-*co*-AA) (PO(N/A)) triblock terpolymers were prepared by reversible addition-fragmentation chain transfer (RAFT) polymerization from a PO-CTA macroinitiator, chain transfer agent (CTA) removal, and acid hydrolysis (Scheme 2.1).

Scheme 2.1. Synthesis of PO(N/A) triblock terpolymers

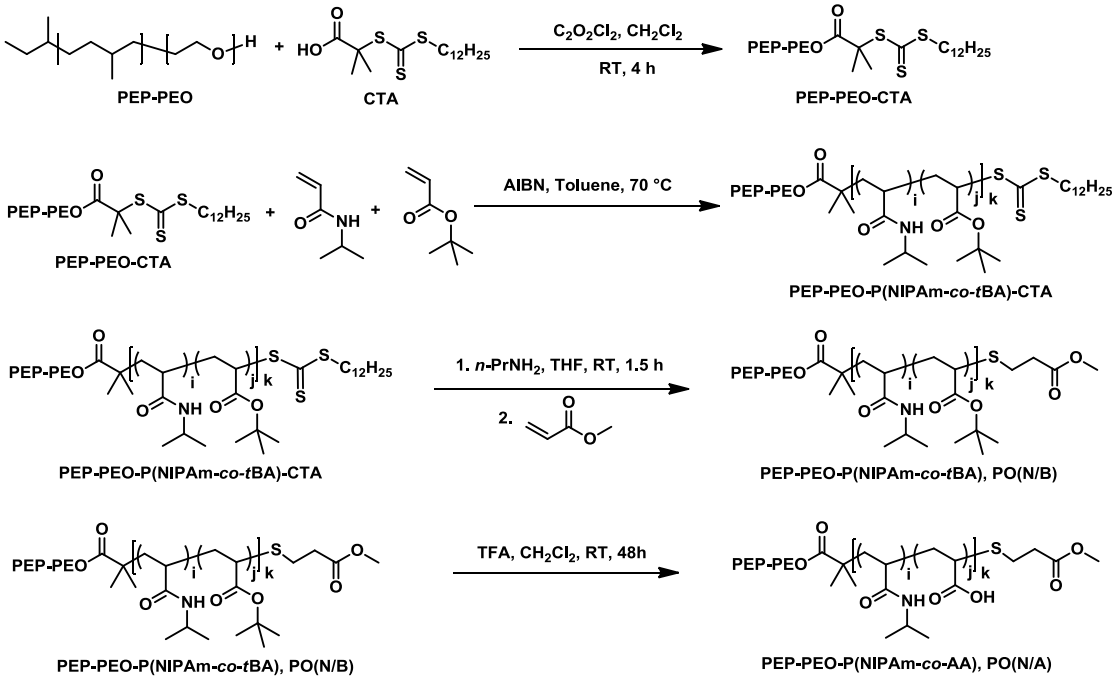

First, PO-CTA was prepared by anionic polymerization and end-functionalization according to the procedure reported by Zhou, et al.[121] The PO-CTA was then used to grow a P(NIPAm-*co*-*t*BA) random copolymer to obtain a PEP-PEO-P(NIPAm-*co*-*t*BA)-

CTA (PO(N/B)-CTA) triblock. In order to avoid the effect of CTA end groups on polymer solution behavior [141], the trithiocarbonate functionality on PO(N/B)-CTAs was removed by aminolysis and Michael addition in the same manner as described for the PON terpolymers [121]. Finally, the *t*BA of PO(N/B) was hydrolyzed to AA *via* acid hydrolysis, resulting in PO(N/A), the desired polymer [142].

Detailed procedures for each reaction step, including a summary of steps for forming PO-CTA, are provided in Supporting Information. Intermediates and products were confirmed by ^{1}H-NMR spectroscopy and characterized by size exclusion chromatography (SEC). The AA content in the P(NIPAm-*co*-AA) block of the PO(N/A) terpolymers was determined by potentiometric titration. Samples investigated in this work and their molecular characteristics are listed in Table 2.1. The percent degree of substitution of *t*BA and ultimately AA in the N block is designated following the comonomer identifier in the polymer acronym.

2.3.3. Reactivity ratios

Reactivity ratios of NIPAm and *t*BA were estimated by traditional free radical copolymerization of NIPAm and *t*BA with six NIPAm:*t*BA feed ratios (80:20, 65:35, 50:50, 35:65, 20:80 and 10:90) (Table 2.2 and Figure 2.10 in Supporting Information). The polymerizations were performed in deuterated toluene in NMR tubes at 70°C and monomer conversion monitored over time. The data were analyzed by nonlinear least squares fitting to the Mayo-Lewis equation. Details of sample preparation and analysis can be found in the Supporting Information.

Table 2.1. **Molecular characteristics of PO(N/B) and PO(N/A) block polymers**

Sample	Molecular composition[a]	*t*BA content (feed)[b]	*t*BA or AA content (polymer)[c]	$Đ^d$
PO(N/B7)	PEP_{45}-PEO_{565}-P(NIPAm$_{80}$-*co*-*t*BA$_5$) (3-25-9-0.7)	10	7	1.09
PO(N/A7)	PEP_{45}-PEO_{565}-P(NIPAm$_{80}$-*co*-AA$_5$) (3-25-9-0.4)	10	7	-
PO(N/B11)	PEP_{45}-PEO_{565}-P(NIPAm$_{71}$-*co*-*t*BA$_9$) (3-25-8-1.1)	20	11	1.08
PO(N/A11)	PEP_{45}-PEO_{565}-P(NIPAm$_{71}$-*co*-AA$_9$) (3-25-8-0.6)	20	11	-

[a]Numbers in parentheses correspond to molecular weights of individual blocks in kg/mol as determined by ^{1}H NMR spectroscopy and potentiometric titration. Subscript indicates number average degree of polymerization of each block. [b]Mol % of *t*BA in reaction mixture of NIPAm and *t*BA as determined by ^{1}H NMR spectroscopy. [c]Mol % of AA in the P(NIPAm-*co*-AA) block of PO(N/AA) as determined by potentiometric titration. Mol % of *t*BA in the P(NIPAm-*co*-*t*BA) block of PO(N/BA) is equal to mol % of AA due to the complete hydrolysis of *t*BA to AA, confirmed by ^{1}H NMR. [d]Dispersity was measured by SEC with THF/*N*,*N*,*N*',*N*'-tetramethylethylenediamine as the eluting solvent.

2.3.4. Sample Preparation

Aqueous solutions of PO(N/B) and PO(N/A) triblock terpolymers were prepared at 0.5 wt% and 5 wt% concentration by the thin film hydration method. Appropriate amounts of bulk polymer were dissolved in CH_2Cl_2, followed by evaporation of solvent to yield a thin film on the walls of the vial. The thin film was hydrated, and the resulting mixture was stirred at room temperature for at least 2 weeks. The aqueous PO(N/A) solutions were then diluted by buffered aqueous solutions prepared at pH 2 (maleate, 0.075 M), 4 (acetate buffer, 0.25 M), 6 (piperazine, 0.05 M) and 8 (phosphate buffer, 0.015 M), at 85 wt% polymer solution/15 wt% buffer, followed by at least one day of

stirring at room temperature. All buffers had initial ionic strength ~0.04 M, hence the buffered polymer solutions had ionic strength ~0.006 M.

2.3.5. Dynamic Light Scattering

Micellar aggregation of the triblock terpolymers was investigated by dynamic light scattering (DLS). The solutions were passed through 0.45 μm filters into glass tubes (ID=0.25 in). Light scattering was carried out in a Brookhaven BI-200SM DLS system equipped with a Mini L-30 HeNe laser operating at 637 nm, a BI-NDO detector, and a TurboCorr correlator. The sample tube was immersed in decalin. Experiments were performed at temperatures from 25 to 55 °C. Intensity correlation functions $g^2(t)$ were recorded at scattering angles of 60°, 90° and 120° and converted to size distribution using the REPES program,[143-145] provided in the GENDIST analysis package.[146] The average hydrodynamic radius R_h and the reduced second cumulant μ_2/Γ^2 were also extracted from $g^2(t)$. In cases where two significant and well-separated peaks were observed in the size distribution, $g^2(t)$ data were fit to a biexponential decay curve at each scattering angle, and characteristic radii corresponding to micelles and aggregates were calculated, as detailed in the Supporting Information.

2.3.6. Rheology

Rheological measurements were carried out in an AR-G2 rheometer, with a Couette geometry confining the sample in a 1 mm concentric cylindrical gap between the cup (inner diameter 30 mm) and the bob (diameter 28 mm). About 15 mL of the sample was first loaded into the cup at room temperature (25 °C). This amount filled the gap as the bob was lowered. Temperature was controlled by a Peltier accessory. To avoid water

evaporation, the assembly was covered with a metal cover with a wet sponge attached to the cover rim. Dynamic frequency sweeps were conducted in the linear viscoelastic regime. Temperature dependences of G' and G'' were measured at 10 rad/s and 1 °C/min.

2.4. Results

2.4.1. Synthesis of PO(N/A) triblock terpolymers

In the present work, the PO-CTA macroinitiator was used to grow P(NIPAm-*co*-*t*BA) blocks by RAFT polymerization.[121] Subsequent removal of the dodecyltrithiocarbonate end group was confirmed by the absence of the methylene protons next to the trithiocarbonate unit (δ=3.3 ppm) and the presence of methylene protons of the added methyl acrylate (δ=2.6, 2.8 ppm) (Figure 2.7). In the final step, hydrolysis of *t*BA of PO(N/B) to acrylic acid (AA), TFA was the catalyst. An excess of triethylsilane was used as a carbocation scavenger, ensuring complete hydrolysis of *t*BA, as confirmed by the disappearance of the methyl protons of *t*BA (δ=1.4 ppm) (Figure 2.7).

The AA content in the P(NIPAm-*co*-AA) block of the PO(N/A) triblock terpolymer was determined by potentiometric titration (Figure 2.9). We found that it was lower than the *t*BA content in the feed. This suggested that *t*BA was incorporated to a lesser extent than NIPAm in the P(NIPAm-*co*-*t*BA) block. (The *t*BA content could not be quantified by ^{1}H-NMR due to peak overlap). To confirm this we carried out a reactivity ratio study for the free radical polymerization of NIPAm and *t*BA, without the CTA. Reactivity ratios of NIPAm and *t*BA were estimated to be $r_{t\mathrm{BA}} = 0.88$ and $r_{\mathrm{NIPAm}} = 2.1$ (Figure 2.10),

suggesting that the P(NIPAm-*co*-*t*BA) block starts out relatively rich in NIPAm and more *t*BA units are located towards the chain end.

2.4.2. Micellar aggregation of PO(N/B) and PO(N/A) triblock terpolymers

DLS experiments were performed on 0.5 wt% aqueous solutions of four PO(N/B) and PO(N/A) terpolymers for a series of temperatures over the range 25–55 °C. Figure 2.1 displays mean hydrodynamic radii and scattering intensities as a function of temperature for PO(N/B) and PO(N/A) copolymers in dilute aqueous solutions (0.5 wt%).

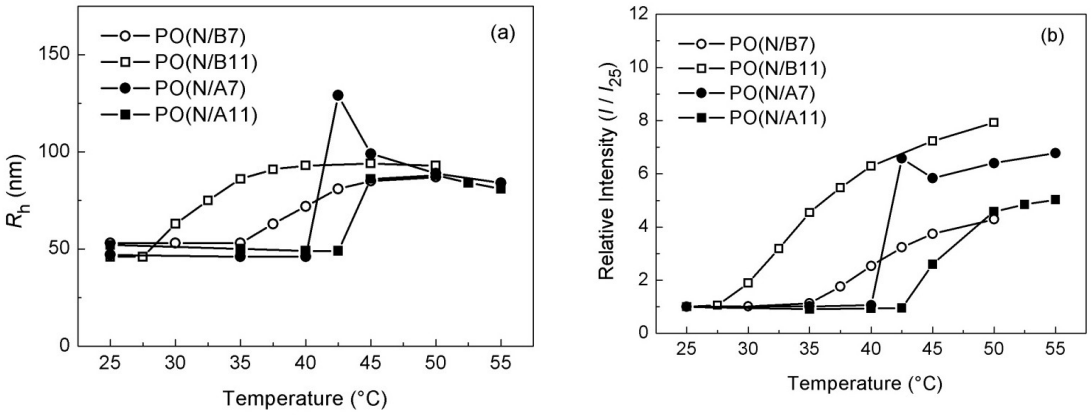

Figure 2.1. (a) Mean micelle size (R_h) and (b) scattering intensity as a function of temperature for aqueous solutions of PO(N/B7) (○), PO(N/B11) (□), PO(N/A7) (●) and PO(N/A11) (■). Polymer concentration: 0.5 wt%. R_h was calculated from DLS data at three different angles (60°, 90°, 120°) by the cumulant method. Intensity was measured at 90°. Ordinate is relative intensity (I/I_{25}) where I_{25} is intensity recorded at 25 °C.

At 25 °C, the micelle radii were around 50 nm for both PO(N/B) and PO(N/A) terpolymers, irrespective of composition. As the solution was heated above a critical temperature, both hydrodynamic radius and scattering increased, indicating formation of micellar aggregates. This transition temperature will henceforth be called the "critical

micellar aggregation temperature" or CMAT. Dispersity in R_h was evident both above and below CMAT. The reduced second cumulant (μ_2/Γ^2) was ~0.20 at lower temperatures, and tended to increase around CMAT, as expected for an aggregation transition.

The full size distribution curves leading to the mean R_h values in Figure 2.1(a) are displayed in Figure 2.2. While the PO(N/B) distributions are essentially unimodal (save for very small blips), the PO(N/A) distributions are often bimodal at high temperatures, indicating that both micelles and micellar aggregates are present. Thus the CMAT should be taken as the onset of a subpopulation of aggregates, rather than a complete transition from the micellar to the aggregated state.

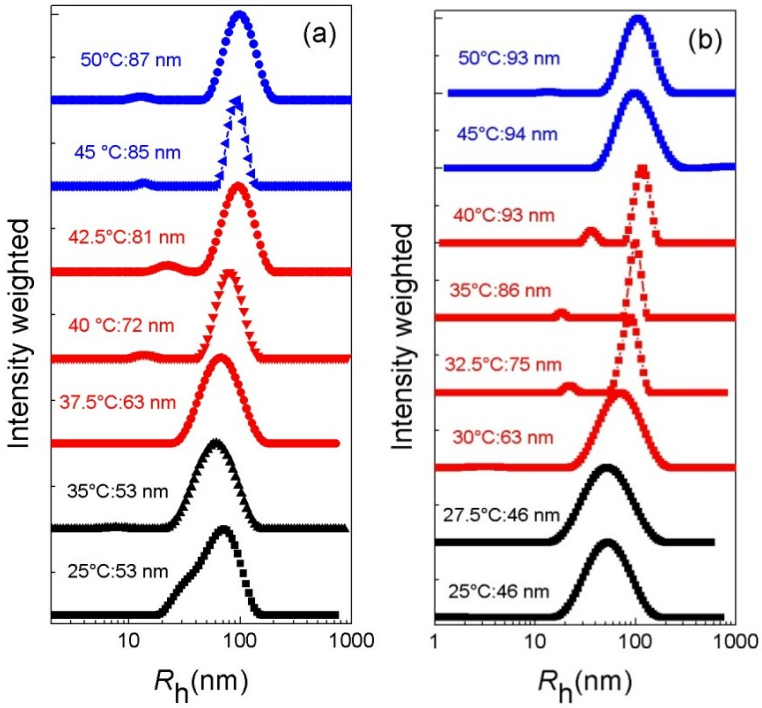

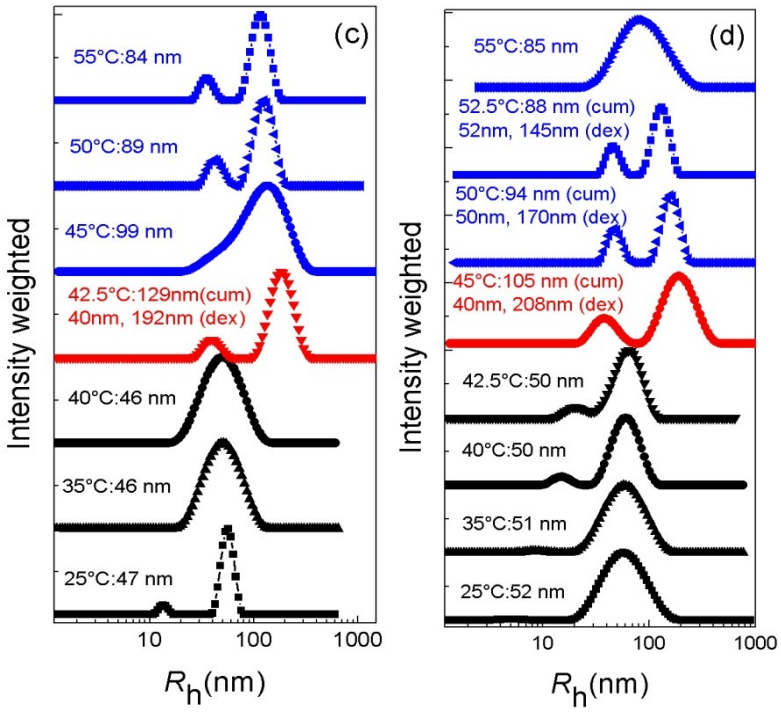

Figure 2.2. Micelle size (R_h) distribution as a function of temperature for (a) PO(N/B7), (b) PO(N/B11), (c) PO(N/A7) and d) PO(N/A11) micelles, as determined by DLS at 90° (0.5 wt% polymer concentration). The designations (cum) and (dex) stand for R_h obtained by cumulant and double exponential fitting, respectively.

For the PO(N/B7) terpolymers, CMAT≈35 °C while for the PO(N/B11) polymers, CMAT≈27 °C. This implies that CMAT decreases with increasing *t*BA fraction. This observation is consistent with literature observations that substitution of *tert*-butyl acrylate, *n*-butyl acrylate, and other alkyl analogs lowers the LCST of PNIPAM [147, 148]. On the other hand, for the PO(N/A) terpolymers, the aggregation trend as a function of polymer composition was reversed, with the CMAT increasing with increasing AA fraction. The PO(N/A7) terpolymer micelles aggregated at 40 °C while PO(N/A11) terpolymer began forming micellar aggregates at a slightly higher temperature of 42.5 °C. Overall, PO(N/B) terpolymer micelles exhibited lower aggregation temperatures than the PO(N/A) triblocks. It should be noted that there was no pH adjustment for these samples.

The pH for the PO(N/B) aqueous solutions was around 7.0 while that for the PO(N/A) aqueous solutions was around 4.0, indicating significant release of acidic protons and ionization of the AA groups ($pK_a \approx 4.3–4.8$).

2.4.3. Micellar aggregation of PO(N/A) triblock terpolymers as a function of pH

DLS experiments were also performed with 0.4 wt% PO(N/A) terpolymer aqueous solutions for pH values ranging from 2 to 8 over the 25–55 °C temperature range. Figure 2.3 presents DLS data for 0.4 wt% PO(N/A7) terpolymer solutions. Full size distribution curves are present in Figure 2.11. At pH 2, the CMAT was 37.5 °C, and the aggregation transition shifted to 40 °C and 45 °C for the pH 4 and 6 solutions, respectively. No aggregation was observed for pH 8 up to 55 °C.

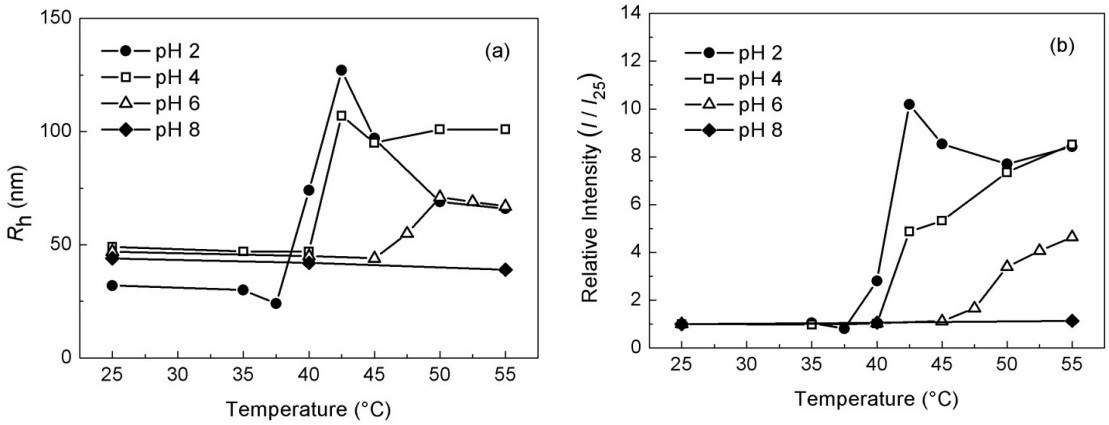

Figure 2.3. (a) Micelle size and (b) scattering intensity as a function of temperature for PO(N/A7) in buffered aqueous solutions at pH 2 (●), 4 (□), 6 (Δ) and 8 (◆). Polymer concentration: 0.4 wt%. R_h was calculated from DLS data at three different angles (60°, 90°, 120°) by the cumulant method. Intensity is measured at a 90° scattering angle, and the vertical axis is the relative intensity (I/I_{25}) where I_{25} is the intensity recorded at 25 °C.

An increase in mean hydrodynamic radius correlated with the rise in scattering intensity upon aggregation, and the ratio of scattering intensity provides a rough estimate of the aggregation number of the average micellar cluster. At room temperature, the

typical micelle size was ~50 nm at pH 4, 6 and 8. However, at pH 2, the micelle size was reduced to ~30 nm. The source of this reduction, which is also observed for PO(N/A11) (see below), is not certain. We note however that the pH 2 condition is the only one in which the corona is essentially completely unionized. It is also noteworthy that protonated AA has been proposed to form hydrogen bonds with NIPAm[128] and PEO [149], which may also encourage contraction of the corona at pH 2.

Results for the PO(N/A11) samples are shown in Figure 2.4. (See Figure 2.12 for the size distribution curves.) Trends are similar to the PO(N/A7) sample, but with quantitative differences. CMAT was shown to be 40 °C and 42.5 °C at pH 2 and 4, respectively, while no aggregation was observed up to 55 °C for the pH 6 and pH 8 solutions. Similar to PO(N/A7), the micelle radius was ~50 nm at 25 °C for the pH 4, 6 and 8 solutions and shrank to ~30 nm at pH 2.

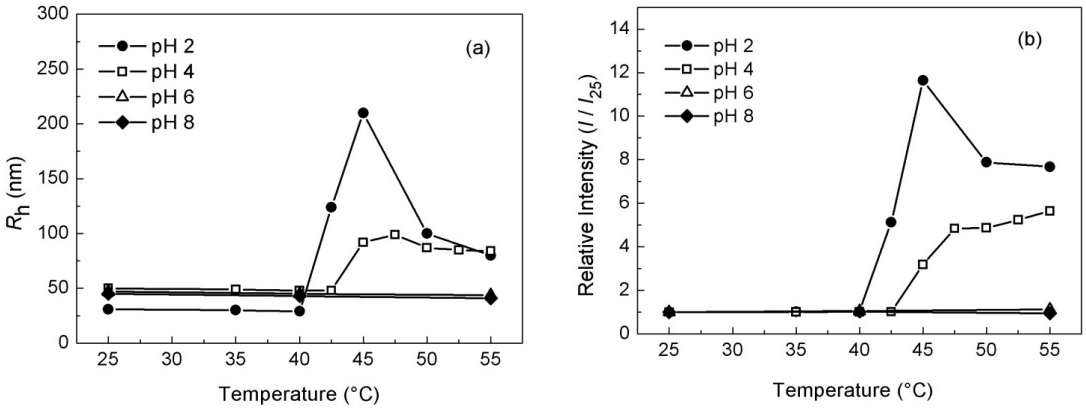

Figure 2.4. (a) Micelle size and (b) Intensity as a function of temperature for PO(N/A11) in buffered aqueous solutions at pH 2 (●), 4 (□), 6 (Δ) and 8 (◆). Polymer concentration: 0.4 wt%. R_h was calculated from DLS data at three different angles (60°, 90°, 120°) by the cumulant method. Intensity is measured at a 90° scattering angle, and the vertical axis is the relative intensity (I/I_{25}) where I_{25} is the intensity recorded at 25 °C.

The CMATs for PO(N/A7) and PO(N/A11) in buffered pH 4 aqueous solution were the same as those for the corresponding unbuffered solutions, which were of pH ~3.8 and 4.0, respectively. It may therefore be inferred that ionization of the coronal polymer chains was nearly identical in these two cases. At and above the CMAT, the micelles aggregated, as indicated by increasing mean R_h and intensity. At pH 2, the mean aggregate size peaked near CMAT and then decreased to a smaller R_h value that remained nearly constant with further increase in temperature. This pH value was also distinguished from the others in the more significant bimodality of the size distributions above the CMAT, as shown in Figures 2.11(a) and 2.12(a). Near the CMAT, aggregate sizes above 300 nm were detected, which were reduced at higher temperatures, at pH 2. This nonmonotonic behavior, also evident in the mean R_h values, is unexplained.

The DLS results for the PO(N/A) triblock are summarized as a phase diagram in Figure 2.5, which reflects the following trends. First, the CMAT increases with increasing pH, reflecting increased ionization of the corona. Second, the CMAT increases with AA content, for essentially the same reason. The phase diagram is truncated due to lack of data above 55 °C. For comparison, we also include the CMAT of PON, which is 42 °C.[121] Under acidic conditions, the CMAT for PONA is lower than that for PON due to intra-chain H-bonding between the unprotonated AA groups [44, 150]. At higher pH values, PONA CMAT increases due to acrylic acid ionization.

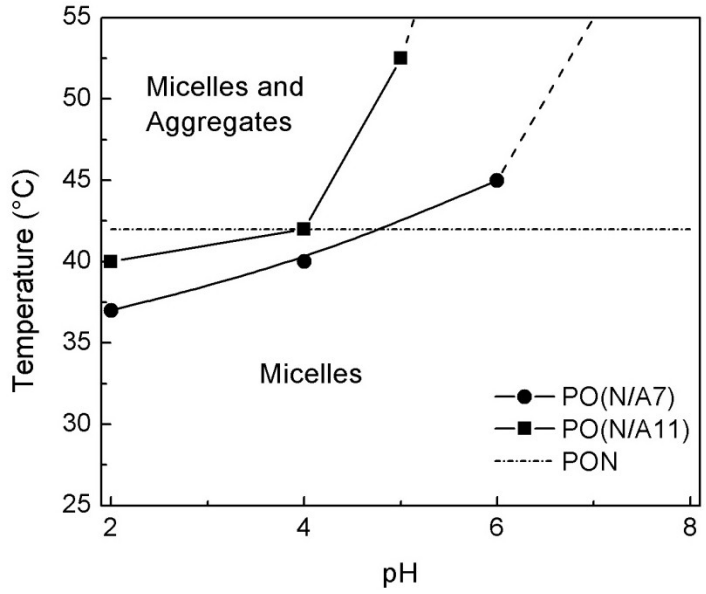

Figure 2.5. Phase diagram for PO(N/A7) (●), PO(N/A11) (■) as a function of temperature and pH. Points and solid lines represent measured and interpolated values of CMAT, which separate regions featuring micelles from regions in which aggregates are present. The aggregate phase may also include a subpopulation of micelles. Dashed lines are extrapolations of trends, which cannot be well specified since data was not taken above 55 °C. PON CMAT (dash dot) (from the previous study by Zhou et al.[121] and assumed to be pH-independent) is presented here for comparison. Similar horizontal lines could be included for PO(N/B7) and PO(N/B11) at 35 °C and 27.5 °C, respectively.

2.4.4. Gelation of PO(N/A) triblock terpolymers

Results of oscillatory shear measurements conducted with 4 wt% PO(N/A11) in buffered solutions at pH = 2 and 8 over the temperature range 25–60 °C are shown in Figure 2.6. PO(N/A7) samples showed similar behavior (Figure 2.13). Figure 2.6 clearly demonstrates a sharp sol-gel transition near 45 °C at pH 2, but no such transition at pH 8. Below 42.5 °C, G' was nearly constant and the same at both pH values while G'', again identical at the two pH values, decreased slightly with increasing temperature. The temperature dependence of G' and G'' displayed no evidence of aggregation at pH 8, up

to the highest measured temperature (60 °C). At pH 2 both G' and G'' increased abruptly near the transition point, with G' crossing over G''. The sol-gel transition was thermoreversible throughout repeated heating and cooling cycles (not shown).

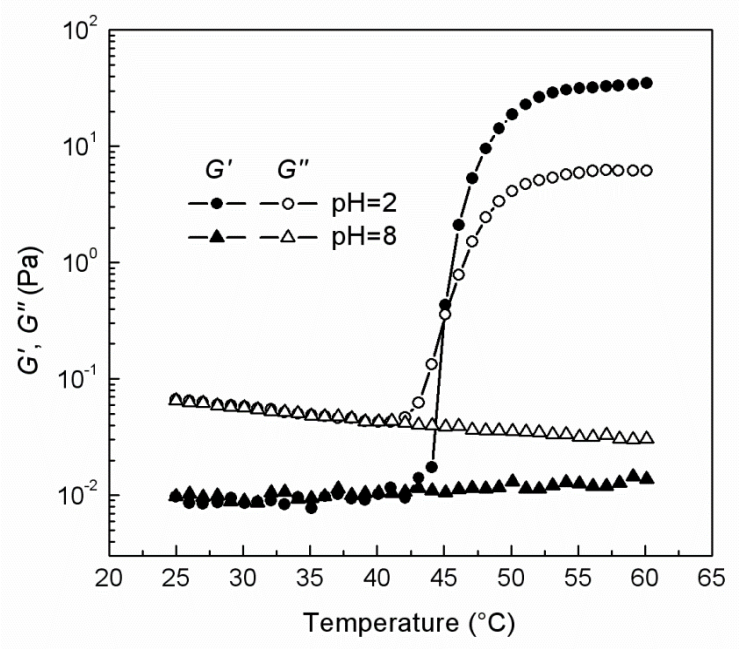

Figure 2.6. Temperature-dependent dynamic shear moduli (G' and G'') for 4 wt% PO(N/A11) in buffered aqueous solutions at ω=10 rad/s and heating rate 1 °C/min. The pH 2 solution was measured at strain amplitude γ= 0% at low temperatures (below gel point) and γ=2% at high temperatures (above gel point). The pH 8 solution was measured at γ = 2%.

The sol-gel transition for the pH 2 solution and sol state for the pH 8 solution were verified using dynamic frequency sweep measurements. Representative data for the pH 2 solution at 25, 43, and 60 °C are shown in Figure 2.14. At 25 °C, G' was smaller than G'' indicating a free-flowing sol state. At 60 °C, G' was larger than G'' at all frequencies and was nearly frequency independent, indicating solid-like behavior. At 43 °C, the sample showed intermediate behavior with nearly identical values for G' and G'', signifying the transition between liquid-like and solid-like behavior. Dynamic frequency sweeps of the

pH 8 solution at 25 and 60 °C are presented in Figure 2.15, and clearly show that G' is smaller than G'' at both temperatures, indicating that the pH 8 solution was in the sol state over the temperature range of 25 – 60 °C.

2.5. Discussion

The PON materials we previously reported, and the present PO(N/B) and PO(N/A) triblock systems share a short chain, non-glassy hydrophobic core (PEP), a hydrophilic shell (PEO), and a stimulus sensitive corona. The coronas all contain NIPAM, a monomer exhibiting LCST behavior, as the majority monomer. Incorporating *t*BA augments the hydrophobic character of the N/B coronas. Hydrolysis of *t*BA in N/B converts it to acrylic acid, a species that is not only more hydrophilic than both NIPAM and *t*BA, but is also ionizable.

In the previous paper on PON and the present work on PO(N/B) and PO(N/A) triblocks, the observed transition was between a micelle solution and a highly aggregated state, which is manifested as a collection of micelle clusters at low concentrations, and an elastic network at high concentrations. The temperature at which micellar aggregates appear, the CMAT, is analogous to the LCST for polymer solutions. However, the transitions for PON and PO(N/A) triblocks occurred at 37.5 °C or above, in all cases several degrees higher than the LCST of PNIPAM. The covalent linkage of the well solvated PEO to the PNIPAM-based corona increases the temperature at which the coronal chains aggregate [72, 151-153]. This effect is countered in the PO(N/B) systems, with CMAT reduced to 35 °C and 27.5 °C with 7% and 11% substitution by *t*BA,

respectively. These results are in accord with literature in which LCST of PNIPAm is lowered upon incorporation of small amounts of *n*-butyl acrylate [39, 103, 154].

At pH 2, virtually all AA units are expected to be protonated and electrically neutral, while increasing fractions of AA will be ionized at the higher pH values, including the case where the PO(N/A) is suspended in pure water, where the pH was observed to be approximately 4. At and above pH 4, the PO(N/A) micelles had approximately the same radii at low temperatures, around 50 nm. The micelles of PON[121] and PO(N/B) also had $R_h \approx 50$ nm. At pH 2, however, the PO(N/A) micellar radius was ~30 nm. We speculate that the substantially reduced radius of PO(N/A) at pH 2 is due to condensation of the corona into the shell resulting from hydrogen bonding between the protonated AA units and PEO. Although AA can also hydrogen bond within the corona with PNIPAm, intra-coronal PNIPAm and PAA hydrogen bonding alone is not likely to be sufficient to bring about a micelle size reduction of this magnitude. Hence, it appears that H-bonding between protonated PAA and PEO is causing the P(NIPAM-*co*-AA) corona to collapse onto the PEO shell.

The effects of pH and degree of incorporation of AA into the PO(N/A) micelles on the CMAT are consistent with the literature reporting the LCST of NIPAm/AA copolymers, except for the overall shift toward higher temperatures seen in the micellar systems, as discussed above. Consistent with literature on N/A copolymers, a slight decrease in the CMAT was observed in PO(N/A) as compared to PON terpolymers [128]. Also as expected, the CMAT increased with increasing degree of ionization, brought

about either by increased pH at constant AA substitution or by increased degree of AA substitution at constant pH.

The light scattering measurements were taken at low polymer concentrations, with turbidity and increased R_h reflecting the presence of relatively small, dispersed aggregates. The rheological measurements with PO(N/A) polymers were taken at higher concentrations (4 wt%) in order to identify gelation conditions. Figure 2.5 illustrates distinct rheological behaviors at pH 2 and 8. At pH 2, viscous behavior was dominant below 42.5, at which point both G' and G'' rose sharply with temperature, and G' surpassed G'', signaling a transition to elastically dominant behavior. At pH 8, viscous behavior was dominant at all temperatures. (It should be noted that these results reflect measurements at 10 rad/sec. At higher frequencies there was less relative dominance of viscosity over elasticity at pH 8, or at lower temperatures for pH 2. However, the moduli in those cases were much lower; see Fig 2.15. These results may be interpreted as follows. At pH 2, the PO(N/A) micelles have a relatively small diameter and do not overlap substantially at low temperatures. Above the CMAT, the coronae become so interconnected as to form a percolating network of adherent micelles. At pH 8, however, such overlap is not permitted at any temperature since it would lead to substantial increase in fixed charge density in the overlapping coronae, leading to osmotic forces that draw water back into the coronae.

The gelation temperature at 45 °C, observed for PO(N/A11) at pH 2, is a few degrees higher than the corresponding CMAT (40 °C). This difference between the CMAT and gelation temperature is not unexpected. While the CMAT, determined by DLS, signals

the onset of aggregation, the gelation temperature, as measured by rheology, indicates the point at which micellar aggregates form a percolating three dimensional network strong enough to result in a modulus crossover. Another factor that could account for the difference in transition temperature is the difference in heating rate.

In the present study the observed aggregation and gelation transitions were completely reversible, and the reversibility was not influenced by polymer concentration. At 0.5 wt%, upon cooling, the micellar aggregates disaggregated into individual micelles with radius of ~50 nm. Similarly, the gels formed on heating 4wt% PO(N/A) solutions reverted to sol form on cooling.

2.6. Conclusions

Doubly thermo- and pH-responsive PO(N/A) triblock terpolymers were prepared via hydrolysis of PO(N/B) triblock terpolymers, which were synthesized by a combination of anionic and RAFT polymerization, followed by acid hydrolysis of *t*BA to AA. As shown in Scheme 1.2. the PO(N/A) terpolymers spontaneously self assemble into core-shell-corona micelles with PEP cores, PEO shells and P(NIPAm-*co*-AA) coronae in aqueous solution at room temperature. Upon heating, the polymer micelles aggregate in the dilute solutions and form a three dimensional network at higher concentrations. The micelle-micellar aggregate transition is completely reversible and is brought about by interchain collapse of the corona p(NIPAm-*co*-AA) chains. The critical micelle aggregation temperature can be controlled by changing pH of the medium and by varying the copolymer composition.

Scheme 2.2. Proposed self assembly of PO(N/A) triblock

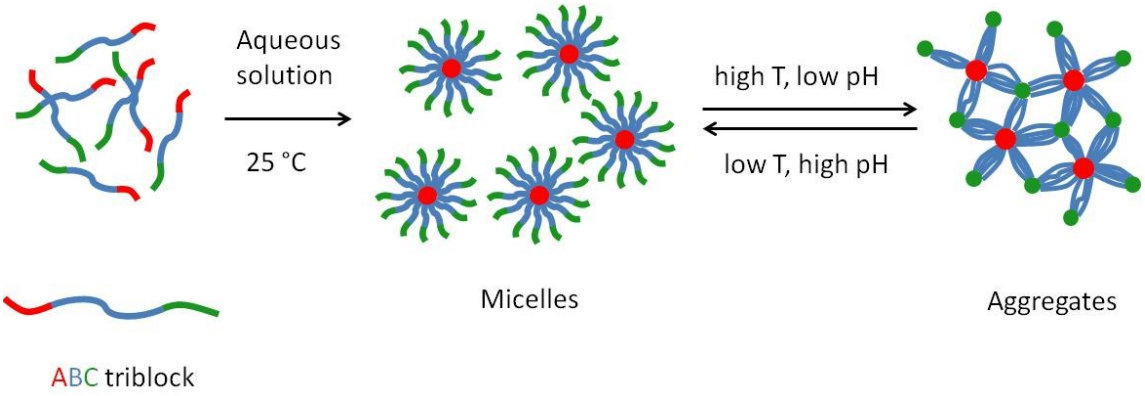

It should be apparent that while measurements were carried out by sweeping temperature at fixed pH, one could fix temperature and vary pH instead. The joint temperature/pH behavior may lead to biomedical applications of these or analogous triblock polymer systems. For example, one might consider an intravaginal drug delivery system incorporating a hydrophilic antiviral, antibacterial, anti-inflammatory or spermicidal agent into a concentrated micellar solution which, at room temperature, remains in the fluid state. Because of the large PEO content relative to PEP and N/A, the agent will reside primarily in the shell region. Upon application in the relatively acidic (pH 4-5) vaginal cavity [155], the increased temperature could instigate gelation. Release of drug could be by relatively slow, passive diffusion through the resulting hydrogel, or it could be triggered by introduction of sperm, whose pH is ~7.5, which would promote disaggregation of the micellar network. Properties of the terpolymers (CMAT, pH sensitivity, biocompatibility, etc.) would need to be tuned for such physiological applications.

Numerous variations can be imagined around the present theme, in which a sol-gel transition of micellar systems is triggered by both temperature and a second stimulus. By

incorporating appropriate comonomers, the LCST of NIPAM has been shown to be modulated by other stimuli such as light[156, 157] and glucose.[158-165] Further, the pH-mediated transition can be altered using acidic comonomers besides AA,[44, 45, 166] or by replacing acidic monomers with monomers containing tertiary amines or other weak base sidechains.[133] Finally, the LCST can be raised or lowered by incorporating hydrophilic or hydrophobic comonomers, respectively, into the coronal C block.[39] We envision that all these variations can be carried over to the triblock micellar system studied here, with the LCST of the C block correlated with the CMAT and the gelation transition. Similarly the core polymer, PEP, might be replaced by other very hydrophobic polymers.

2.7. Supporting Information

2.7.1. Polymer synthesis I. PEP-PEO macro-CTA (PO-CTA)

First, A PEP-PEO (PO) diblock copolymer was synthesized by anionic polymerization following a previously reported procedure.[167] PEP and PEO block molar masses were 3,000 and 25,000, respectively, with very narrow molecular weight distribution ($Đ$ = 1.02).[121] The chain transfer agent (CTA), *S*-1-dodecyl-*S*′-(*α, α*′-dimethyl-*α*″-acetic acid) trithiocarbonate was then coupled to the hydroxyl end-groups of PO diblock to give PEP-PEO-CTA (PO-CTA) macroinitiator *via* an acid chloride intermediate.[168]

2.7.2. Polymer synthesis II. PEP-PEO-P(NIPAm-co-tBA)-CTA

In a representative synthesis, PO-CTA macroinitiator (3.0 g, 0.11 mmol), NIPAm (2.1 g, 19 mmol), *t*BA (0.255 g, 2.0 mol) and AIBN (1.8 mg, 0.011 mmol) were

dissolved in toluene (30 mL), degassed by three freeze-pump-thaw cycles and reacted at 70 °C for 3.2 h. The reaction mixture was then cooled to 0 °C, diluted with CH_2Cl_2, precipitated in pentane three times, and dried at 40 °C in a vacuum oven overnight. Conversion of NIPAm was around 50% as determined by ^{1}H NMR. The content of *t*BA in the P(NIPAm-*co*-*t*BA) block was varied by controlling the feed ratio of NIPAm to *t*BA.

2.7.3. Polymer synthesis III. Removal of trithiocarbonate end groups

CTA was removed by aminolysis and Michael addition according to the procedure reported by Qiu and Winnik.[169] In a typical example towards the synthesis of PEP-PEO-P(NIPAm-*co*-*t*BA) (PO(N/B)), PO(N/B)-CTA (2.7 g, 0.069 mmol), *n*-propylamine (0.2 g, 3 mmol) and tris(2-carboxyethyl) phosphine hydrochloride (20 mg, 0.069 mmol) were dissolved in THF (40 mL). The reaction mixture was stirred for 24 h at room temperature with methyl acrylate (1.5 mL, 17 mmol) added at 2.5 h. The reaction mixture was precipitated in pentane. The product was then dissolved in 100 mL CH_2Cl_2, filtered through a 0.45 μm HVHP Durapore membrane and passed through a basic alumina column. It was then precipitated two more times in pentane and dried at 40 °C in the vacuum oven overnight.

2.7.4. Polymer synthesis IV. Hydrolysis of tBA to AA

PO(N/B) (1.0 g, 0.0028 mmol), trifluoroacetic acid (3.0 mL, 39 mmol) and triethylsilane (4.0 mL, 25 mmol) were dissolved in 10 mL CH_2Cl_2 and stirred at room temperature for 24 h. After hydrolysis, most of the trifluoroacetic acid and triethylsilane were removed under vacuum. The reaction mixture was then redissolved in CH_2Cl_2,

precipitated in diethyl ether twice and pentane once and dried at 40 °C in a vacuum oven overnight.

2.7.5. Characterization

^{1}H nuclear magnetic resonance (^{1}H NMR) spectroscopy was conducted using a Varian Inova 500 MHz instrument spectrometer with CDCl3 as the solvent. Size exclusion chromatography was performed on a Waters 150C ALC/GPC equipped with three Phenogel (Phenomenex) columns with pore sizes of 10^3, 10^4, and 10^5 Å, a Wyatt DAWN multiangle light-scattering detector and a Wyatt OPTILAB rEX refractive index detector. THF containing 1 % tetramethylethylenediamine by volume was used as the eluent at a flow rate of 1.0 mL/min.

2.7.6. Determination of AA content by potentiometric titration

0.1 wt% aqueous solutions of PO(N/A) polymer were titrated against 0.05 M sodium hydroxide aqueous solution using a Metrohm 719S Titrino equipped with a Metrohm LL Micro glass electrode. AA content was calculated from the titration curve endpoint, as estimated by the titration freeware CurTiPot.

2.7.7. Reactivity ratio determination

NIPAm, *t*BA and AIBN were dissolved in deuterated toluene in Wilmad LabGlass 7" NMR tubes and sparged with argon. The sample was analyzed by ^{1}H NMR in a Varian Innova 300 spectrometer at 70 °C. Monomer conversion in the reaction mixture and NIPAm:*t*BA ratios in the feed and polymer were estimated from the NIPAm and *t*BA peak integrals calculated at approximately 10% conversion.

Results were fitted to the Mayo-Lewis equation,

$$F_2 = \frac{f_1 f_2 + r_2 {f_2}^2}{r_1 {f_1}^2 + 2 f_1 f_2 + r_2 {f_2}^2}$$

where f_1 and f_2 = monomer compositions in feed, F_1 and F_2 = monomer compositions in polymer, and r_1 and r_2 are the reactivity ratios, with 1= NIPA and and 2=*t*BA.

2.7.8. Dynamic Light Scattering

The squared electric field correlation functions $g_1^2(t)$ was calculated from the measured intensity correlation functions $g_2(t)$ according to Siegert relation $g_2(t) = 1 + \beta g_1^2(t)$.

Then, the cumulant method was used to fit the autocorrelation functions to extract the average decay rate Γ.

$$g_1^2(t) = A \exp(-2\Gamma \cdot t)(1 + \frac{\mu_2}{2!} t^2 - \frac{\mu_3}{3!} t^3 + \cdots)^2$$

The mutual diffusion coefficient D_m was determined by linear regression of Γ vs q^2 according to the relation $D_m = \Gamma/q^2$, where q is the scattering vector [$q = 4\pi n/\lambda \sin(\theta/2)$, where n is the refractive index of the solution, λ is the wavelength of the light in vacuum, and θ is the scattering angle] Then, the hydrodynamic radius (R_h) was determined using the Stokes-Einstein equation,

$$R_h = \frac{k_B T}{6\pi \eta_s D_m}$$

The estimated uncertainty of R_h was ±5 %. The size dispersity was estimated by the reduced second cumulant (μ_2/Γ^2), which is a measure of the width of the decay rate distribution, assuming it is monomodal. The hydrodynamic radius distribution could also

be extracted from the decay rate distribution generated by the inverse Laplace transform program REPES.

In cases where the size distribution was bimodal with well separated peaks, the correlation data was fit to a double exponential decay.

$$g_1^2(t) = [A_1 \exp(-\Gamma_1 t) + A_2 \exp(-\Gamma_2 t)]^2$$

$D_{m,1}$ and $D_{m,2}$ were calculated by linear regression of Γ_1 and Γ_2 vs q^2, respectively, using OriginPro 7.5 software. The corresponding hydrodynamic radii $R_{h,1}$ and $R_{h,2}$ for the two distinct populations were obtained by the Stokes-Einstein equation.

Table 2.2. NIPAm:*t*BA ratios in the feed and polymer by free radical polymerization

Sample	Ratio in the feed (NIPAm:*t*BA) [a]	NIPAm Conversion (%) [b]	*t*BA conversion (%) [c]	Ratio in the polymer (NIPAm:*t*BA) [d]
1	80:20	11	10	83:17
2	65:35	8	4	80:20
3	50:50	10	6	65:35
4	35:65	11	7	49:51
5	20:80	9	7	25:75
6	10:90	7	9	9:91

[a]NIPAm:*t*BA molar ratio in the feed as determined by ^{1}H NMR spectroscopy. [b,c]Percent molar conversion of NIPAm and *t*BA, respectively, as determined by ^{1}H NMR spectroscopy. [d]NIPAm: *t*BA molar ratio in the polymer as determined by ^{1}H NMR spectroscopy.

Table 2.3. Hydrodynamic radii (R_h) at 25 °C and transition temperatures (T_t) of PON(N/B) and PO(N/A) micelles

Sample	R_h initial (nm) [a]	μ_2/Γ^2 (θ=90°)	T_t (°C) [b]
PO(N/B7)	53	0.21	35
PO(N/B11)	47	0.25	27
PO(N/A7)	47	0.24	40
PO(N/A11)	52	0.26	42
PO(N/A7) pH 2	32	0.23	37
PO(N/A7) pH 4	49	0.18	40
PO(N/A7) pH 6	47	0.24	45
PO(N/A7) pH 8	44	0.22	- [c]
PO(N/A11) pH 2	31	0.21	40
PO(N/A11) pH 4	50	0.22	42
PO(N/A11) pH 6	47	0.23	- [c]
PO(N/A11) pH 8	45	0.20	- [c]

[a] R_h calculated from DLS data at three angles (60°, 90°, 120°) by the cumulant method. [b] Micelle→aggregate transition identified at temperature at which micellar size and scattering intensity starts to increase. [c] No transition was observed over the measured temperature range i.e. 25 to 55 °C.

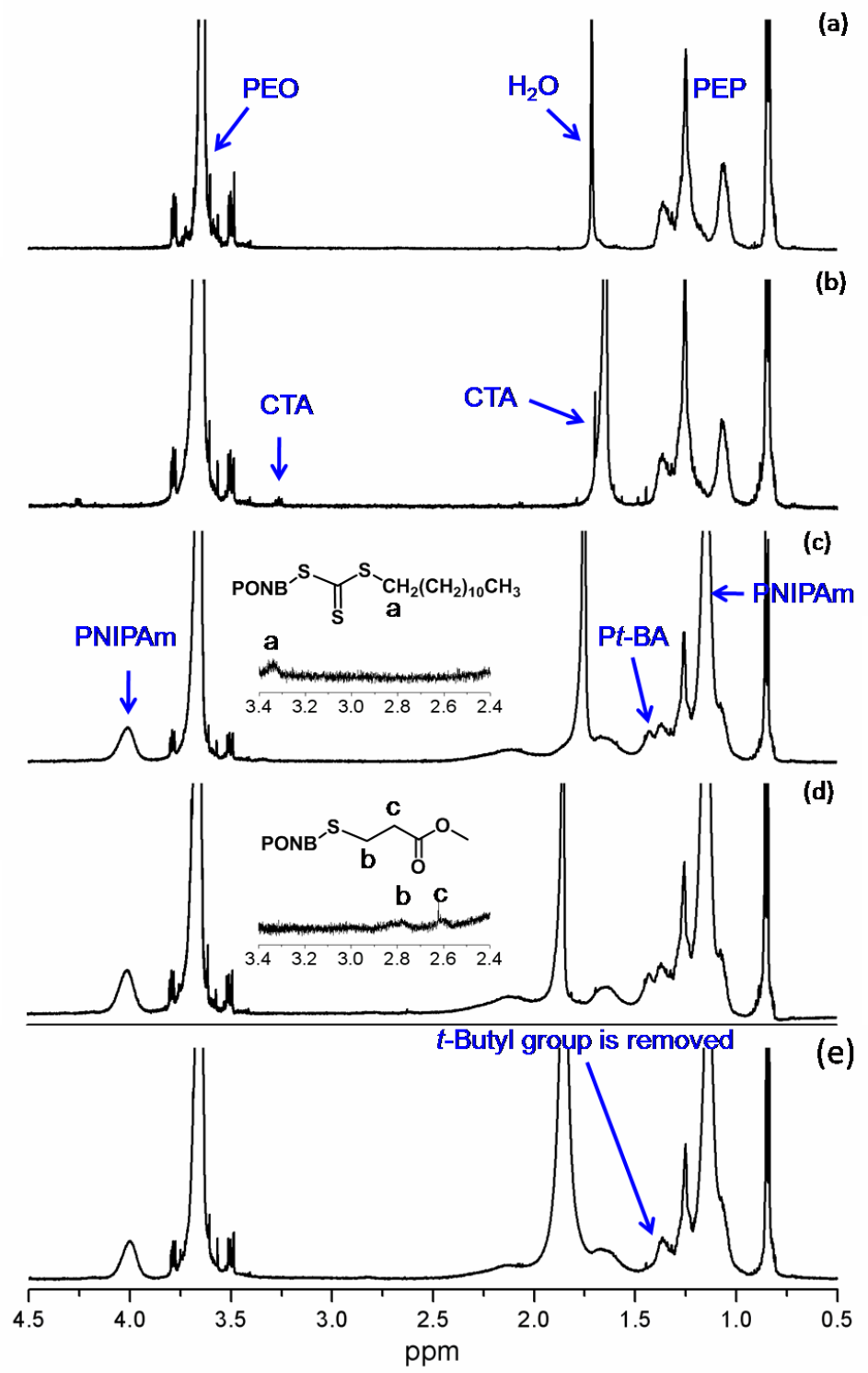

Figure 2.7. ^{1}H NMR (500 MHz) spectra of (a) PO and (b) PO-CTA, (c) PO(N/B)-CTA (d) PO(N/B7) and (e) PO(N/A7) polymers in $CDCl_3$. Area from 3.4 to 2.4 ppm of (c) and (d) is enlarged in each spectrum to monitor end group conversion.

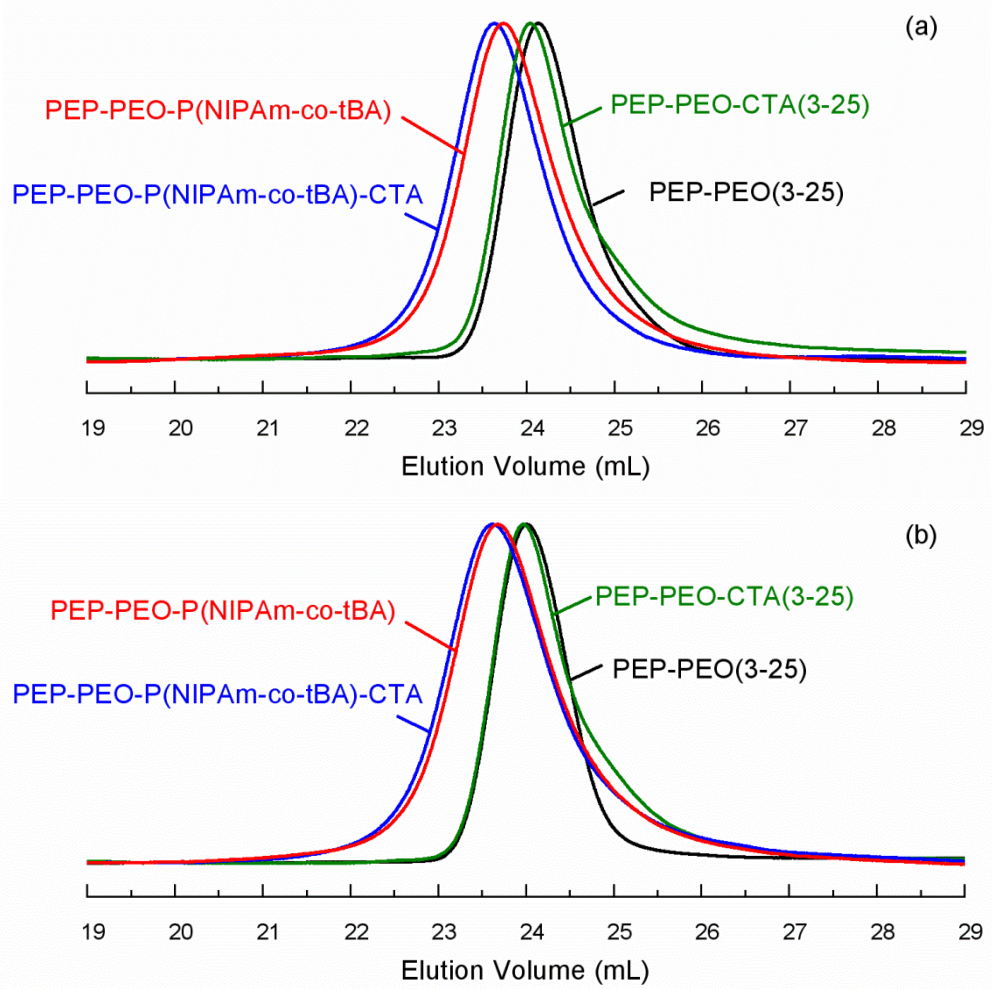

Figure 2.8. GPC curves for (a) PO(N/B7) and (b) PO(N/B11) and the corresponding precursors.

Note: In the elugrams, some amount of 'tailing' is observed for samples end capped with CTA. Polymer chains with this particular CTA attached may have a tendency to 'stick' to the column, which would lead to the broadening of the MW distribution. We have seen this on several other occasions. Note that the broadening goes away once the dodecyl chain is cleaved off.

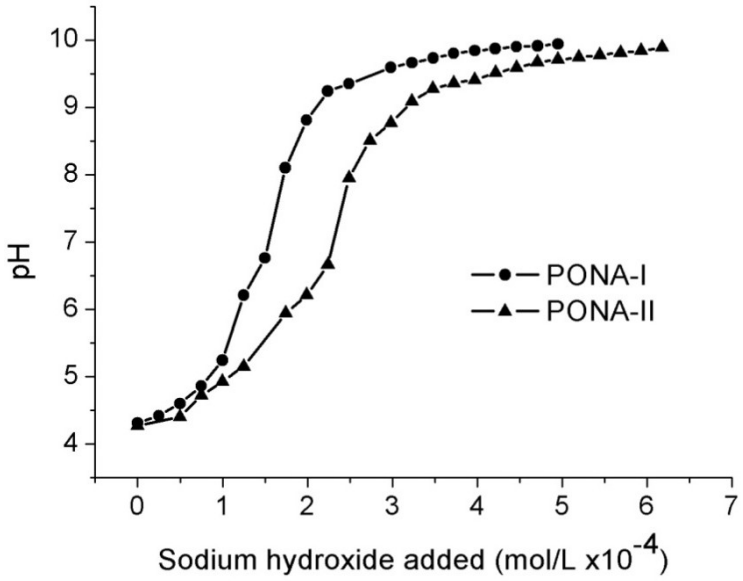

Figure 2.9. Titration curves for PO(N/A7) (●) and PO(N/A11) (▲) when titrated against 0.05 M sodium hydroxide solution

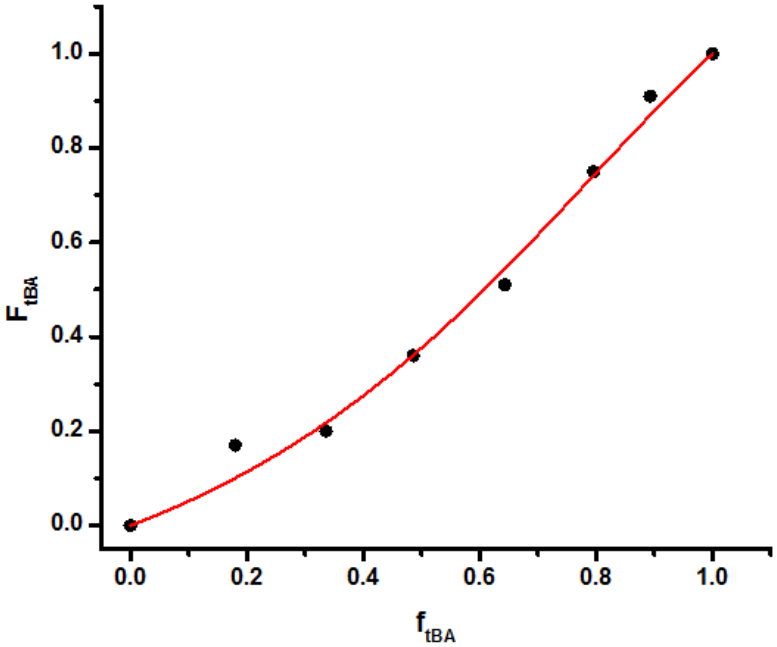

Figure 2.10. Plot of *t*BA composition in polymer (F_2) vs feed (f_2)

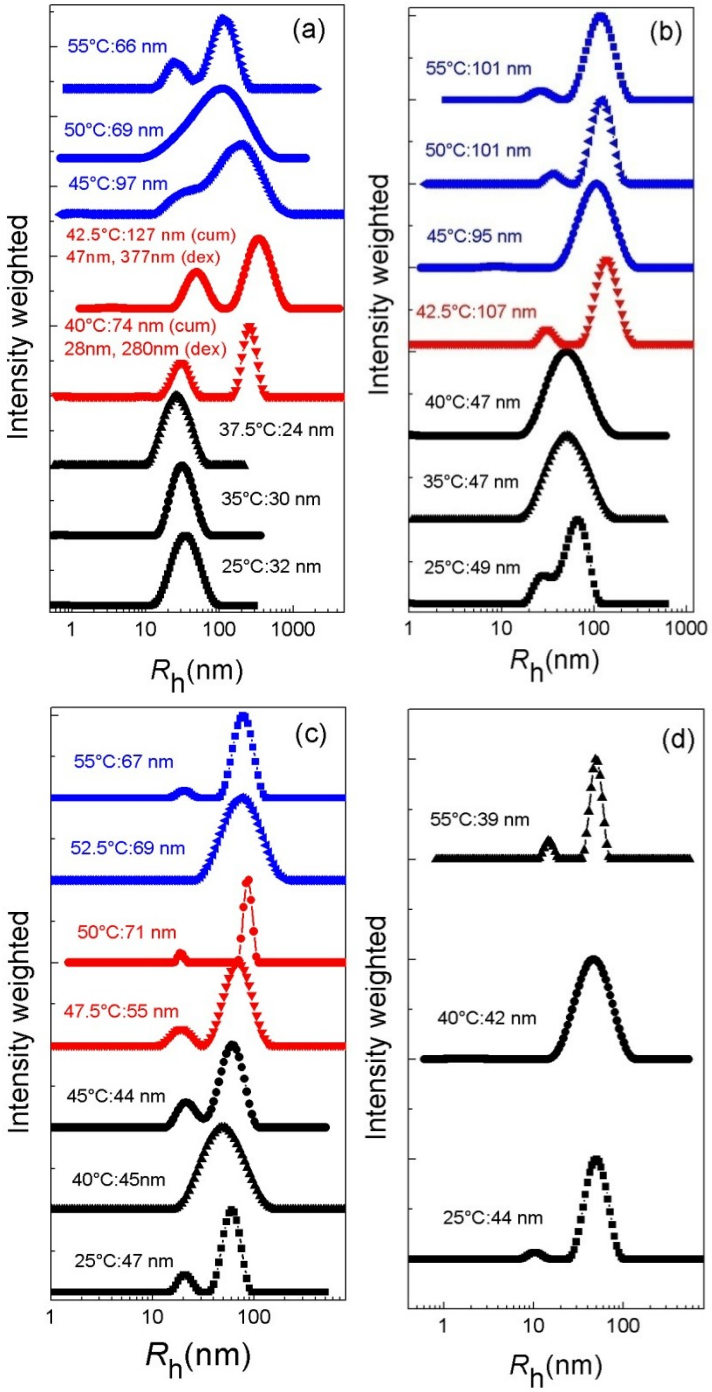

Figure 2.11. Micelle size (R_h) distribution as a function of temperature for PO(N/A7) micelles at (a) pH 2, (b) pH 4, (c) pH 6 and (d) pH 8, as determined by DLS at 90° (0.4 wt% polymer concentration) [(cum) and (dex) stand for R_h obtained by cumulant and double exponential fitting, respectively]

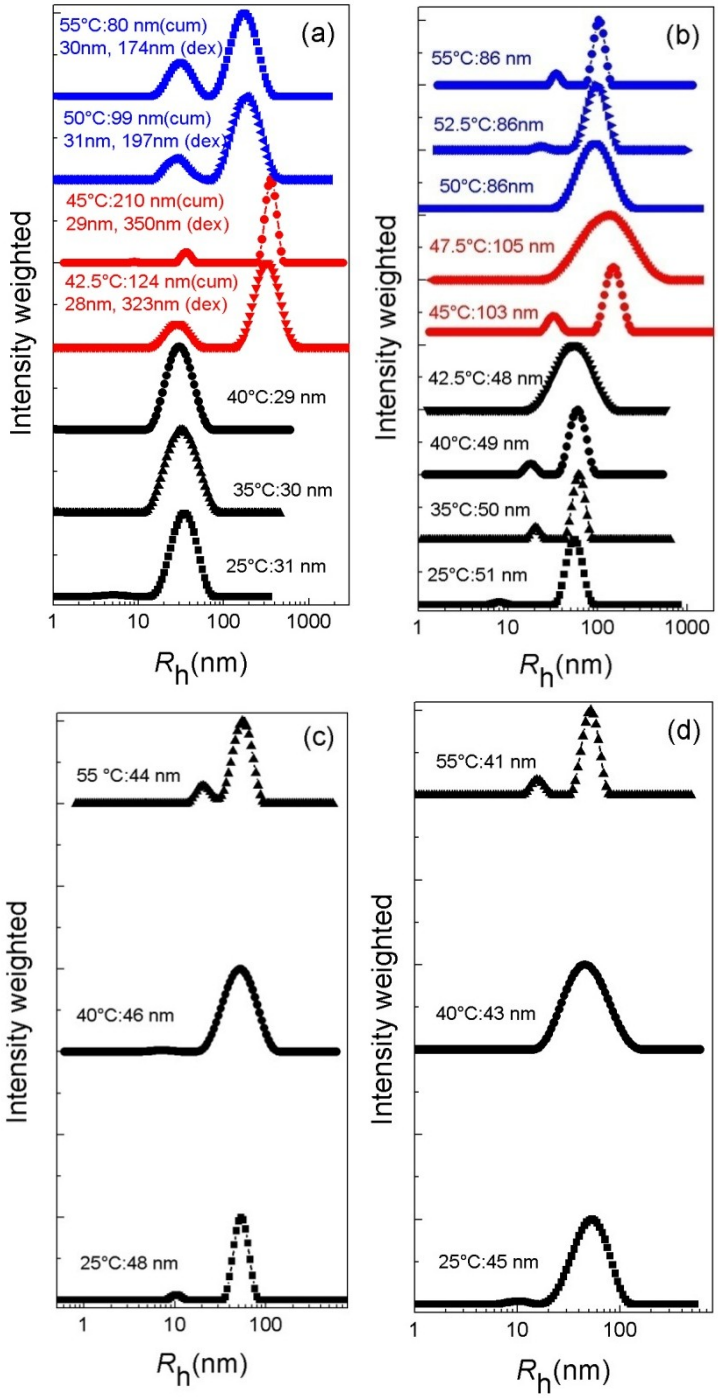

Figure 2.12. Micelle size (R_h) distribution as a function of temperature for PO(N/A11) micelles at (a) pH 2, (b) pH 4, (c) pH 6 and (d) pH 8, as determined by DLS at 90° (0.4 wt% polymer concentration) [(cum) and (dex) stand for R_h obtained by cumulant and double exponential fitting, respectively]

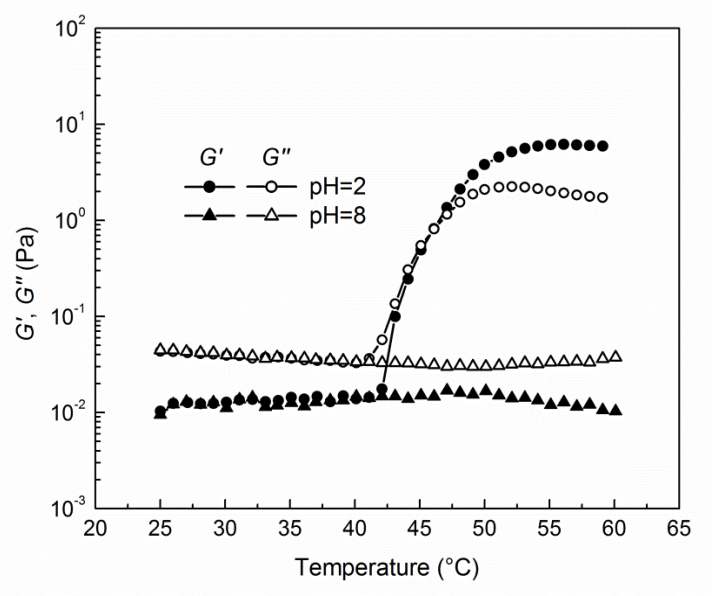

Figure 2.13. Temperature dependent dynamic shear moduli (G' and G'') for 4 wt% PO(N/A7) in buffered aqueous solutions at ω=10 rad/s and heating rate 1 °C/min. The pH 2 solution was measured at strain amplitude γ=50% at low temperatures (below gel point) and γ=2% at high temperatures (above gel point). The pH 8 solution was measured at γ=50%.

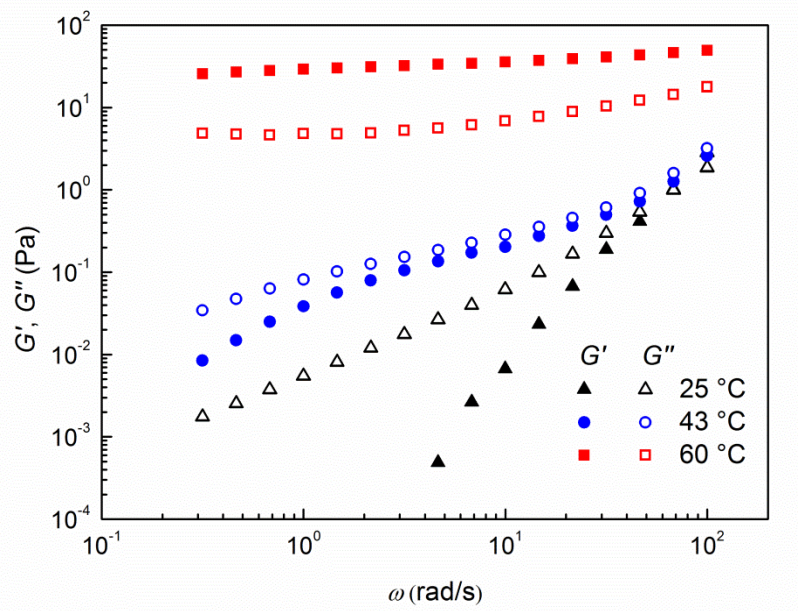

Figure 2.14. Dynamic shear moduli (G' and G'') as a function of frequency for 4 wt% PO(N/A11) in pH 2 buffered aqueous solutions measured at indicated temperatures.

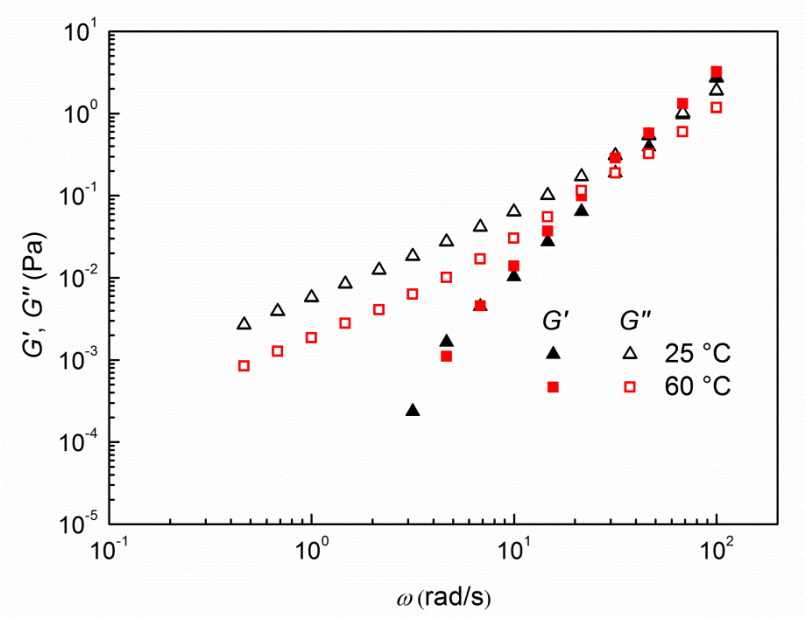

Figure 2.15. Dynamic shear moduli (G' and G'') as a function of frequency for 4 wt% PO(N/A11) in pH 8 buffered aqueous solutions measured at indicated temperatures.

Chapter III

Synthesis and Characterization of Stimuli-Responsive Triblock Polymers*

3.1 Extract

Temperature- and pH-sensitive ABC triblock polymers were prepared and studied for stimuli sensitive micellization and aggregation. The flanking A and C blocks contained N-isopropylacrylamide (NIPAm) and diethylacrylamide (DEAm), respectively, while the B block consisted of a random copolymer of NIPAAm and acrylic acid (AA). The polymer was prepared by reversible addition fragmentation chain transfer (RAFT) polymerization. RAFT synthesis was performed in three successive steps to form A, AB and finally an ABC triblock. BA and BC diblocks were also synthesized. Each block was fully analyzed by MALDI (matrix-assisted laser desorption ionization/mass spectrometry) and ^{1}H-NMR techniques in terms of monomer conversion, MW, PDI and composition. The final triblock's MW was 43,000 Da with narrow chain length distribution (PDI < 1.1), characterized by a high monomer conversion ratio (> 90%) and a controlled AA percentage (5 and 10%). Investigation of the triblock's behavior as a function of the pH and temperature was performed by turbidity and DLS measurements.

---

* This chapter describes results obtained from a collaborative research project performed with Marie Gaumet, a former postdoctoral research associate, who is now working at TRB Chemedica International SA (Geneva, Switzerland).

As expected, such a polymer showed thermo- and pH-sensitivity in aqueous solution. ABC cloud points observed at pH 2, 4, 6, 8 and 10 were 27°C, 27°C, 39°C, 43°C and 42°C, respectively. Furthermore, micelle formation was evidenced above the cloud points, mainly at pH 10 in case of AB and BC diblocks.

3.2. Introduction

There is considerable interest in preparing hydrogels based on environmentally sensitive polymers. Such membranes alter their swelling, partitioning, and permeability properties with changes in external conditions such as temperature, pH, ionic strength, and composition of specific solutes [170-176]. In the present contribution we focus on pH-sensitive hydrogels, which can be used for on demand delivery of drugs, or when configured with an appropriate chemical or biochemical reacting system, they can deliver hormones in a either an open or closed loop manner [45, 177].

Conventional hydrogel membranes are typically prepared by crosslinking during polymerization. These membranes, however, may be mechanically weak due to structural nonuniformities, may retain toxic unreacted monomers and sol fraction, and are difficult to process after polymerization [13, 178, 179]. ABC triblock polymers, with hydrophobic and temperature responsive flanking A and C blocks and a pH-sensitive B block, could overcome these limitations, since preparing and purifying the block polymer is separate from processing it into a hydrogel membrane. The strategy explained in the present paper involves the self assembly of A and C microdomains that physically crosslink the polymer chains at body temperature. Swelling and shrinking of the membrane is modulated through the pH-sensitive B block.

Poly(N-isopropylacrylamide) (PNIPAm) was chosen as the A block because of its sharp lower critical solution transition (LCST) behavior in response to temperature changes, which is normally observed around 32-33°C [180-182]. Poly(diethylacrylamide) (PDEAAm), which has an LCST in the range of 28-33°C, was chosen as the C block. Other thermosensitive polymers, such as poly(N-vinylcaprolactam), were tested unsuccessfully and rejected, mainly due to synthesis difficulties.

The B block was formed by substituting acrylic acid, a pH-sensitive monomer, into a PNIPAm chain. Polyacrylic acid (PAA) is an ionizable polymer with a pKa of 4.7. Due to the presence of carboxyl groups, PAA gels exhibit pH dependent swelling, with lower swelling ratios at pHs below pKa ~5 and higher swelling ratios at higher pH values. The combination of AA and NIPAm should thus create a system responding to microenvironmental changes in both pH and temperature. PNIPAm-*b*-PAA diblocks have been fully explored for solution behavior as a function of pH, temperature and polymer composition [128, 132, 183]. Experiments [45] with poly(NIPAm-*co*-α-alkylacrylic acid) hydrogels showed that increasing the side chain length of the α-alkylacrylic acid comonomer enhances the overall hydrophobicity of the copolymer and directs the transition pH closer toward physiological pH. Thus, by modulating the AA content and by using AA derivatives, the solubility transition of the block copolymer can be set to a specific pH range. This would enable polymer self assembly at pH values of interest.

The recent development of living/controlled free radical polymerization methodologies, including reversible addition-fragmentation chain transfer (RAFT) polymerization, permits synthesis of linear block polymers with precisely controlled molecular weight (MW) and monomer assembly. For the present work, RAFT was selected due to its applicability to a wide range of monomers and its efficiency in yielding low polydispersity polymers [83, 184, 185], well defined micelle formation, and sharp solubility transitions. The present paper reports the synthesis and characterization of a new ABC triblock polymer and the study of its behavior in aqueous solution as a function of environmental conditions, pH and temperature.

3.3. Experimental Section

3.3.1. Materials

NIPAAm (Polysciences Inc.) was recrystallized from a mixture of toluene and hexane and dried under vacuum overnight prior to use. Acrylic acid (Sigma-Aldrich) was distilled under reduced pressure in order to remove the polymerization inhibitor. DEAAm (Polysciences Inc.) was used as received. The initiator (2RS, 2'RS)-azobis(4-methoxy-2,4-dimethylvaleronitrile) (V-70: Wako Chemicals USA, Inc.), and the solvent N,N-dimethylformamide (DMF: Sigma-Aldrich) (99.9%) were used as received. Industrial grade argon was used. The trithiocarbonate based RAFT chain transfer agent, 2-dodecylsulfanylthiocarbonylsulfonyl-2-methylpropionic acid (DMP), was synthesized and purified according to the method reported by Lai [140]. In this procedure, 1-dodecanethiol, acetone and tricaprylylmethylammonium chloride were used as starting

materials. All chemicals were purchased from Sigma-Aldrich, unless otherwise noted, and used as received. Water was purified with a Millipore MilliQ® system.

3.3.2. ABC triblock copolymer synthesis

Scheme 3.1. Polymer synthesis

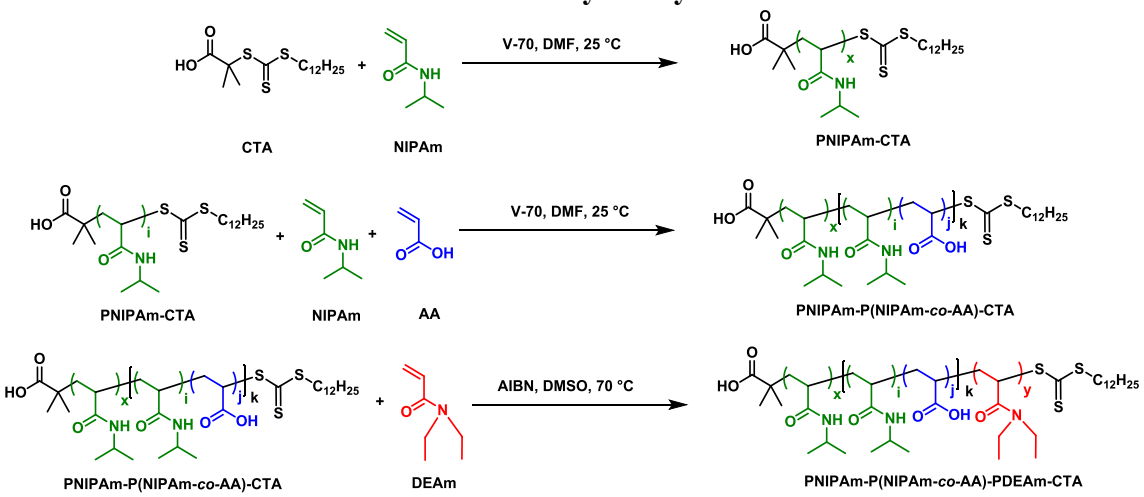

Polymers were synthesized by RAFT polymerization. In a typical procedure, an O-ring sealed vial was charged with NIPAm (2.2632 g, 0.02 mol), DMP (72.92 mg, 0.2 mol), and DMF (4.8 mL). The initiator V-70 was added according to a specific $[DMP]_0/[V\text{-}70]_0$ ratio. Ratios of [DMP]/[NIPAm] and [DMP]/[V-70] were optimized at 1:100 and 5:1 (mol:mol), respectively. The mixture was degassed by three cycles of freeze-pump-thaw [186]. Polymerization was carried out at room temperature under argon for 24 hours, and was quenched by exposure to air. An aliquot was extracted and stored in a freezer prior to NMR analysis. The rest of the product was precipitated in a large excess of ethyl ether, collected onto a glass filter, and exposed to vacuum overnight. The solid PNIPAm-CTA obtained (A block) was then dissolved and used as a macro chain transfer agent, and subsequently extended with additional NIPAAm and AA

monomers, under identical synthetic conditions to those described previously, to yield AB diblock polymers consisting of PNIPAm-P(NIPAm-*co*-AA)-CTA (PN(N/A)-CTA). A single P(NIPAm-*co*-AA) B block was also synthesized.

A final RAFT polymerization with DEAAm completed the triblock (Scheme 3.1). Conditions applied to form the C block were the following. The solid PN(N/A)-CTA, used as macro chain transfer agent, was dissolved in DMSO with AIBN as initiator and DEAAm monomers, in an O-ring sealed vial and degassed by three cycles of freeze-pump-thaw, then warmed up to 70°C under argon. Polymerization proceeded for 24 hours, yielding the ABC triblock consisting of PNIPAm-P(NIPAm-co-AA)-PDEAm-CTA (PN(N/A)D-CTA). Unreacted monomer was washed off with acetone and the polymer was further purified by precipitating in ether. Ratios of [AB diblock]/[DEAAm] and [AB diblock]/[AIBN] were optimized at 1:100 and 5:1 (mol:mol), respectively. The BA diblock P(N/A)N was synthesized in a similar manner wherein the P(N/A) diblock (~ 20 kDa) was first synthesized. For synthesis of P(N/A)N, a ratio of [P(N/A)]:[NIPAm] of 1:100 (mol:mol) was used. The macroCTA:[AIBN] ratio was kept the same as for the other polymerizations at 5:1. The BC diblock was synthesized in the same manner using a [P(N/A)]:[DEAm] ratio of 1:100.

In the present report, polymer blocks are designated A, B or C. Where necessary, a number indicates the percentage of AA used for the B block preparation. For instance, B10 stands for a B block containing 10% of AA (mole%).

3.3.3. Homopolymer and block polymer characterization

3.3.3.1. Molecular weight (M_n, M_w)*, Polydispersity index (*PDI*)*

MALDI-TOF (Matrix-Assisted Laser Desorption Ionization-Time Of Flight) mass spectrometry was performed on a Bruker Reflex III spectrometer equipped with a 337 nm N_2 laser. Data were processed with Matlab® software to determine molecular weight (M_n, M_w) and PDI (see Supporting Information). Samples were prepared from a THF solution by mixing the matrix (2,5-dihydroxybenzoic acid, 20 mg/ml), salt (sodium trifluoroacetate, 10 mg/ml) and sample (10mg/ml) in a ratio of 10:1:1[187, 188]. Samples were analyzed in linear or reflection modes, depending on their MW range.

3.3.3.2. Monomer conversion

Degrees of conversion of monomers to polymer and copolymer composition were determined by ^{1}H-NMR analysis (Advance 400 MHz NMR spectrometer, Bruker) in deuterated chloroform. Regarding NIPAm conversion, quartets around 5.6, 6.1, and 6.2 ppm, associated with vinylic protons, were chosen to mark the monomer, while the single peak around 4 ppm, associated with the methine proton in the isopropyl group, was chosen to label the monomer plus polymer. Average integrals of the three quartets and of the single peak around 4 ppm were used to calculate conversion (Supporting Information, Figure 3.8). DEAm conversion was determined by average integrals of the vinylic protons (quartets around 5.7, 6.4 and 6.6 ppm) only present in the monomer, and of the –CH_2 peak at 3.4 ppm occurring for monomer and polymer as well.

3.3.3.3. Acrylic acid percentage

pH titration was used to determine composition of NIPAm and AA in the copolymers. AA monomers incorporated in the copolymers were quantified by acid-base titration, using a Brinkmann Metrohm 719s Titrino®. B block samples at concentration 1 mg/mL were titrated against 0.05 M NaOH at room temperature. The amount of AA monomer incorporated in the copolymer was determined from the inflection point of the titration curve (Supporting Information, Figure 3.9).

3.3.4. Thermo- and pH-Sensitivity Study

3.3.4.1. Cloud Point (CP) determination

Thermal behaviors of the individual blocks A, B and C, and their di- and triblocks were investigated by UV spectrophotometry using a Perkin Elmer Bio40 UV-Vis spectrometer (λ=542 nm) equipped with a sample cell that was thermostated in a circulator bath. Absorbance by aqueous polymer solutions was assessed at λ=500 nm and recorded over a temperature ramp from 20°C to 80°C. The experimental conditions were first optimized by testing polymer concentrations from 0.2 mg/mL to 20 mg/mL and rates of temperature increase from 0.06°C/min to 1°C/min. The cloud point (CP) of a polymeric solution was defined as, the onset of increase in optical absorbance, or decrease in transmittance [189, 190].

3.3.4.2. Aggregate and micelle diameters

A ZetaPlus dynamic light scattering detector (Brookhaven Instruments Corporation, 27 mW laser, 658 nm incident beam, 90° scattering angle), equipped with a temperature control device, was used to study micellation and aggregation behavior of

AB diblock copolymers. AB diblock copolymer samples were prepared with concentration 0.2 mg/mL in basic and acidic aqueous solutions. Measurements were performed at temperatures from 20-50°C, waiting 20 min for temperature stabilization at each point, and were analyzed using Zetaplus® particle sizing software.

3.4. Results

3.4.1. Molecular weight (M_n, M_w), Polydispersity index (PDI)

By optimizing the RAFT polymerization conditions, A, B, C, AB, BA, BC and ABC polymers were obtained. As shown in Table 3.1, individual blocks and their combinations were of low polydispersity (PDI<1.1). In the case of homopolymers, MALDI-TOF mass spectrometry led to one narrow peak near 10,000 Da for A and C blocks and primary narrow peaks near 30,000 Da and 40,000 Da for AB and ABC di- and triblocks, respectively. In the case of copolymers, the presence of AA, which is ionizable, led to the presence of a couple of smaller peaks attributed to doubly and triply charged polymers. A higher molecular weight peak was also observed and is speculated to result from chain association (Supporting Information, Figure 3.7).

3.4.2. Monomer conversion

Degrees of conversion (24 hours synthesis of each block) estimated from ^{1}H-NMR analysis of the polymerization medium, were above 90% for all polymerized monomers (Table I and Supporting Information, Figure 3.8).

Table 3.1. Molecular weight, polydispersity and monomer conversion of the polymeric blocks

Sample	Polymer composition	Molecular weight (M_n) expected* (Da)	Molecular weight obtained (Da)		
			M_n	M_w	PDI
A	PNIPAm, (PN)	11,000	10,000	10,200	1.02
B2	P(NIPAm-*co*-AA), P(N/A2)	25,000	24,000	25,000	1.05
B5	P(N/A5)	25,000	23,000	24,000	1.05
B10	P(N/A10)	25,000	24,000	24,000	1.01
B15	P(N/A15)	25,000	24,000	25,000	1.03
C	PDEAm (PD)	12,000	11,000	12,000	1.06
AB(5)	PN-P(N/A5)	31,000	32,000	33,000	1.02
AB(10)	PN(N/A10)	30,000	28,000	29,000	1.03
B(10)A	P(N/A10)N	31,000	27,000	28,000	1.02
B(10)C	P(N/A10)D	30,000	30,000	32,000	1.06
AB(5)C	PN(N/A5)D	46,000	42,000	44,000	1.04
AB(10)C triblock	PN(N/A10)D	39,000	36,000	37,000	1.04

* Assuming 100% conversion**,** the number in brackets indicates acrylic acid % in the P(NIPAm-co-AA) block

3.4.3. Acrylic acid percentage

Compositions of samples with different AA mol% in the feed are listed in Table 3.2. Mol fractions of AA in the polymer samples were determined by acid-base titration (see Supporting Information, Figure 3.9). Polymer AA compositions were similar to the feed

compositions, as should be expected since polymerizations were carried out to near completion. The AA content estimated in polymers P(N/A2) and P(N/A5) was greater than the AA feed composition. This may be due to the CTA-derived free acid group at the polymer chain end. At low AA compositions, the CTA –COOH may result in a significant contribution towards the estimation of acid groups. Since NIPAm and AA have significantly different reactivity ratios, a gradient in composition is expected for NIPAm-AA copolymers run to high conversions.

Table 3.2. Acrylic acid content in B block

Sample	Feed AA composition (mol%)	Polymer AA composition[a] (mol%)
P(N/A2)	2	2.6
P(N/A5)	5	5.5
P(N/A10)	10	8.9
P(N/A15)	15	13.7

[a] Acrylic acid composition in the polymer determined by potentiometric titration.

3.4.4. Cloud Point (CP) Determination

3.4.4.1. Optimization of experimental conditions

Cloud points are known to be sensitive to polymer concentration and to the temperature ramp rate. As shown in the Figures 3.1a and b, this statement holds true for the p(NIPAm-*co*-AA) B block. In dilute polymer solution, a fivefold concentration change (0.2 mg/mL to 1 mg/mL), resulted in a change in CP of up to 8°C whereas no large difference was noticed between concentrations from 1 to 20 mg/mL. A change in temperature ramp rate from 0.06°C/min to 1°C/min led to a CP change of up to 10.6 °C.

In subsequent experiments, the polymer concentration was chosen to be 0.2 mg/mL and the temperature ramp rate was the lowest possible in the device, which was 0.06°C/min.

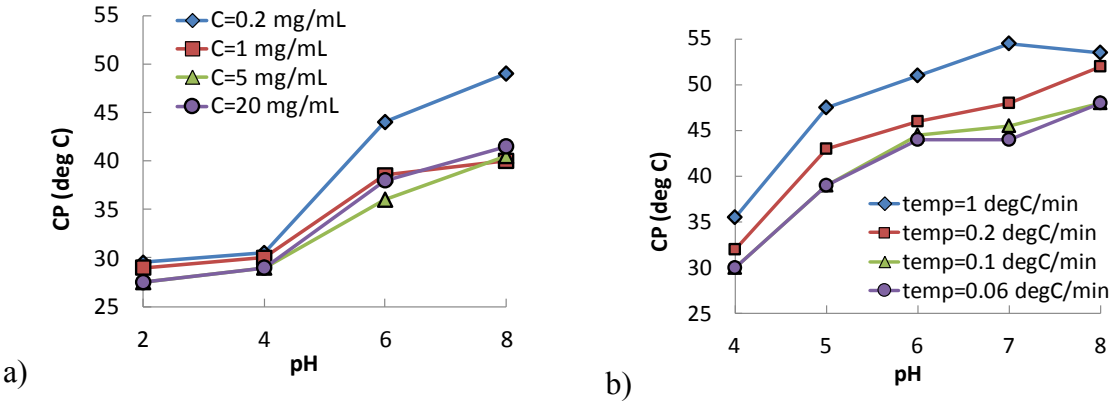

a) b)

Figure 3.1. Influence of polymer concentration (a) and temperature increase rate (b) on cloud point. Experiments performed on AB10 diblock. (C=0.2 mg/mL in b).

3.4.4.2. Study the A, B and C blocks

Cloud points of the A, B and C blocks were studied separately. As shown in Fig 3.2., the A and C blocks exhibited well defined CPs along the pH range at which the data were collected. PNIPAm and PDEAm are well studied polymers that exhibited cloud points in the range of 30-33 °C, in agreement with literature values [103, 182, 191, 192].

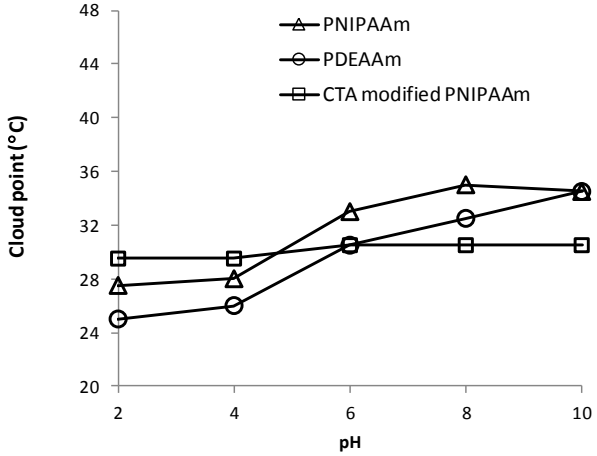

Figure 3.2. Cloud points of PNIPAAm and PDEAAm as a function of pH

Cloud points were typically lower for PDEAm compared to PNIPAm, reflecting the greater hydrophobicity of PDEAm. Unexpectedly, a slight but noticeable increasing trend in pH dependence was observed here for PNIPAm and PDEAm, as shown in Figure 3.2.

The rise in CP with pH was speculated to be due to the RAFT CTA attached to the end of the polymers. Following RAFT synthesis, the polymer is end capped by the CTA groups, the COOH group on one end and the trithiocarbonate dodecyl group on the other. The free carboxylic acid end group may lead to pH effects [141]. To test this hypothesis, the free acid end group was modified into a non-ionizable amide using 1-ethyl-3-(-3-dimethylaminopropyl) carbodiimide (EDC) crosslinker chemistry. UV-Vis measurements performed on the modified polymer exhibited a cloud point of ~30 °C, irrespective of pH, as shown in Figure 3.2 for CTA-modified PNIPAm. This confirms that the observed pH sensitivity for PNIPAm and PDEAm homopolymers is a result of the CTA-derived free carboxylic acid present at the end of the polymer chains. It also is a likely explanation of the apparent excess in AA incorporation in the B copolymer at low substitutions reported in Table 3.2.

Solution behavior of the B block, P(N/A)-CTA, was also studied as a function of temperature, pH and AA content (Figure 3.3). Polymer solutions were set to varying degrees of AA ionization, α by addition of proper amounts of base (See Supporting Information), and transmittance of the solutions was measured over the range 25-50 °C.

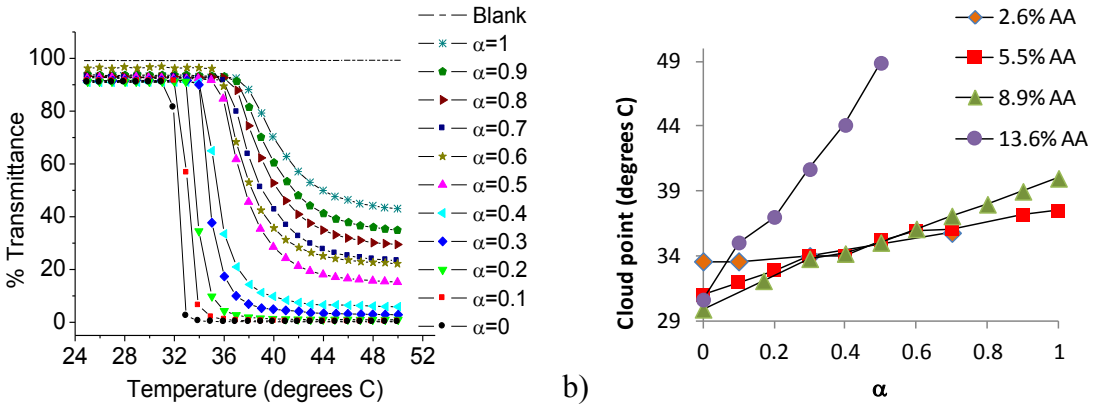

Figure 3.3. Cloud point determination of B block (a) Transmittance vs temperature curve for poly(NIPAm-*co*-AA) containing 5.5% AA at different degrees of ionization (α). (b) Cloud points of P(NIPAm-*co*-AA) as a function of degree of AA ionization (α) (See Supporting Information). CP defined as the onset temperature of decrease in transmittance (temperature at which transmittance drops to 90% of original value)

As shown in Figure 3.3a for the B5 polymer containing 5.5% AA, P(N/A5), transmittance decreased upon heating, with a rather sharp onset. The temperature at which transmittance dropped to 90% was used to define CP. Also, in agreement with literature reports [127], CP increased with increasing amounts of AA ionization (α). In Figure 3.3b, the CPs for B blocks with 2.6% to 13.7% AA are plotted at different degrees of ionization, α, which were set by varying pH. P(NIPAm-co-AA) containing 2.6% AA, P(N/A2), exhibited a cloud point of 33.5 °C at 0% ionization. At 70% ionization, CP shifted to 36 °C. At 13.7% AA substitution, CP was 30.7 °C at 0% ionization and 49 °C at 50% ionization. Thus, the pH dependence of B block CP became steeper with increasing AA substitution. Polymers containing higher amounts of AA displayed stronger pH dependence.

In the fully protonated state, i.e. at 0% ionization, there was a reversal in pH dependence of CP in the B blocks. At 0% ionization, the CP the B polymer containing

2.6% AA [P(N/A2)] was 33.5 °C, close to the LCST of PNIPAAm homopolymer, 32 °C. At low pH, increasing AA substitution caused a reduction in the CP values. For polymers containing 5.5% AA and 8.9% AA, (P(N/A5) and P(N/A10) respectively, the CPs reduced to 31.0 and 29.9 °C. However, at 13.7% AA substitution [P(N/A15)], CP increasesd slightly to 30.7 °C.

3.4.4.3. Study of the AB, BC and BA diblocks

Cloud points were estimated for AB, BC and BA diblocks as a function of temperature and pH (SI, Figure 3.10). The diblocks demonstrated two types of thermoresponsive behaviors, as shown in Figure 3.4.

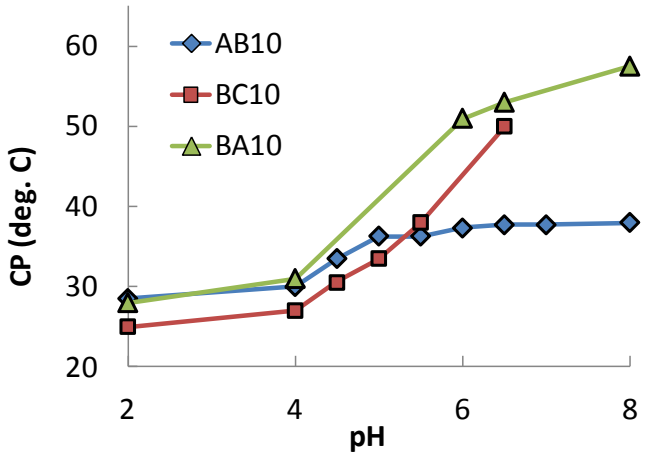

Figure 3.4. Diblock cloud point determination as a function of pH

First, AB10, i.e. PN(N/A10), exhibited well defined CPs for each pH tested, namely 28.7°C, 30.0°C, 38.2°C and 39.8°C for pH 2, pH 4, pH 6 and pH 8, respectively. This confirms the increase in solubility of the AB diblock, due to ionization of AA units, with increase in pH and therefore CP elevation (>10°C) at high pH. The BC [P(N/A10)D] and BA [P(N/A10)N] diblocks displayed similar dependence of CP on temperature at low pH

but became more soluble on increasing pH. At pH 2, CP was at 24.9 °C for BC and 28.3 °C for BA. With increasing pH, the CPs reached 50.0°C at pH 5.5 for BC, and 58.3°C at pH 6 for BA, before becoming essentially undetectable above pH 6. At most pH values tested, the CPs were slightly lower for BC [P(N/A10)D] than for BA [P(N/A10)N] due to the presence of PDEAm, which was expected since PDEAm has a lower LCST than PNIPAM.

3.4.4.4. Study of the ABC triblock

Cloud point measurements were performed on ABC [PN(N/A)D] triblocks with 5 and 10% AA (Figure 3.5 and Supporting Information, Figure 3.11).

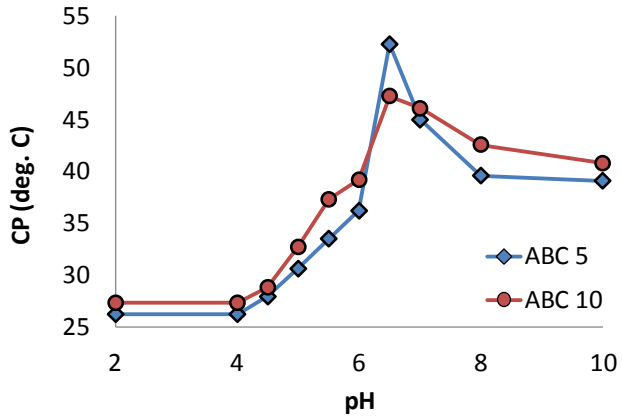

Figure 3.5. Cloud point determination as a function of pH for ABC5 and ABC10

As expected, the more AA present in the B block, the higher the cloud point, although there was a reversal at pH 6.5, where CPs were maximal. The cloud points for AB(5)C [PN(N/A5)D] and AB(10)C [PN(N/A10)D] began at pH 2 at 26.9°C and 27.3°C, finished at 39.4°C and 41.5°C at pH 10, respectively.

a) 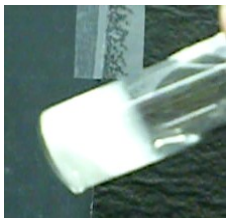 b) 

Figure 3.6. ABC (10wt%) solutions when heated to 40 °C at a) pH 4.5 and b) pH 7.4

To test for gelation, 10 wt% solutions of AB(10)C were heated to 40 °C and observed for visual signs of aggregation/gelation. At pH 4.5, the polymer phase separated out of solution to form a gel as shown in Figure 3.6a. At pH 7.4, the polymer formed a viscous solution upon heating (Figure 3.6b) but there was no sign of gelation. These results are consistent with the cloud point results since 40 °C is decidedly larger than the CP at pH 4.5, but lies below the CP at pH 7.4, which is close to 40 °C.

3.4.5. Aggregate and micelle diameters

DLS measurements on the A block revealed a multimodal size distribution upon heating. At 40°C, pH 2, small aggregates around 79 nm and large aggregates of 2–8 μm were observed. DLS studies were also carried out to study the behavior of AB and BC diblock polymers at high pH, where the B block was highly ionized. At pH 10, the AB(10) and BC(10) diblocks were in solution at room temperature. Upon heating, the mean diameter of AB diblock in solution was 90 nm at 40 °C. On heating further to 50 °C, a bimodal size distribution was observed with particle diameters of 83 nm and 575 nm (see Figure 3.12 in Supporting Information). The BC [P(N/A)D] diblock on the other hand exhibited slightly different solution behavior at elevated temperatures. At 40 °C, the

BC diblock measured 65 nm in diameter while at 50 °C, the mean size dropped down to 48 nm (Supporting Information Figure 3.13).

3.5. Discussion

In the present work, PNIPAm and PDEAm based polymers were synthesized by RAFT polymerization. The final triblock ABC as well as the intermediate blocks exhibited M_n values very close to expected, with narrow chain length distributions (Table 3.1). The reproducibility from batch to batch was very good, with a standard deviation <4% (n=3). Furthermore, the high monomer conversion (>90%) confirmed the success of the polymerization process applied to NIPAm, AA and DEAm. Regarding the copolymerization of NIPAm and AA, conversion data are in agreement with literature [193]. Content analysis by pH-titration showed that AA incorporation within the B block was nearly complete.

The blocks based on NIPAAm-AA copolymers: B, AB, BA, BC and ABC (Figure 3.2-3.5) exhibited both temperature and pH response, as determined by turbidity experiments. Because of the LCST behavior of PNIPAm and PDEAm, the various block polymers also exhibited inverse phase solubility. Although there was slight pH sensitivity due to the CTA at the end of the homopolymer chains, much stronger pH dependence resulted from AA incoroporation in NIPAm. Starting in their protonated, unionized form at low pH, with increasing pH more of the AA units in the B block become ionized, conferring higher solubility to the copolymers.

The degree of AA substitution had a significant influence on the polymer CP both in the ionized and the unionized states. As previously demonstrated for P(NIPAm-co-

AA), cloud points increased with increasing AA substitution in the B blocks, when the AA groups were partially or fully ionized [45, 132]. Increased AA substitution resulted in greater density of ionizable groups along the polymer chains, which exerted repulsive electrostatic forces on neighboring charges, thus increasing polymer solubility. So, higher temperatures were needed for the polymer to precipitate out of solution. In the unionized state, an inversion in this trend was observed. Polymers with higher AA substitution displayed lower CPs, sometimes even lower than the CP for a PNIPAm homopolymer, probably due to H-bonding between NIPAm and AA when AA is present in the protonated state [132]. When acting alongside the existing hydrophobic interactions between NIPAm-derived isopropyl groups, such H-bonding facilitates phase separation of the polymer at lower temperatures.

In the case of diblocks, some interesting differences were observed in solution behavior depending on the block arrangement. The tremendous difference in behavior of AB solutions, compared to BA and BC solutions at pH above 5, may be due to a chain transfer agent (CTA) effect on the shrinking of the whole polymeric chain at pH > 5. The BA and BC diblocks share common architectural characteristics: a -COOH soluble moiety from the CTA at one end, followed by the pH sensitive B block and then the A or C thermo-sensitive block, and finally the $–C_{12}H_{25}$ hydrophobic moiety from the CTA.

As depicted in Scheme 3.2, in the case of BC [P(N/A)D] and BA [P(N/A)N], the -COOH moieties are positioned on the left side whereas the $–C_{12}H_{25}$ chains are on the right side, creating therefore only two distinct domains in terms of solubility, the predominant one being the B block which becomes more soluble by increasing pH.

Scheme 3.2. Schematic of proposed difference in micellar assembly behavior of AB vs BA and BC diblocks

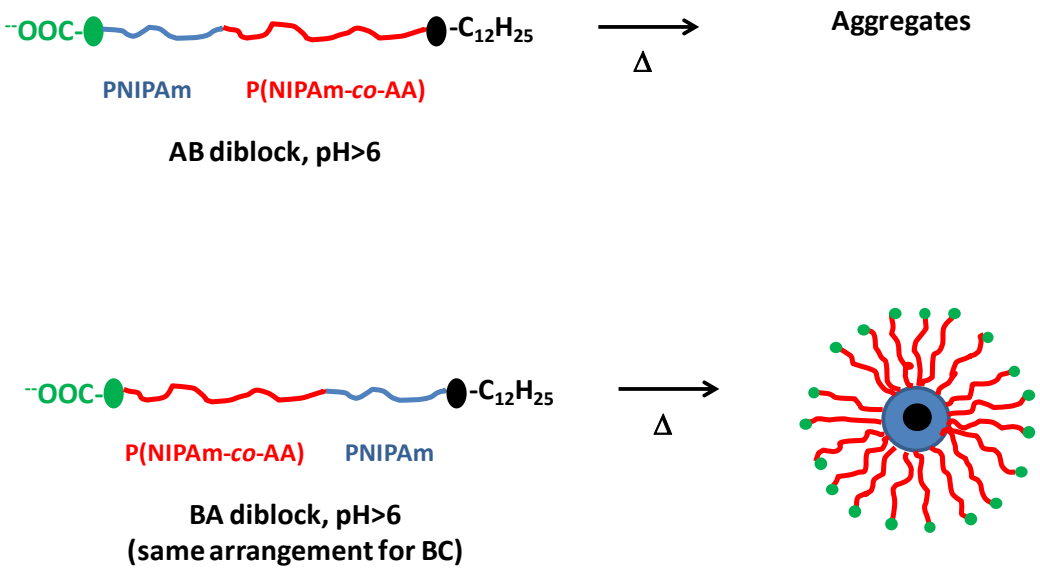

For AB diblocks, the structure is more complex and one can suppose that the alternating presence of the four hydrophilic/hydrophobic domains is more favorable to polymer precipitation over the temperature range studied. This could explain why, at high AA ionization, the AB cloud points are clearly defined whereas those of BC and BA could not be determined. The presence of the hydrophilic –COOH moieties in close proximity to AA units may help to stabilize the BA and BC micelles at high pH. Also worth speculating on is the effect of a likely gradient structure of the B block, arising from unequal reactivities of the comomomers. If present, the acidic monomers will be distributed differently in polymers with first *versus* second B blocks.

DLS studies also indicated greater stability of BC micelles as compared to AB. The AB diblock, at pH 10 formed micelles (90 nm) at 30 °C, comprised of a PNIPAm

core and a P(NIPAm-co-AA) corona. On heating, two subpopulations were observed at 83 and 575 nm (Supporting Information, Figure 3.12). The larger size indicated micellar aggregation with a fraction of the micelles remaining free in solution. The BC diblock exhibited smaller micelles at 40 °C measuring ~65 nm. The smaller micelle size for the BC diblock may be attributed to the more compatible arrangement of CTA hydrophobic and hydrophilic domains with the hydrophobic and hydrophilic domains of the polymer. On heating, the micelle size reduced to 48 nm, but no aggregation was observed. This could explain the absence of a defined CP for BC above pH 6.

Taken together, these results suggest that the better segregation of hydrophobic and hydrophilic domains in BC diblock, when the B block is ionized, leads to greater stabilization of BC micelles as compared to AB. The CTA-derived $–C_{12}H_{25}$ hydrophobic chain represents a significant part of the polymer in comparison to the A and C blocks, and its position relative to the polymeric hydrophobic and hydrophilic blocks can govern micellar aggregation. It should also be noted that the free micelle size in both AB and BC diblock solutions decreased upon heating. This indicates B chain shrinkage with increasing temperature. DLS experiments provide us with more information about particle size in solution than was afforded by UV spectroscopy. In addition to measurement of soluble to aggregate transition, it also provides an estimate of the size of the respective assemblies.

This study also demonstrates that the double sensitivity of the B block to pH and temperature in the ABC triblock system. As seen for the B block, the triblocks with greater AA incorporation, PN(N/A10)D, exhibit slightly higher CPs than PN(N/A5)D

(Figure 3.5). This trend highlights two opposing effects: on the one hand, hydrophobic interactions operating between the alkyl side chains of the outer PNIPAm and PDEAm drive polymer phase separation, and on the other, hydrophilic interactions due to ionization of AA units facilitate midblock solubility.

Aqueous solutions containing 10wt% of ABC triblock, when tested in vials, exhibited pH-dependent behavior. As shown in Figure 3.6, at pH 4.5 the polymer phase separated to form aggregates. Since a significant fraction of the AA units were protonated at pH 4.5, the B block phase separated out of solution along with the thermoresponsive A and C blocks leading to polymer aggregation. At pH 7.4, the polymer solution became turbid on heating but no phase separation was evident. In this case, turbidity may arise due to collapse of the thermoresponsive side blocks, but the hydrated B chains help maintain the polymer in solution.

In conclusion, RAFT polymerization was used to synthesize dual temperature and pH responsive ABC triblock copolymers with controlled architecture and MW distribution. Chemical structure and composition of these complex block polymers were characterized using MALDI and ^{1}H-NMR. Phase behavior of the block polymers in aqueous solution was characterized as a function of pH and temperature. The combination of PNIPAm, PDEAm and P(NIPAAm-co-AA) in a triblock polymer leads to a system that responds to both pH and temperature. One important and unexpected finding of the present work is the tremendous influence on phase behavior of the CTA used for RAFT polymerization.

3.6. Supporting Information

3.6.1. Molecular weight estimation

Molecular weights were estimated by MALDI mass spectrometry. Mass (m) vs frequency (n) data was obtained for each i-monomer long polymer chain. The number average molecular weight (M_n), the weight average molecular weight (M_w) and the polydispersity index ($Đ$) were calculated as follows:

$$M_n = \sum M_i n_i \Big/ \sum n_i \; ; \; M_w = \sum M_i^{\,2} n_i \Big/ \sum M_i n_i \text{ and } Đ = M_w / M_n$$

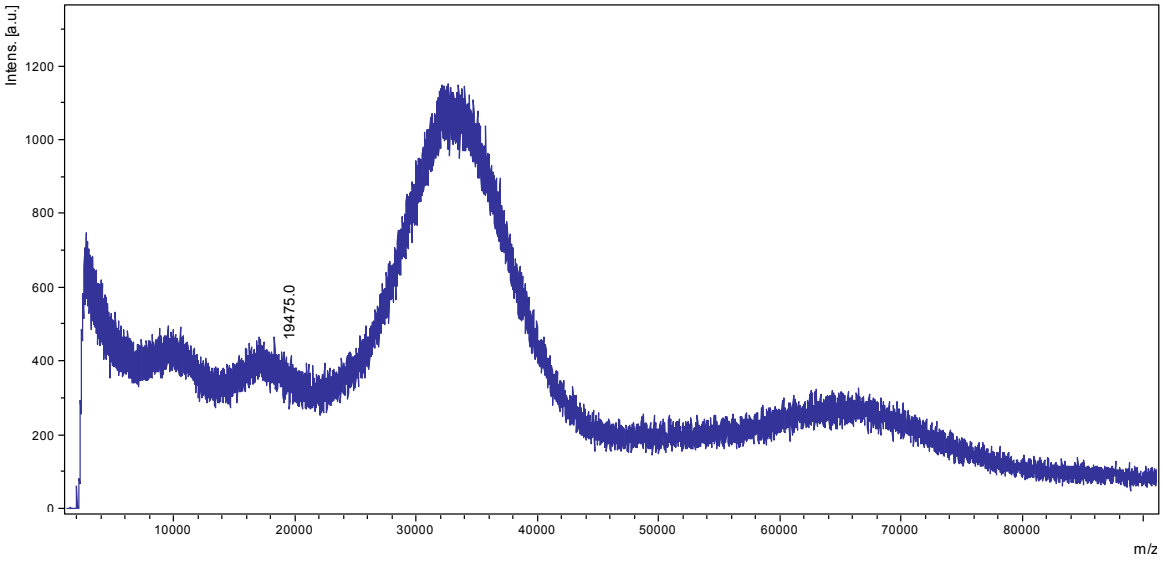

Figure 3.7. MALDI spectrum of AB diblock

Note: There were multiple peaks observed in MALDI spectra due to formation of dimers and multiply charged chains. This led to peak overlap due to which the baseline of the main peak could not be accurately determined. This may lead to error in determination of $Đ$. The principal peak from the MALDI spectrum was fitted to a Gaussian using the equation:

$$y = y_0 + \frac{A}{w\sqrt{\pi/2}} exp^{\frac{-2(x-x_c)^2}{w^2}}$$

Where y = intensity at a given molecular weight; y_0 = baseline offset; w = 2σ; x = molecular weight; x_c = mean molecular weight. From the intensity (y) vs molecular weight data (x), parameters y_0, σ and x_c can be calculated. Dispersity, *Đ*, is further calculated by using the equation:

$$Đ = 1 + \left(\frac{\sigma}{x_c}\right)^2$$

By comparing *Đ* estimates obtained using the two approaches, it was seen that although Gaussian fitting results in a slightly larger *Đ* estimate, it closely matches with the *Đ* value calculated using M_w/M_n.

3.6.2. Monomer conversion

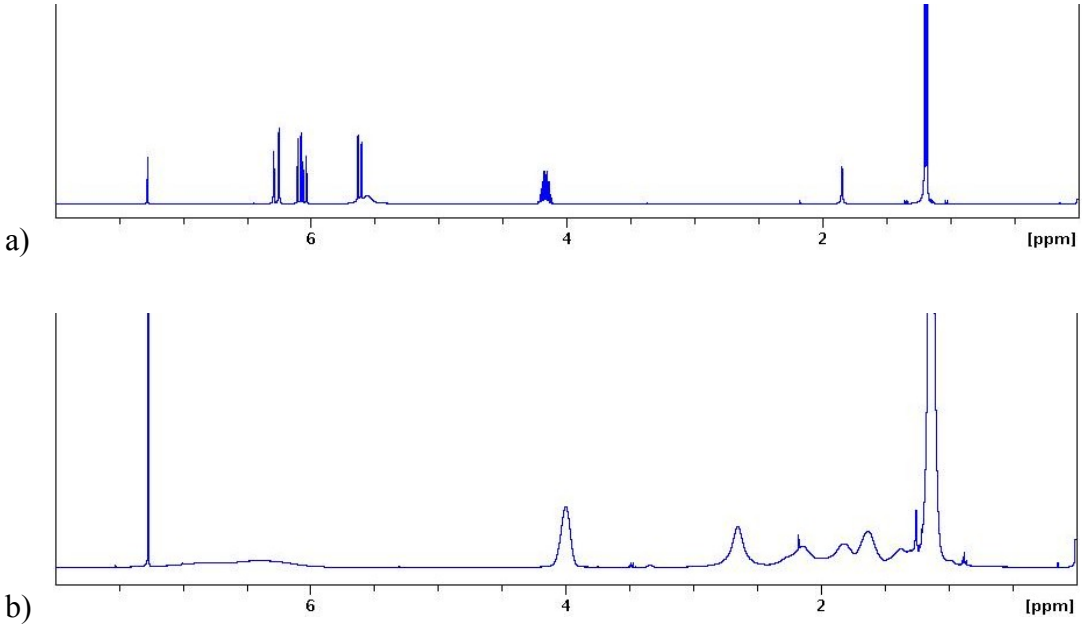

Figure 3.8. ^{1}H-NMR spectra a) before and b) after polymerization of NIPAAm in deuterated chloroform.

Monomer conversion calculated from the peak integrals of vinylic (=CH and =CH_2) (5.5-6.5 ppm) and methine (-CH) protons (~ 4 ppm). In Figure 3.8, the vinylic protons disappear after polymerization thus suggesting almost 100% conversion.

3.6.3. Determination of AA composition

AA content in the polymers was determined by acid-base titration. Polymer was dissolved in distilled water at a concentration of 1 mg/mL. The polymer solution was then titrated against 0.05 M NaOH. The inflection points of the titration curve were determined using CurTiPot software.

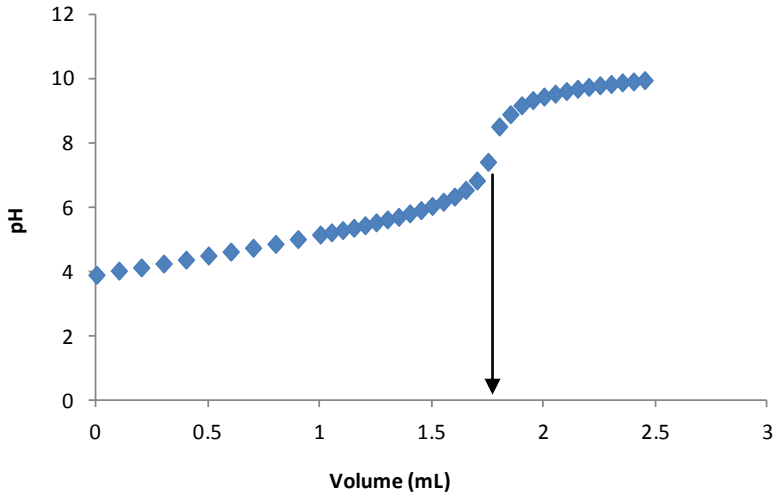

Figure 3.9. Titration curve of P(NIPAAm-co-AA) vs 0.05 N NaOH, arrow indicates inflection point

3.6.4. Degree of ionization (α)

Degree of ionization was calculated as follows:

$$\alpha = \frac{Moles\ of\ NaOH}{Moles\ of\ AA}$$

AA content of polymers was determined as described above. Aqueous polymer solutions

were then prepared, with known amount of polymer, and thus known amount of moles of AA. Calculated volume of 0.05 N NaOH, equivalent to the amount of acid (AA) in the sample was added to set the sample to a given degree of ionization.

3.6.5. Cloud point determination

Cloud points were determined using UV-Vis spectroscopy. Polymer solutions were gradually heated from 25-50 °C and transmittance was measured. Cloud point was defined as, the onset temperature of increase in absorbance, or decrease in transmittance.

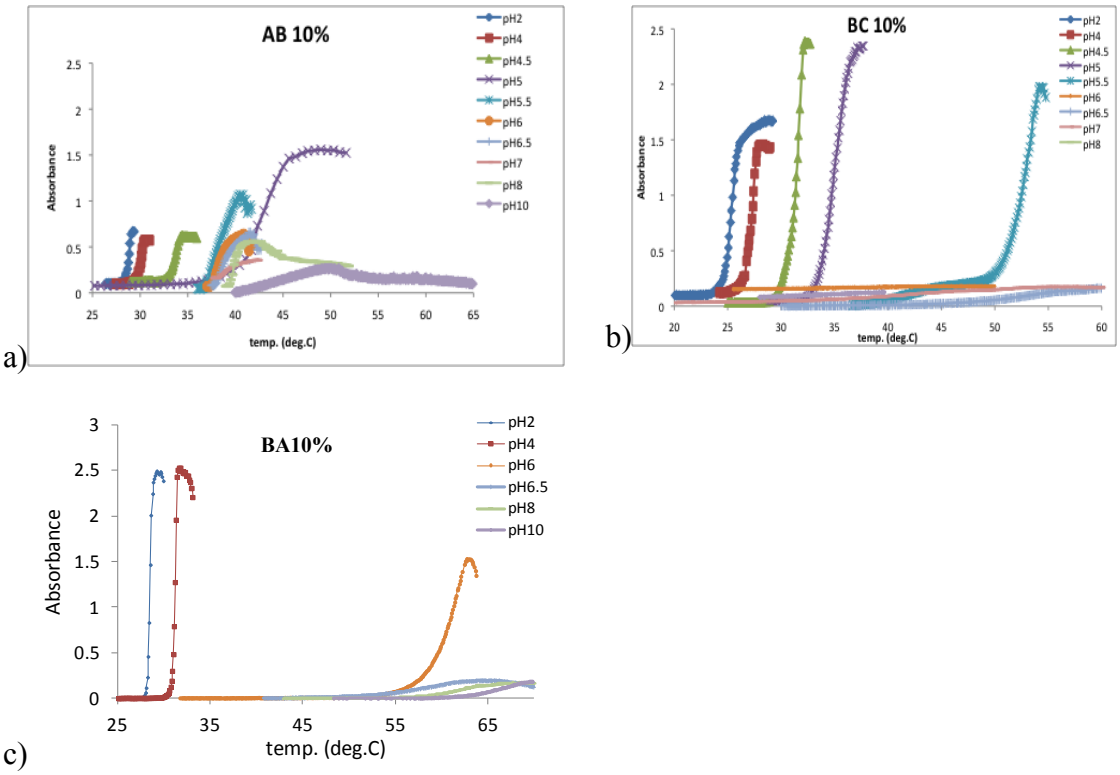

Figure 3.10. Absorbance curves for a) AB 10% , b) BC 10% and c) BA 10% diblock polymers as a function of temperature and pH

a)

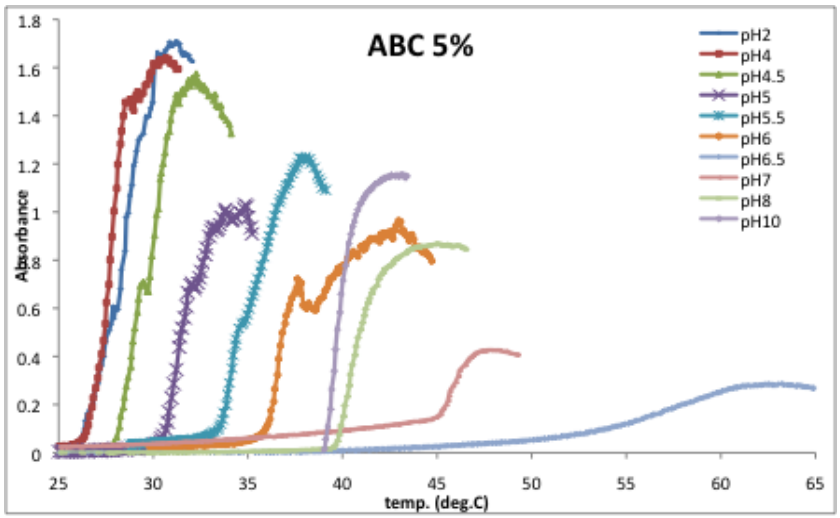

b)

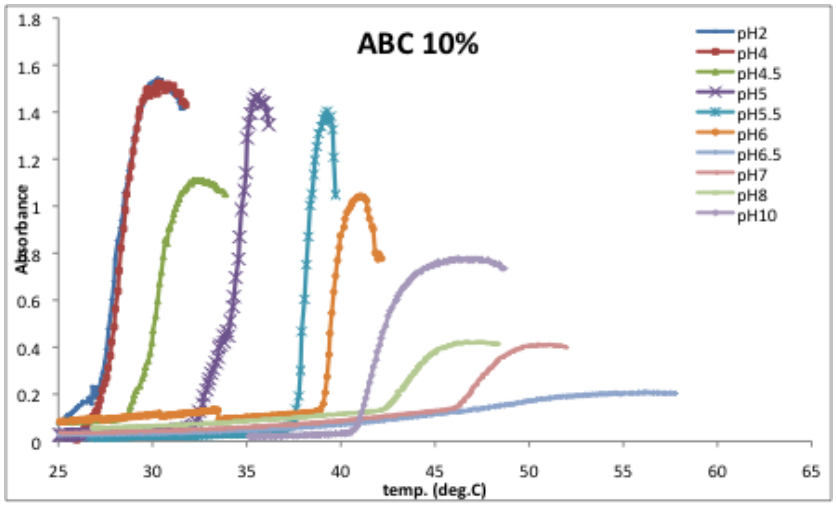

Figure 3.11. Absorbance curves for a) ABC 5% and b) ABC 10% triblock polymers as a function of temperature and pH

a)

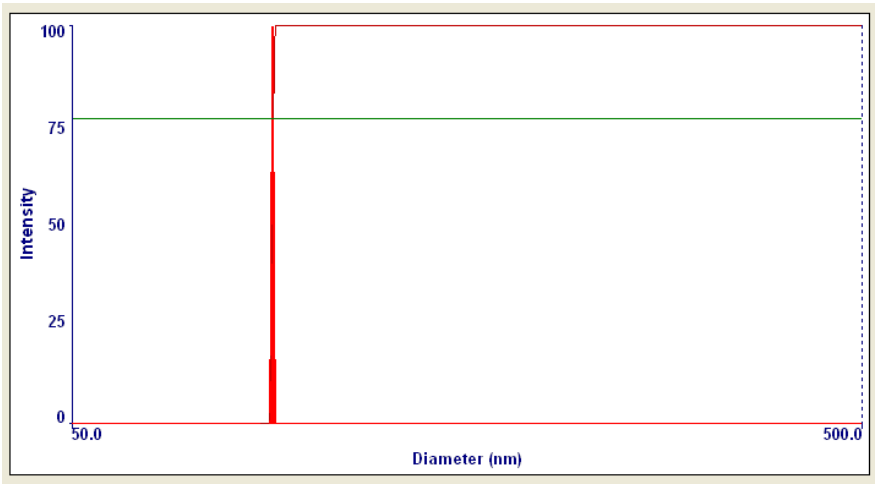

b)

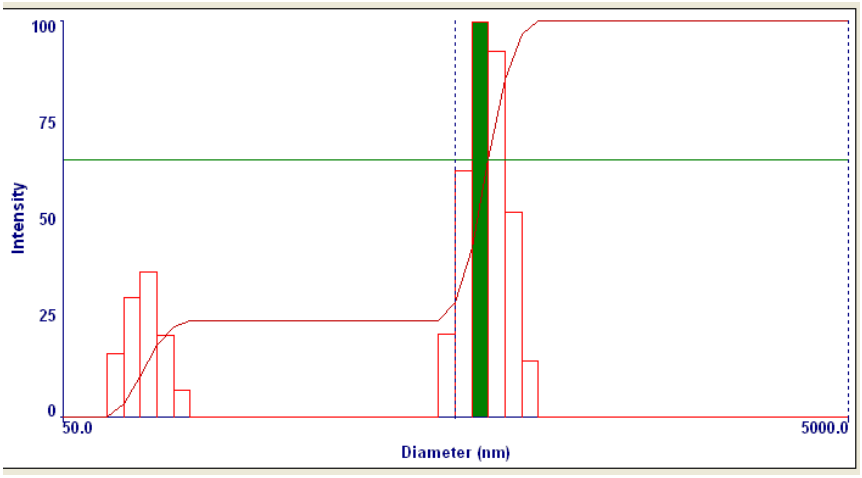

Figure 3.12. Size distributions of AB diblock in solution at pH 10, estimated by DLS at 40°C (a) and 50°C (b).

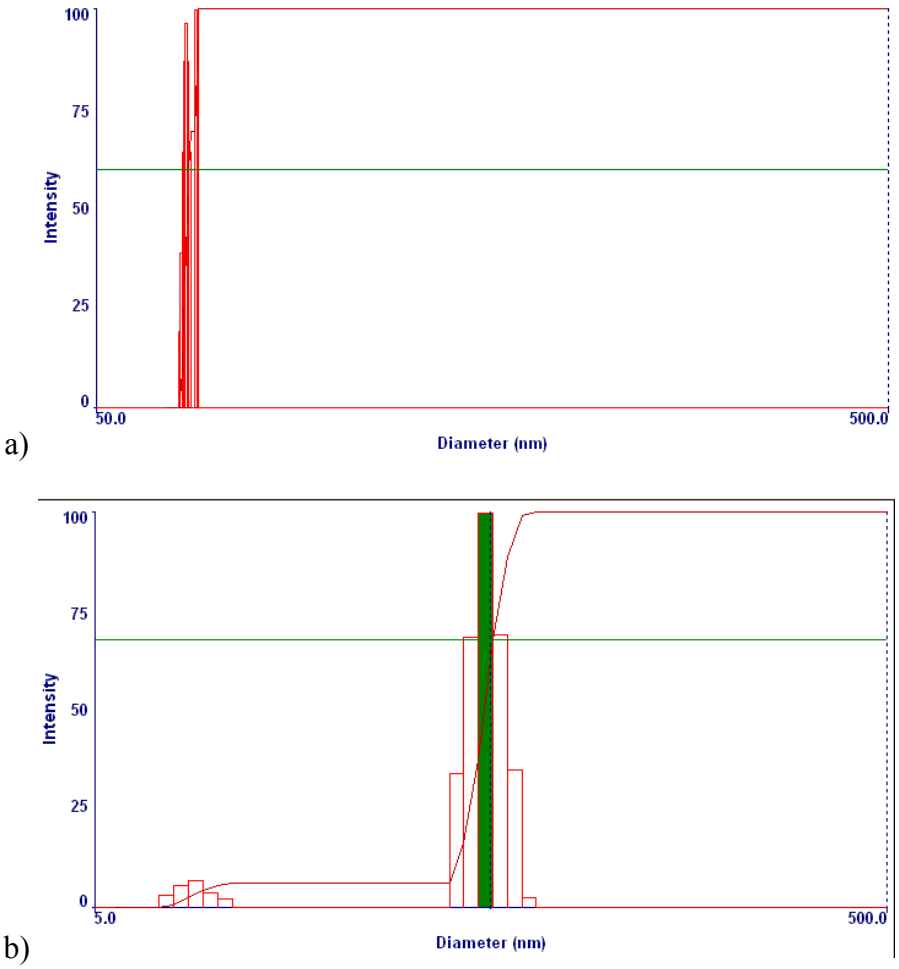

Figure 3.13. Size distributions of BC diblock in solution at pH 10, estimated by DLS at 40°C (a) and 50°C (b).

Chapter IV

Temperature and pH Responsive ABC Triblock Polymers

4.1. Extract

The solution behavior of an ABC triblock polymer with dual temperature and pH response has been studied in concentrated solutions. The polymer PNIPAm-P(NIPAm-*co*-AA)-PDEAm is comprised of thermoresponsive side blocks, poly(N-isopropylacrylamide) (PNIPAm) and poly(N,N-diethylacrylamide) PDEAm, and a dual temperature and pH responsive copolymer poly(NIPAm-*co*-acrylic acid) (PNIPAm-*co*-AA) as the midblock. The polymers were prepared by RAFT polymerization with postpolymerization modification of the RAFT CTA end group, and tested for mechanical properties under different temperature and pH conditions. RAFT polymerization yielded well defined polymers with good control over molecular weight and dispersity $Đ \sim 1.20$. The triblock consisted of A and C flanking blocks with MW~11,000 and a B midblock twice as long with $M_n \sim 23{,}000$. At pH 2.0, 10% w/v solutions of the polymers phase separated and aggregatde upon heating to 30 °C. On increasing pH to 7.4, the polymers formed a viscoelastic fluid at 57 °C. While each block in the triblock exhibited temperature sensitivity, the solubility of the midblock P(NIPAm-co-AA) influenced the phase transition of the triblock. The results were also compared with the ABA triblock PNIPAm-P(NIPAm-*co*-AA)-PNIPAm. The ABC and ABA triblocks exhibited similar phase behaviors over the range of tested temperatures. This may be because of hydrogen bonding interactions between PDEAm and PNIPAm and close LCST temperatures of 30 and 32 °C, respectively.

4.2. Introduction

Polymers that can self assemble to form three dimensional networks have gained widespread importance in the fields of drug delivery, tissue engineering and coatings [117, 178, 194-197]. The property of self assembly usually comes about due to the presence of blocks with differing chemical affinities in a single molecule. The simplest example is surfactants, in which the hydrophobic and hydrophilic regions cause the surfactant molecules to assemble into micelles in solution with the core internalizing the solvophobic region. The same is true in the case of polymers that contain both hydrophilic and hydrophobic segments. Amphiphilic polymer molecules self assemble to form micelles as well as other supramolecular assemblies such as wormlike micelles, bilayers and vesicles [198].

An advance in the area of amphiphilic polymers was the introduction of stimuli responsive components in which the solubilities of the various components depend on environmental conditions [199]. For example, thermoresponsive polymers that exhibit LCST behavior undergo a hydrophilic to hydrophobic transition with increasing temperature. The assembly behavior of stimuli responsive polymers is thus not only affected by the polymer composition, but also by environmental conditions. This imparts an added level of control to molecular assembly. Stimuli responsive polymers also enable reversible self assembly [200-202]. For example, the triblock polymer poly(N,N-diethylacrylamide)-*b*-poly(acrylic acid)-*b*-poly(N,N-diethylacrylamide) undergoes reversible sol-gel transitions as a function of temperature [115]. This is attributed to the structural make up of the polymer, in which the side blocks are formed of PDEAm, a

polymer that exhibits LCST behavior [203]. This implies that it can undergo a hydrophobic to hydrophilic transition and vice-versa, on change in temperature. The midblock is formed of a hydrophilic polymer poly(acrylic acid), whose water solubility is essentially independent of temperature. On increase in temperature, the flanking PDEAm blocks undergo reduction in solubility and phase separate. The hydrophobic PDEAm blocks, in a bid to reduce contact area with water, cluster together into hydrophobic domains, and this leads to formation of physical crosslinks comprised of PDEAm that hold together the soluble PAA chains. Such a three dimensional network is termed a gel. If the gel has appreciable affinity for water, it is termed a hydrogel.

The pH responsive component for that study, polyacrylic acid, was a weak mucoadhesive polyacid [204]. Polyacrylic acid and its derivatives such as polymethacrylic acid have been used to enhance retention time of various topical and oral drug delivery systems [42]. NIPAm and acrylic acid can be coincorporated to render polymers that are both temperature and pH responsive [44, 205]. Chemically crosslinked hydrogels of NIPAm-acrylic acid copolymers have been studied as enteric delivery systems for pH regulated delivery of indomethacin [206]. In that work, Dong and Hoffman were among the first to present the concept of incorporating pH sensitivity to PNIPAm by using acrylic acid as a comonomer.

Water soluble associating block polymers can undergo assembly into higher order structures in solution with a corresponding change in solution viscosity. Assembly may be from single polymer chains to micelles, from micelles to micellar aggregates, or from sol to gel. Thus, such block polymers have garnered interest as injectable drug delivery

and tissue engineering systems [207-210]. They can also serve as thickeners in paints, drilling fluids and detergents. Triblock polymers have been extensively investigated as gelators [77, 85, 116, 118, 211, 212]. The triblock architecture, with a long hydrophilic midblock and short hydrophobic sideblocks, results in the formation of a physical hydrogel in which the end hydrophobic blocks serve as physical crosslinks. Such water soluble associating polymers can either be rendered thermoresponsive by using LCST polymers such as PNIPAm and PDEAm, or pH responsive by addition of polyelectrolytes such as polyacrylic acid. As mentioned earlier, the temperature and pH responsive functionalities can also be combined to design multi responsive polymers. Interest in triblock polymers is based on the expectation that the end blocks should phase separate into different hydrophobic domains, thus increasing the efficiency of network formation. This would result in lowering the gelation concentration, i.e., the concentration required to establish a three dimensional transient network.

Angelopoulos and Tsitsilianis studied poly(N,N-diethylacrylamide)-*b*-poly(acrylic acid)-*b*-poly(N,N-diethylacrylamide) for its gelation properties as a function of temperature and ionic strength [115]. At low temperatures and high pH, the polymer was water soluble while above pDEAAm's LCST, the PDEAAm chains phase separated out of solution with the PAA block still being preferentially dissolved. This led to a sol-gel transition with formation of a physical hydrogel. It was also observed that increasing ionic strength lowered the gelation temperature.

Zhu et al. studied micellization of poly(N-*n*-propylacrylamide)-b-poly(N-isopropylacrylamide)-b-poly(N,N-ethylmethylacrylamide) as a function of temperature.

The polymer underwent a solution to micelle transition at 28 °C due to dehydration of poly(N-*n*-propylacrylamide) block. On further heating, the poly(N-isopropylacrylamide) and poly(N,N-ethylmethylacrylamide) blocks dehydrated at specific temperatures leading to micellar rearrangement. In this way, by tying together different LCST polymers, various micellar morphologies could be assessed by changing temperature [213]. Here, the dual thermal/pH modulation of structural transitions is not present. Instead, the sequential nature of thermal transitions due to differing LCSTs of the constituent blocks is noted.

In the present work, we designed a poly(N-isopropylacrylamide)-*b*-poly(N-isopropylacrylamide-co-acrylic acid)-*b*-poly(N,N-diethylacrylamide) (PNIPAm-P(NIPAm-*co*-AA)-PDEAm) triblock polymer. The polymer is comprised of thermoresponsive sideblocks and a dual temperature and pH responsive midblock. Polymer phase behavior was studied as a function of temperature and pH by rheology.

4.3. Experimental Section

4.3.1. Materials

All chemicals were purchased from Sigma Aldrich and used as received unless otherwise noted. NIPAm was recrystallized from hexane. The monomer *tert*-butyl acrylate was washed 3 times with 5% aqueous sodium hydroxide, followed by 3 washings with distilled water. Water was removed by drying *t*BA overnight over anhydrous sodium sulfite. It was then distilled under reduced pressure. The initiator 2,2'-azobisisobutyronitrile (AIBN) was recrystallized from methanol. Methyl acrylate was passed over a basic alumina column to remove the polymerization inhibitor.

4.3.2. Polymer synthesis

Scheme 4.1. PN(N/A)D synthesis and chain end modification

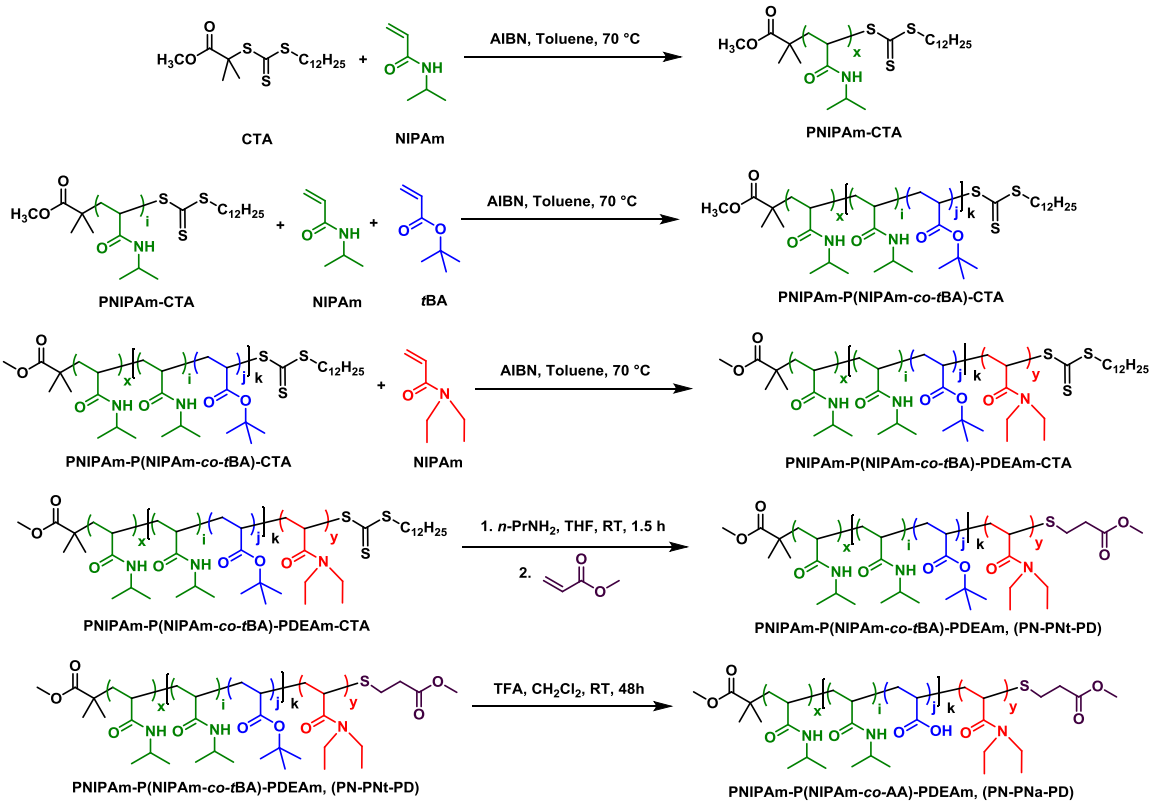

PNIPAm-P(NIPAm-*co*-AA)-PDEAAm [PN(N/A)D] triblocks were synthesized by sequential radical addition-fragmentation chain transfer (RAFT) polymerization, followed by acid hydrolysis (Scheme 4.1). First, PNIPAm-P(NIPAm-*co*-*t*BA)-PDEAAm-CTA [PN(N/*t*)D-CTA] and PNIPAm-P(NIPAm-*co*-*t*BA)-PNIPAm-CTA [PN(N/*t*)N-CTA] triblocks were prepared by RAFT polymerization. The CTA end group was modified by aminolysis and Michael addition to overcome any hydrophobic end group effects exerted by the CTA on polymer solution behavior. The *t*BA groups in the triblock were then hydrolyzed to AA by acid hydrolysis, resulting in the final polymer PNIPAm-P(NIPAm-*co*-AA)-PDEAAm [PN(N/A)D]. The ABA triblock PNIPAm-P(NIPAm-*co*-

AA)-PNIPAm [PN(N/A)N] was prepared in an identical manner by growing a PNIPAm (PN) chain off the PN(N/A) diblock.

All polymerization steps were monitored by ^{1}H-NMR of feeds and products, and molecular weight distributions of the block polymers at the end of each step were determined by gel permeation chromatography (GPC). CTA removal was confirmed by elimination of a UV-Vis absorbance peak at 310 nm.

4.3.3. ^{1}H-NMR Spectroscopy

NMR experiments were performed on Bruker Avance II 400 MHz spectrometer comprised of a 5 mm broadband observe (BBO) probe and a BACS 60-tube sample changer for continuous operation. Data was processed with TOPSPIN 2.0 software coupled to the spectrometer. NMR samples were prepared by dissolving the polymer in deuterated chloroform**.**

4.3.4. UV-Vis spectroscopy

UV-Vis measurements were performed on a Cary 100 Bio UV-Vis spectrophotometer equipped with a Peltier thermostatted multicell holder and controlled by Cary WinUV software. For estimation of CTA removal, polymer solutions were prepared in $CHCl_3$ at a concentration of 1mg/mL in quartz cuvettes. Absorbance scans of the polymer solutions were then collected over the wavelength range of 200-800 nm. An instrumental baseline showing a sharp increase in absorbance at short wavelengths was found even in blank solutions (Figure 4.9 b), and was accounted for. For cloud point measurements, the samples were prepared in distilled water and scanned at λ=500 nm.

4.3.5. Gel Permeation Chromatography (GPC)

GPC was performed on an Agilent Technologies 1260 Infinity GPC, equipped with three Phenogel columns with pores sizes 10^5, 10^4 and 10^3 Å, a Wyatt DAWN DSP light scattering detector, and a Wyatt OPTILAB rEX refractive index detector. Tetrahydrofuran (THF) containing 1 % tetramethylethylenediamine (TEMED) by volume was used as the eluent at a flow rate of 1.0 mL/min. GPC samples were prepared by dissolving the polymer in THF. The solution was then filtered through 0.25 μm PTFE membrane filters.

4.3.6. Sample preparation

10% w/v solutions of the polymers were prepared by dissolving the polymer in distilled water. The solutions were allowed to stir for 2 weeks at room temperature before performing mechanical measurements. 0.1 % w/v solutions were prepared by dilution of the 10% w/v solutions. pH was adjusted using strong acid/base. For UV spectroscopy measurements, the solutions were filtered through 0.45 μm GHP ACRODISC membrane filters.

4.3.7. Dynamic Mechanical Analysis

Viscosity measurements were performed on an AR-G2 rheometer using the parallel plate geometry with an upper plate diameter of 40 mm. The upper and lower plates confined the sample in a gap ranging from 0.5-1 mm. Approximately 1 mL of the polymer solution was loaded onto the lower plate at room temperature (25°C). The upper plate was slowly brought down to make contact with the sample. The gap was gradually reduced until the sample was flush with the edge of the upper plate. The rheometer was

equipped with a temperature controlling Peltier accessory. The following tests were performed:

a) Strain sweep experiments were conducted at a frequency of 1 rad/s. The sample was subjected to strain amplitudes ranging from 0.5-100%. The modulus was plotted on a log-log scale and region of linear viscoelasticity was determined for further experiments.
b) Flow temperature ramp experiments were performed over the range 25-60 °C. To avoid evaporation of water at higher temperatures, the upper and lower plates were covered with a metal cover with an underlying sponge moistened with water. The flow temperature ramp experiments were conducted at strain amplitudes of 1 and 2%, at angular frequency 1 rad/s and ramp rate 1 °C/min.
c) Frequency sweep experiments were conducted at fixed strain amplitude (0.5 or 1%). The sample was subjected to frequencies ranging from 0.5-100 rad/s. The modulus was plotted against frequency on a log-log scale.

4.4. Results

4.4.1. Molecular weight and polymer composition

Polymer molecular weight was estimated by GPC. Measurements were made on the *t*BA-containing polymers prior to hydrolysis of the *t*BA units to AA. (AA-containing polymers, when analyzed using GPC, exhibited appreciable retention on the GPC column.) Polymer samples were prepared in THF (4-8 mg/mL) and THF/*N*,*N*,*N*′,*N*′-tetramethylethylenediamine was used as the eluting solvent. Molecular weights were

estimated from the LS chromatograms using refractive index increment. The calculated molecular weights are listed below in Table 4.1.

Table 4.1. Molecular weight characteristics

Sample	Composition	M_n[a] dn/dc = 0.107 gm/mL(LS)	$Đ$[b] dn/dc = 0.107 gm/mL(LS)
PN	PN_{100}-CTA	11,000	1.06*
PN(N/B)	PN_{100}-PN_{181}-*co*-*t*BA_{16}-CTA	34000	1.05/1.19*
PN(N/B)D	PN_{100}-PN_{181}-*co*- *t*BA_{16}-PD_{90}-CTA	45000	1.05
PN(N/B)N	PN_{100}-PN_{181}-*co*- *t*BA_{16}-PN_{99}-CTA	45000	1.21*
PN(N/A)D	PN_{100}-PN_{181}-*co*-AA_{16}-PD_{90}-CTA	45,000	1.05
PN(N/A)N	PN_{100}-PN_{181}-*co*-AA_{16}-PN_{99}	44,000	1.21*

[a] M_n estimated from refractive index signal using dn/dc increment of 0.107 ml/gm^{-1} for polyNIPAm. [b] Dispersity $Đ$ calculated using PNIPAm refractive index increment, dn/dc = 0.107 gm/mL. Subscripts refer to number of monomer units per block. * PDI estimated using pure THF as the mobile phase (without 1% TEMED)

The molecular weight of PN-CTA was estimated to be 11,000 Da, which was close to the desired molecular weight of 10,000 Da. As the polymer almost completely consisted of PNIPAm, the molecular weights were estimated from the light scattering signal using PNIPAm's refractive index increment (dn/dc) of 0.107 mL/gm^{-1} [214]. In a separate study, it was determined that the molecular weights calculated using PNIPAm dn/dc correlated well with values obtained using Universal Calibration (see Supporting Information Table 4.2).

Polymerization of the second block P(NIPAm-*co*-*t*BA) increased the molecular weight to 34,000 Da. Thus, the midblock was ~23,000 Da, i.e., twice in length as compared to the first block PNIPAm. Monomer conversion was estimated by 1H-NMR.

A 10% *t*BA: NIPAm polymer feed was found to have converted 54% of NIPAm and 49% of *t*BA with the overall monomer conversion amounting to 53%. *t*BA in P(NIPAm-*co*-*t*BA) was calculated to be 8.5%. This estimate is in agreement with %tBA calculated using Mayo Lewis copolymerization equation [215]

$$F_2 = \frac{r_2 f_2^2 + f_1 f_2}{r_1 f_1^2 + 2 f_1 f_2 + r_2 f_2^2}$$

where F_2 is the mol fraction of monomer 2, in this case *t*BA, in the polymer, f_1 and f_2 are the mol fractions of NIPAm and *t*BA in the feed, and r_1 = 2.12 and r_2 = 0.88 are the reactivity ratios of NIPAm and *t*BA, respectively, which were evaluated previously [216]. The reactivity ratio values suggest that the polymer chains add more NIPAm towards the start of the polymerization and add more *t*BA units in the later part of the chain.

Sequential polymerization of the third block PDEAm resulted in M_n of 45,000 Da for PN(N/B)D triblock, implying that the PDEAm block formed was 11,000 Da in weight. The GPC chromatograms (Supporting Information, Figure 4.11) showed single peaks thus suggesting complete growth of sequential blocks, with essentially no dead A or AB blocks formed *en route*. The dispersities of the PN(N/B)D triblock and PN-PN/B diblock were equal, $Đ$ = 1.05. This also suggests that the diblock chains successfully propagated to add the third block. In the past, problems were encountered with obtaining a triblock free from unreacted diblock. This can sometimes occur due to inactivation of the growing CTA end. In polymerizations where there is incomplete propagation of the macro-CTA, the dispersity $Đ$ is known to increase. Incomplete propagation is sometimes encountered when running polymerizations to high extents (>80% conversion). This problem was avoided by quenching the diblock polymerization at ~ 50% conversion.

Similar to the ABC triblock, PN(N/B)N triblock was grown off PN(N/B) macro-CTA by polymerization with NIPAm. The estimated molecular weight of PN(N/B)N was 44,000 Da implying that the end PNIPAm block length was 10,000 Da. This polymer was characterized on a different GPC column using THF (without TEMED) as the eluting solvent. (TEMED is usually added to the mobile phase to prevent retention of PNIPAm on the column.) As expected, absence of TEMED led to 'tailing' in the GPC chromatograms due to delayed elution of the polymer. The estimated dispersity *Đ* was thus much higher, with a reported value of 1.21. To confirm that increase in dispersity was not related to diblock inactivation, PN(N/B) was analyzed using THF (without TEMED) as the mobile phase. Although the molecular weight estimate was the same i.e. 34,000 Da, the dispersity *Đ* increased from 1.05 to 1.19. Thus, complete propagation of diblock to triblock was confirmed.

4.4.2. Polymer solution behavior

a) 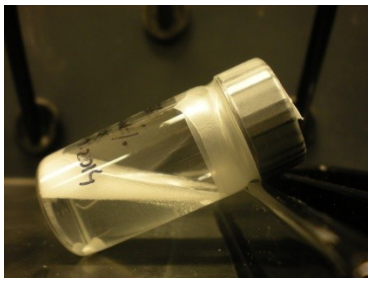 25 °C

b) 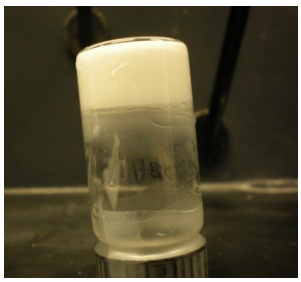 37 °C

Figure 4.1. 10% w/v solutions of PN(N/A)D at temperatures a) 25 and b) 37 °C at pH 2

To look for visual signs of aggregation or gelation in the 10% w/v solutions, PN(N/A)D solutions were kept in vials at different temperatures at pH 2. At room temperature, 10% w/v PN(N/A)D formed a free flowing solution (Figure 4.1 a). The solution tended to foam on stirring which may occur due to structuring of the polymer at

the air-water interface. It was then heated to 37 °C, a temperature above PNIPAm LCST. At 37 °C, the solution phase separated to form a white aggregated mass which stuck to the vial bottom and stayed as such when inverted (Figure 4.1 b) Phase separation took place in less than a minute. The aggregated mass exuded a small amount of water.

4.4.3. Dynamic mechanical analysis

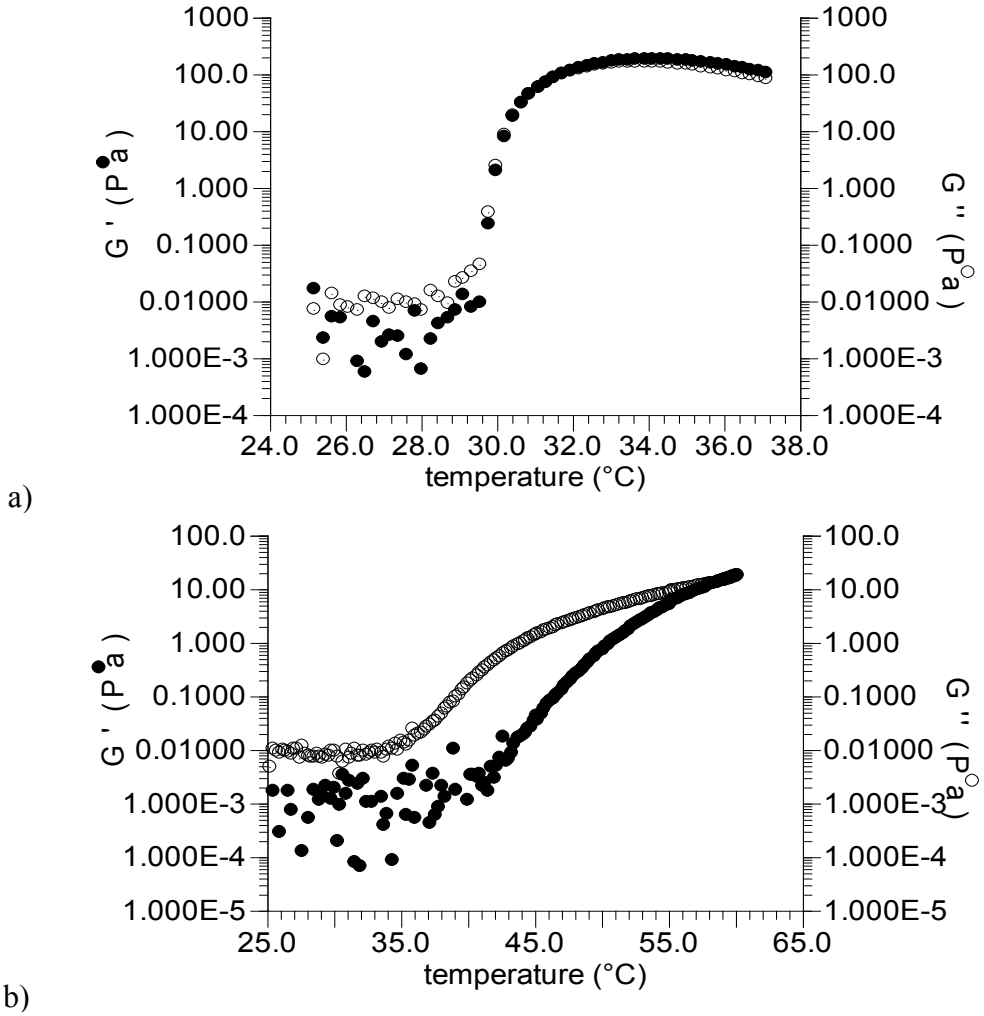

Figure 4.2. Dynamic shear moduli (G′ and G″) as a function of temperature for 10w/v% PN(N/A)D in aqueous solutions at a) pH 2 and b) pH 7.4. The measurements were made at a strain amplitude of 1% and angular frequency of 1 rad/s. Temperature was ramped at 1 °C/min.

To study structural changes in more detail, oscillatory shear measurements were performed at various temperatures and pH conditions. In these experiments, 10% w/v solutions of PN(N/A)D were tested for gelation by performing dynamic mechanical measurements at varying temperatures. Measurements were made at both acidic and alkaline pH values. Shown in Figure 4.2 are the dynamic shear moduli, G′ and G″ as a function of temperature for PN(N/A)D at pH 2 (Figure 4.2 a) and pH 7.4 (Figure 4.2 b). At pH 2, G′ and G″ started out at low values of ~ 0.01 Pa. Upon heating, G′ and G″ started to increase at 29 °C and reached a maximum at 34 °C. No crossover of G′ and G″ was observed. On adjusting pH to 7.4, the modulus profile changed significantly. G″ started out at a low value of 0.01 Pa at 25 °C. With increasing temperature, G″ started to increase at 35 °C. No increase in G′ was observed at this point. However, G′ started to increase at 42 °C. Eventually, G′ and G″ overlapped at ~ 57 °C. No crossover of G′ and G″ was observed, although such a crossover might have been seen at higher temperatures.

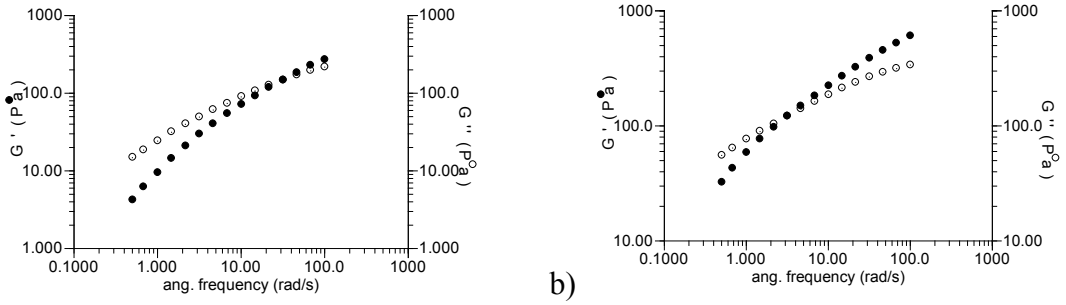

a) b)

Figure 4.3. Dynamic shear moduli (G′ and G″) as a function of frequency for 10% w/v PN(N/A)D in pH 7.4 aqueous solutions at a) 45 °C and b) 60 °C. The measurements were made at strain amplitude of 0.5 %.

Frequency sweeps for 10% w/v PN(N/A)D at pH 7.4. were carried out at 45 °C and 60 °C. The samples were equilibrated at each temperature for 20 minutes and the

frequency sweep was carried out at strain amplitude of 0.5%. At 45 °C, at low frequencies, G″ was almost an order of magnitude greater than G′. At higher frequencies, the difference between G′ and G″ became smaller, and eventually G′ became slightly greater than G″. The G′ - G″ moduli crossover occurred at an angular frequency of 30 rad/s (Figure 4.3 a). On continued heating, at 60 °C, the moduli crossover occurred at a much lower frequency of 3 rad/s (Figure 4.3 b). It should be noted that the modulus amplitude at 1 rad/s in the frequency sweeps were higher than the modulus values measured at the corresponding temperature during the temperature ramp. This dispcrepany occurred because the data were collected from two different runs. The temperature ramp displayed was collected from a second run. There may be some loss of polymer between successive runs which led to dilution of the polymer sample leading to lower modulus values.

4.4.4. Solution behavior of PN(N/A)N

a) 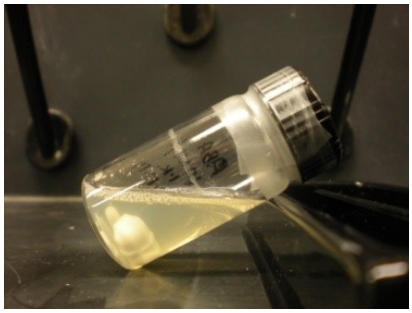 25 °C

b) 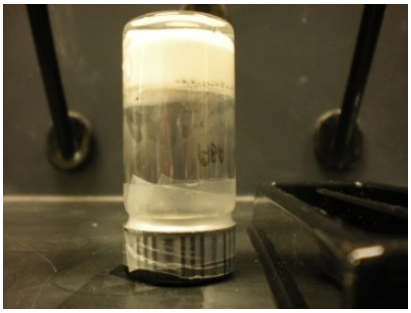 37 °C

Figure 4.4. 10% w/v solutions of PN(N/A)N solutions at temperatures a) 25 and b) 37 °C

It was of interest to see how the ABA triblock PN(N/A)N fared relative to PN(N/A)D. PN(N/A)N triblocks with block composition and weights similar to PN(N/A)D were synthesized by RAFT polymerization (molecular weights listed in Table

4.1). 10% w/v solutions of PN(N/A)N were prepared in distilled water. At room temperature, PN(N/A)N solutions were in the sol state (Figure 4.4 a). On heating to physiological temperature, 37 °C, the solution phase separated and formed a free standing aggregate as demonstrated by vial inversion. Phase separation was accompanied by release of some amount of water from the gel (Figure 4.4 b).

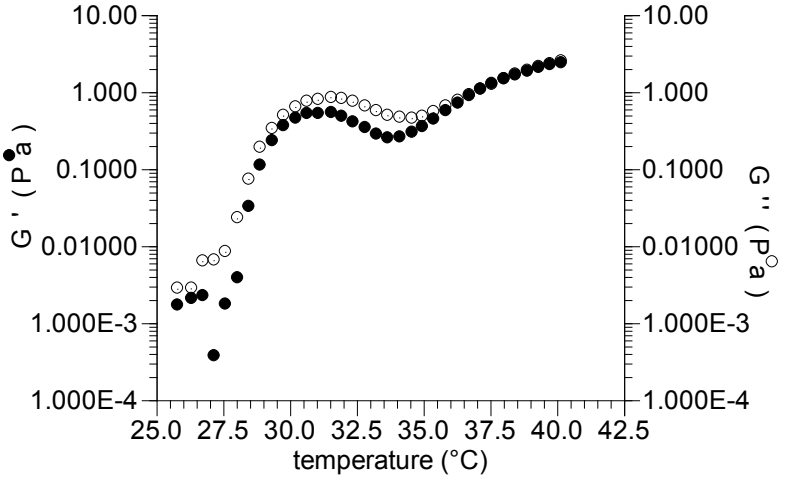

a)

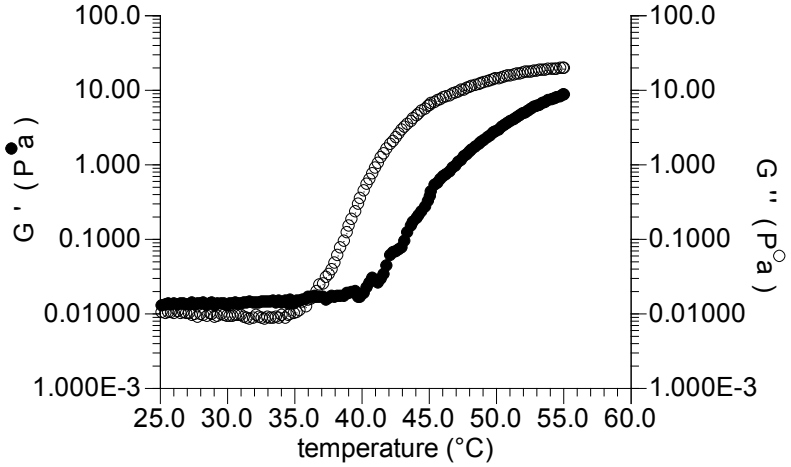

b)

Figure 4.5. Dynamic shear moduli (G′ and G″) as a function of temperature for 10w/v% PN(N/A)N in aqueous solutions at a) pH 2 and b) pH 7.4. The measurements for pH 2 sample were made at a strain amplitude of 2% and angular frequency of 1 rad/s and temperature ramp rate of 2 °C/min. pH 7.4 sample was analyzed at 1% strain, 1 rad/s and ramp rate of 1 °C/min.

Dynamic mechanical measurements were carried out on 10% w/v solutions of 10w/v% PN(N/A)N in aqueous solutions at pH 2 and 7.4. As shown in Figure 4.5 a, at pH 2, G′ and G″ started to increase at ~ 29 °C and remained nearly congruent over the entire range of tested temperatures up to 40 °C. However, no crossover of the moduli was observed. At pH 7.4, the increase in G′ and G″ occurred at higher temperatures. G″ increases at 35 °C and G″ starts increasing at 42 °C. Up to 55 °C, G′ values were less than G″.

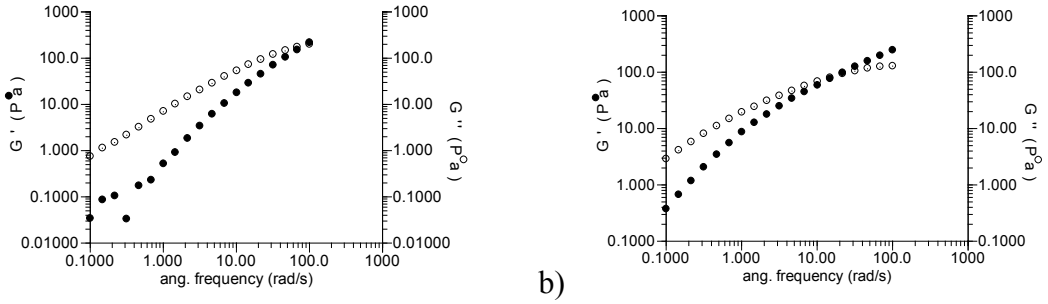

a) b)

Figure 4.6. Dynamic shear moduli (G′ and G″) as a function of frequency for 10w/v% PN(N/A)N in pH 7.4 aqueous solutions at a) 45 °C and b) 55 °C. The measurements were made at a strain amplitude of 1 %.

In order to get a better idea of solution structure at pH 7.4, frequency sweeps were carried out at an intermediate and final temperature during the heating cycle. As shown in Figure 4.6 a, at 45 °C, G″ > G′ at low frequencies. At higher frequencies, G′ approaches G″ and the two become equal at a frequency of 80 rad/s. At 55 °C, the frequency of G′-G″ crossover reduces to 15 rad/s, indicating further development of a viscoelastic structure.

4.4.5. Differences between ABC and ABA

To compare the behaviors of the ABC and ABA systems, 10% w/v aqueous solutions of the triblocks were prepared to look for visual signs of phase separation.

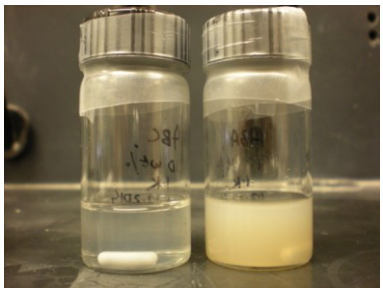

Figure 4.7. 10% w/v solutions of PN(N/A)D (left) and PN(N/A)N (right) when adjusted to pH 7.4 at 25 °C.

At room temperature and pH 7.4, both ABA and ABC were in the fluid state (Figure 4.7). There was a noticeable difference in the turbidity of the ABC and ABA suspensions, however. While ABC was slightly cloudy, ABA was milky, as shown in Figure 4.7.

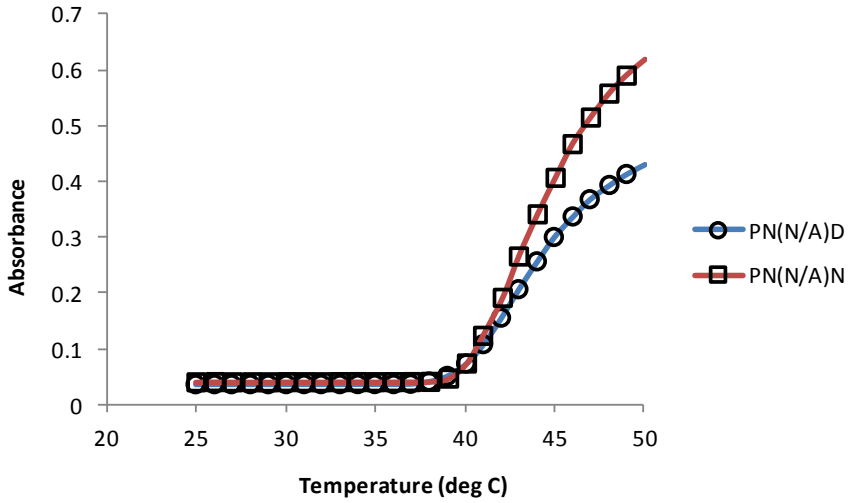

Figure 4.8. Absorbance curves (λ=500 nm) of 0.1% w/v PN(N/A)D and PN(N/A)N aqueous solutions at pH 7.4

Cloud points of the ABA and ABC triblocks were measured in dilute aqueous solution (0.1% w/v) by visible spectroscopy (Figure 4.8). Both ABA and ABC solutions exhibited an increase in absorbance starting at ~ 40 °C. With continued heating, the absorbance of both solutions continued to increase. The increase in absorbance was

sharper for the ABA solution and reached a final absorbance value of 0.6 at 50 °C. ABC solutions exhibited a more gradual increase in absorbance, with a final absorbance value of 0.4 at 50 °C. The onset of aggregation for both polymers occurred at essentially the same temperature ~ 40 °C.

4.5. Discussion

Dynamic mechanical tests were performed to test whether 10% w/v solutions of PN(N/A)D form gels at elevated temperatures. Conventionally, a sol-gel transition is said to occur when initially the viscous modulus, G″, is greater than the elastic modulus, G′. On approaching the gel point there occurs a modulus crossover with G′ becoming greater than G″ [217]. PN(N/A)D solutions, on heating, reached a stage where G′ = G″, but a distinct crossover with G′ > G″ was not observed. At pH 2, G′ and G″ became essentially congruent at 29 °C. This indicates phase separation of PN(N/A)D. As PNIPAm and PDEAm exhibit LCSTs at 32 °C and 30 °C, respectively, they are expected to phase separate at temperatures in that range. The midblock P(NIPAm-*co*-AA) is expected to be more soluble because of the presence of AA, a hydrophilic comonomer. However, at pH 2, with the carboxylic acid moieties in the protonated state, AA is known to form H-bonds with NIPAm leading to a reduction in LCST [39, 47]. Thus, the polymer as a whole crashes out of solution leading to aggregation.

At pH 7.4, the PNIPAm and PDEAm end blocks are expected to exhibit similar solubilities as at pH 2. The midblock solubility, however, will exhibit pH dependence due to the presence of AA which is a weak acid. At pH 7.4, with the majority of the AA carboxylic acid units in the ionized state, PNIPAm-co-AA is more soluble than the

PNIPAm and PDEAm endblocks. On heating PN(N/A)D at pH 7.4, G″ starts to increase at ~35 °C and G′ becomes detectable at ~42 °C. G′ becomes equal to G″ at 57 °C. On increased heating, no crossover of G′ and G″ is observed,

In order to check whether PN(N/A)D forms a gel, a frequency sweep was also carried out at pH 7.4. If G′ and G″ become independent of frequency with G′>G″, it is considered to indicate onset of gelation [218, 219]. Frequency sweeps at elevated temperatures (Figure 4.3) did not indicate a frequency independent modulus for PN(N/A)D solutions. The frequency profiles resembled those for viscoelastic liquids with G″ > G′ at low frequencies, and crossing over at high frequencies leading to a larger elastic modulus G′ relative to G″. Thus, it is suggested that PN(N/A)D undergoes a transition from a viscous fluid to a viscoelastic fluid at high temperatures at pH 7.4.

The viscoelastic structure continued to develop with heating as shown by the frequency sweeps in Figure 4.3. PN(N/A)D 10% w/v solutions, on heating, started to develop viscoelasticitiy. As the sample was heated from 45 to 60 °C, the G′ and G″ crossover frequency dropped from 30 to 3 rad/s. Since the crossover frequency is inversely proportional to structural relaxation time, this implies that as the solution is heated from 45 to 60 °C, polymer entanglements continue to form.

It is speculated that at 35 °C at pH 7.4, when G″ starts to increase with increasing temperature (Figure 4.2 b), the flanking PNIPAm and PDEAm blocks start to phase separate into hydrophobic domains while the midblock P(NIPAm-*co*-AA) stays in solution. This may lead to formation of ‘flower’ micelles whereby the hydrophobic PNIPAm and PDEAm blocks phase separate into a common micellar core causing the

hydrophilic midblock to loop back on to itself forming the micelle corona. With increasing micellization, a portion of the PNIPAm and PDEAm end blocks may traverse two different micellar cores leading to the formation of inter-micellar bridges. These kinds of inter-micellar associations would lead to the emergence of elastic behavior in the polymer solution.

One of the aims of the study was to look for differences in polymer assembly behavior among ABC and ABA triblocks. Similar experiments were conducted on the ABA triblock, PN(N/A)N. It exhibited solution behavior similar to that observed for PN(N/A)D. At pH 2, the polymer aggregated out of solution at 29 °C (Figure 4.5 a). Under relatively alkaline conditions, at pH 7.4, G′ and G″ exhibited a gradual increase on heating with no congruency occurring up to 55 °C. The frequency sweep profiles (Figure 4.6) were characteristic of a viscoelastic liquid with the G′- G″ crossover shifting to lower frequencies with increasing temperatures.

Although ABA and ABC triblocks exhibited similar solution behaviors, some differences were also observed. At room temperature, pH 7.4 solutions of PN(N/A)N were more turbid than those of PN(N/A)D (Figure 4.7). This suggests that PN(N/A)N is less soluble in water as compared to PN(N/A)D. Literature reports suggest that mixtures of PDEAm and PNIPAm resist sedimentation on heating due to complexation between the PNIPAm and PDEAm blocks. PNIPAm contains a lone H atom in the amide group while in PDEAm, the N atom is attached to two alkyl groups but no hydrogen. PNIPAm acts as a H-donor as well as acceptor (because of =C-O groups) while PDEAm acts only as a H-acceptor [220, 221]. The PNIPAm and PDEAm blocks thus may associate with

one another through H-bonding leading to stabilization of the end blocks in PN(N/A)D. The fact that PN(N/A)N is turbid at room temperature, which is lower than LCST of the individual blocks, is not understood.

Also, the magnitude and rate of transition seem to vary for ABA and ABC triblocks. Upon heating 0.1% w/v solutions of PN(N/A)N and PN(N/A)D at pH 7.4, a greater increase in absorbance (measured by UV-Vis spectroscopy) was observed for the ABA triblocks as compared to ABC (Figure 4.3). This may again be explained by differences in the phase transition mechanism of PNIPAm and PDEAm. Upon heating as the polymer chains dehydrate, PNIPAm can have significant intramolecular H-bonding between the carboxyl (=C-O) and the –NH groups of the amide (=C-O---N-H). This leads to PNIPAm chains expelling a significant amount of water and forming compact hydrophobic domains upon phase separation. PDEAm on dehydration also releases bound water but the amount of water released from PDEAm on phase separation is less than for PNIPAm. Due to the absence of a lone H atom in the amide group, PDEAm does not participate in intramolecular H-bonding. So, the increase in turbidity for PNIPAm is greater than that for PDEAm on reaching phase transition temperature [221].

4.6. Conclusions

Triblock polymers with thermoresponsive end blocks and dual thermo- and pH-responsive mid blocks were investigated for their gelation ability. PN(N/A)D triblocks were synthesized by sequential RAFT polymerization. The end blocks PNIPAm and PDEAm exhibit LCST behavior with transition temperatures at 32 and 30 °C, respectively. The polymers existed as a viscous fluid at room temperature. On heating,

the polymer phase transition was governed by pH. At pH 2, the polymers phase separated to form aggregates at 29 °C. At pH 7.4, the polymer solution underwent a transition from a viscous fluid to a viscoelastic fluid at 57 °C, as determined by rheological experiments. As shown in Scheme 4.2, the temperature of the phase transition and structure of the high temperature phase were governed by solubility of the mid block P(NIPAm-*co*-AA). Contrary to expectation, the PN(N/A)D triblock did not form a gel.

Scheme 4.2. pH dependent self assembly of ABC triblock

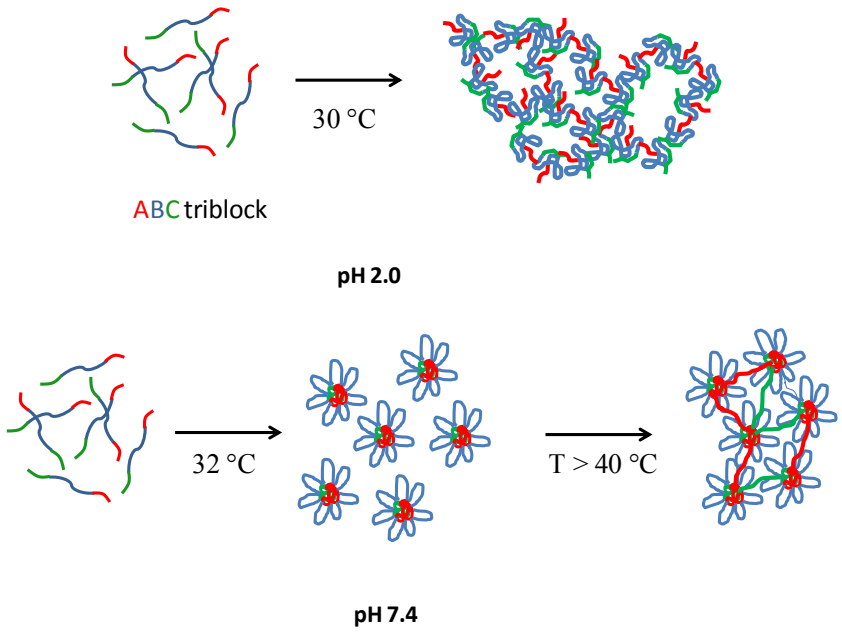

The ABC triblock was also compared to its ABA analogue, PN(N/A)N. ABA and ABC triblocks exhibited similar solution behaviors. This implies that PNIPAm and PDEAm phase separate into common hydrophobic domains. This is in agreement with a literature report stating that mixtures of PNIPAm and PDEAm interact with one another through H-bonds[220]. The proximity in temperature for their phase transitions also makes it difficult to observe block segregation.

4.7. Supporting Information

4.7.1. Synthesis of PNIPAm-CTA

PNIPAm-CTA was prepared by RAFT polymerization of NIPAm in 1,4-dioxane (anhydrous) at 70 °C, using AIBN as the initiator and methyl-2-(dodecylthiocarbonothioylthio)-2-methylpropionate (MDMP) as chain transfer agent (CTA). NIPAm (5.0 gm, 44 mmol), MDMP (0.167 gm, 0.442 mmol) and AIBN (7.23 mg, 0.044 mmol) were dissolved in 1,4-dioxane (anhydrous) (30 mL).

The polymerization flask was evacuated using three freeze-thaw cycles and polymerization was carried out at 70°C for 3 h. The reaction was quenched by immersing the polymerization flask in liquid nitrogen. The polymerization proceeded to 75%, as determined by 1H-NMR spectroscopy. Polymer was purified by repeated precipitation in pentane, followed by drying overnight *in vacuo* at 40°C.

4.7.2. Synthesis of PNIPAm-P(NIPAm-co-tBA)-CTA

The PNIPAm macro-CTA (2 gm, 0.22 mmol) was fed into a reactor along with NIPAm (14.5 gm, 129 mmol) and tBA (1.81 gm, 14.2 mmol). The contents were dissolved in 1,4-anhdyrous dioxane (100 mL). The polymerization flask was evacuated using three freeze-thaw cycles. The polymerization was carried out at 70 °C for 7.0 h. The extent of conversion was around 80% for NIPAm and 65% for tBA, as estimated by 1H-NMR. Reaction was quenched by immersing the polymerization flask in liquid nitrogen. The polymer was purified by repeated precipitation in pentane followed by drying overnight *in vacuo* at 40°C.

4.7.3. Synthesis of PNIPAm-P(NIPAm-co-tBA)-PDEAm-CTA

PNIPAm-P(NIPAm-*co*-*t*BA)-CTA (4.0 gm, 0.069 mmol), DEAm (1.6 gm, 12.5 mmol) and AIBN (1.31 mg, 0.008 mmol) were dissolved in 1,4 dioxane (anhydrous) (60 mL). The polymerization flask was evacuated using three freeze-thaw cycles. The polymerization was carried out at 70 °C for 3.0 h. Reaction was quenched by immersing the polymerization flask in liquid nitrogen. The polymer was purified by repeated precipitation in pentane followed by drying overnight *in vacuo* at 40°C.

PN(N/B)N-CTA was prepared in a similar manner. In a representative example, PN(N/B)-CTA (4.0 gm, 0.069 mmol), NIPAm (0.8 gm, 7.0 mmol) and AIBN (1.31 gm, 0.008 mmol) were dissolved in 1,4 dioxane (anhydrous) (50 mL). The polymerization flask was evacuated using three freeze-thaw cycles. The polymerization was carried out at 70 °C for 3.3 h. The reaction was quenched by immersing the polymerization flask in liquid nitrogen. The polymer was purified by repeated precipitation in pentane followed by drying overnight *in vacuo* at 40°C.

4.7.4. Removal of CTA

The trithiocarbonate moiety at the polymer ends were removed by aminolysis and Michael addition. PNIPAm-P(NIPAm-*co*-tBA)-PDEAm-CTA was dissolved in THF to make a 10% w/v solution. Then, n-propylamine (>50 [CTA] mol) and tris(2-carboxyehtyl) phosphine hydrochloride (equal to [CTA] mol) were added. The reaction mixture was stirred overnight with methylmethacrylate (>250 [CTA] mol) added after 2.5 hours of stirring. CTA removal was confirmed by UV spectroscopy.

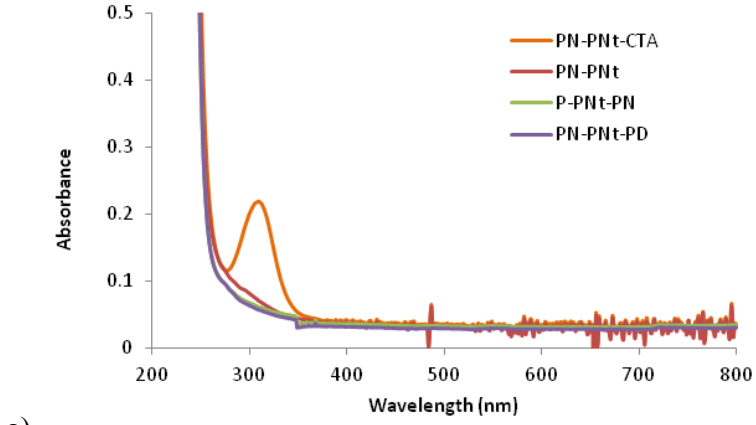

a)

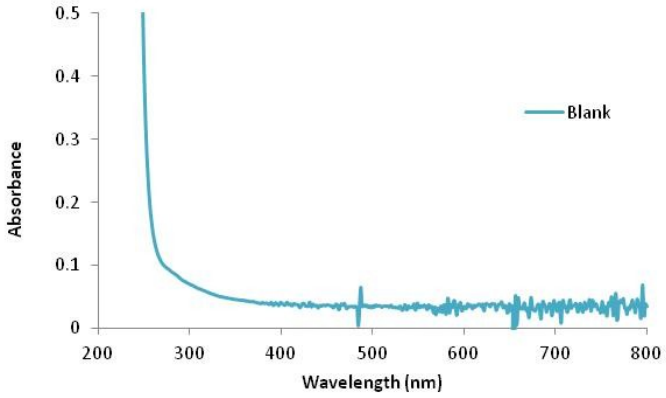

b)

Figure 4.9. UV-Vis spectra of a) *t*BA containing polymers before and after CTA removal and b) blank (water)

The trithiocarbonate moiety of CTA shows a characteristic absorbance peak at 310 nm. As shown in Figure 4.9a in Supporting Information, PN(N/B)-CTA exhibits an absorbance peak at 310 nm, while the PN(N/B), PN(N/B)N and PN(N/B)D polymers show no absorbance peak over the range of scanned wavelengths from 200-800 nm. This implies that CTA removal leads to elimination of the absorbance at 310 nm.

It is to be noted that the CTA absorbance peak does not level off to baseline (Supporting Information Figure 4.9 b. The same is true for the CTA-removed polymers

where the absorbance starts to increase after 400 nm and shoots up around λ=270 nm. This increase in absorbance arises because of instrumental factors as is apparent from the absorbance profile for a blank solution. The absorbance profiles for PN(N/B)N and PN(N/B)D exactly match the profile for the blank solution indicating the complete removal of any photo-active moieties. This confirms CTA removal from the diblock and triblock polymers.

4.7.5. Hydrolysis of tBA groups to obtain PNIPAm-P(NIPAm-co-AA)-PNIPAm

The *t*BA groups were hydrolyzed to acrylic acid (AA) by reaction with trifluoroacetic acid (TFA) in dichloromethane for 24 hours. In a representative example, PNIPAm-P(NIPAm-*co*-tBA)-PNIPAm (1.28 gm, 0.020 mmol) was dissolved in dichloromethane (20 mL). TFA (6 mL, 0.078 mol) was added and the reaction flask was stirred for 24 h. Reaction byproducts were removed by rotary evaporation. Polymer was redissolved in acetone and precipitated in hexane. Purified polymer was dried *in vacuo* at 40°C. The same procedure was followed to obtain PNIPAm-P(NIPAm-*co*-AA)-PDEAm and PNIPAm-P(NIPAm-*co*-AA).

In the NMR spectrum shown in Figure 4.10, a PN-P(N-*co*-*t*BA)-PNIPAm (top) exhibits a peak for the *tert*-butyl group at 1.4 ppm. On hydrolysis of *t*BA (bottom spectrum), the peak at 1.4 ppm disappears. The same is true in case of PN-P(N-*co*-*t*BA)-PDEAm (Figure 4.10 b), where PN-P(N-*co*-*t*BA)-PDEAm is hydrolyzed to PN-P(N-*co*-AA)-PDEAm.

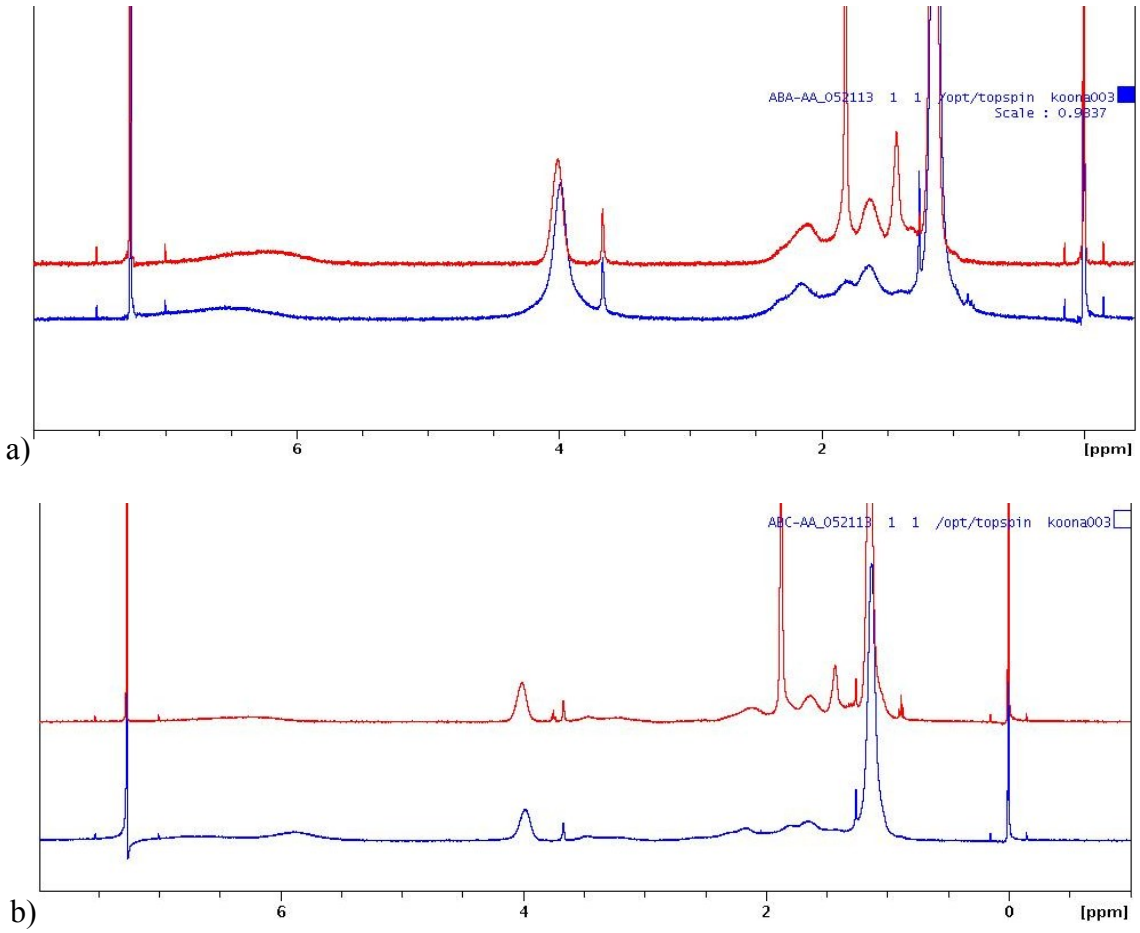

Figure 4.10. 1H-NMR spectra of PN-P(N-*co*-*t*BA)-PNIPAm (top) and PN-P(N-*co*-AA)-PNIPAm (bottom) in $CDCl_3$

4.7.6. Molecular weight estimation by GPC

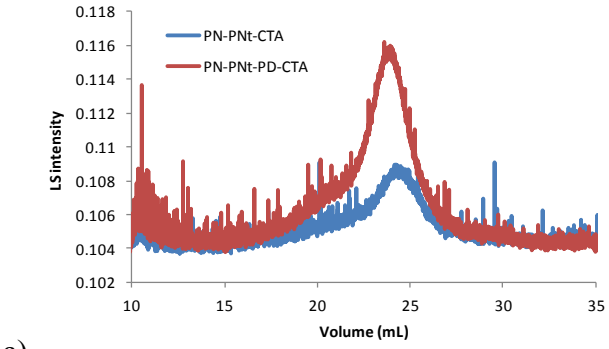

a)

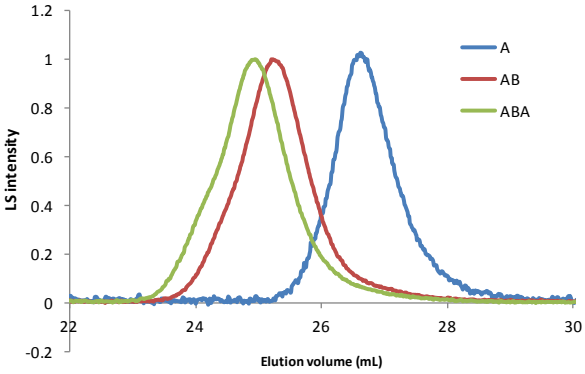

b)

Figure 4.11. GPC curves for a) PN(N/A)D and b) PN(N/A)N

Table 4.2. Molecular weight estimation: comparison of Universal calibration vs Refractive Index increment (dn/dc)

Sample	M_n [a] Universal Cal (RI)	M_n [b] dn/dc = 0.107 gm/mL(LS)
PN_{83}-CTA	11,000	9,000
PN_{83}- PN_{390}-*co*-*t*BA_{34}-CTA	58,000	58,000
PN_{83}- PN_{390}-*co*-*t*BA_{34}-PN_{53}-CTA	64,000	64,000
PN_{83}- PN_{390}-*co*-*t*BA_{34}-PD_{39}-CTA	61,000	63,000

[a]Number average molecular weight (M_n) calculated by universal calibration using Mark-Houwink-Sakaruda (MHS) parameters for polystyrene ($k = 11.4x10^{-5}$ dL gm^{-1}; $a = 0.72$) and polyNIPAm ($k = 9.6x10^{-5}$ dL gm^{-1}; $a = 0.65$). [b] M_n estimated from refractive index signal using dn/dc increment for polyNIPAm (dn/dc = 0.107 gm mL^{-1}). Subscripts refer to number of monomer units per block.

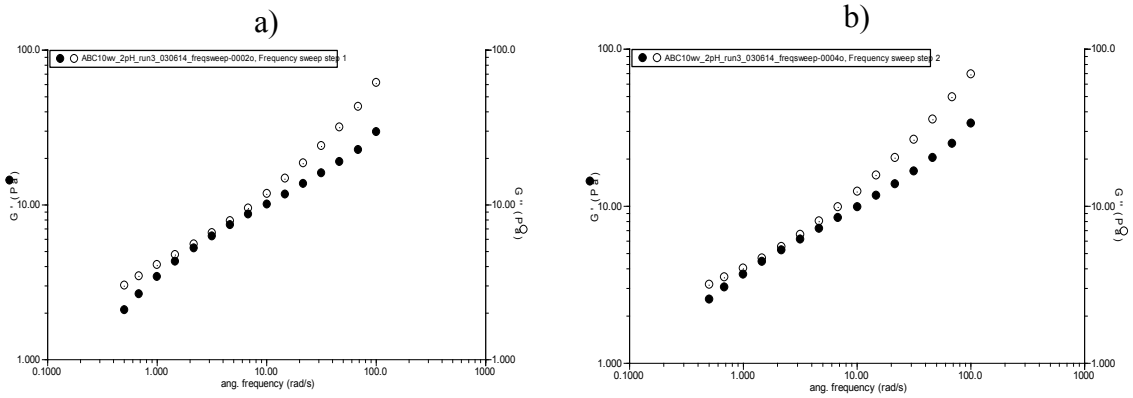

Figure 4.12 Dynamic shear moduli (G' and G") as a function of frequency for 10w/v% PN-PNa-PD in pH 2 aqueous solutions at a) 32 °C and b) 34 °C. The measurements were made at a strain amplitude of 1 %.

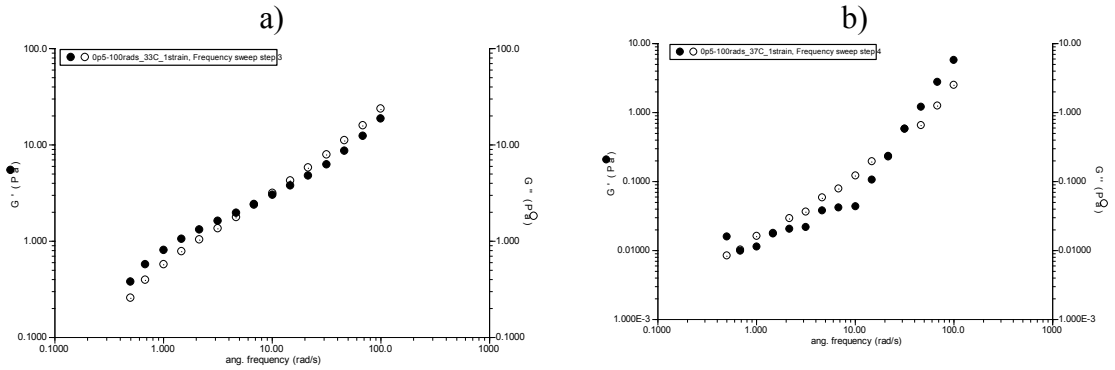

Figure 4.13. Dynamic shear moduli (G′ and G″) as a function of frequency for 10w/v% PN-PNa-PN in pH 2 aqueous solutions at a) 33 °C and b) 37 °C. The measurements were made at a strain amplitude of 1 %.

Chapter V

Summary and Future Direction

5.1. Summary

The aim of the present study was to synthesize and characterize dual temperature and pH responsive triblock polymers. The triblock polymers were designed to undergo temperature and pH-triggered gelation, which was mediated by phase separation of end blocks.

The first system tested was a triblock with a permanently hydrophobic first block, PEP, a hydrophilic midblock, PEO, and a dual temperature and pH responsive third block P(NIPAm-*co*-AA). This work in Chapter II was carried out in equal collaboration with Dr. Can Zhou in the Department of Chemistry. The triblock PEP-PEO-P(NIPAm-*co*-AA) spontaneously formed micelles at room temperature with the hydrophobic PEP block forming the core, the hydrophilic PEO forming the shell and the dual responsive P(NIPAm-*co*-AA) forming the corona. The polymer exhibited a sol-gel transition at high temperatures and low pH values. Gelation was brought about by collapse of the coronal chains into hydrophobic domains. Thus, the triblock was able to form physical gels that were dictated by temperature and pH.

This system also demonstrated that comonomer incorporation can be used as a tool to control gelation conditions. A PEP-PEO-PNIPAm triblock, previously studied by Dr. Zhou, was solely a thermoresponsive gelator. Incorporation of AA in the PNIPAm block led to gelation becoming a function of both pH as well as temperature. It was seen that at low pH values, the triblock worked well as a gelator, while under more alkaline

conditions, gelation did not take place and the polymer remained as a micellar solution. This kind of pH-modulated gelator can be used to switch between controlled and burst release of drugs from polymer matrices.

The second polymer system was a PNIPAm-P(NIPAm-*co*-AA)-PDEAm triblock containing the thermoresponsive end blocks PNIPAm and PDEAm and a dual temperature and pH responsive midblock P(NIPAm-*co*-AA).The three blocks in this case were structurally very similar to one another, and the aim of the project was to see whether minor structural difference in the various blocks can lead to efficient gelators. In Chapter III, solution behavior of the homopolymers, diblocks and triblocks were studied in dilute solution. Cloud point measurements probed polymer solubility under various temperature and pH conditions. The effect of AA substitution on solution properties of AA containing polymers was studied. It was found that degree of AA incorporation has significant influence on block solubility at various pH conditions.The polymers were synthesized by RAFT polymerization. RAFT allowed good control over the molecular weights and low PDIs.

In Chapter IV, gelation behavior of the PNIPAm-P(NIPAm-*co*-AA)-PDEAm triblock was investigated. For this study, the CTA-derived end groups were removed from the triblock in order to avoid chain end effects. At pH 2, the triblock phase separated to form aggregates at 29 °C. At pH 7.4, a polymer solubility transition took place at higher temperatures and the polymer formed a viscoelastic fluid at 45 °C. No gel point was observed for the 10% w/v solution. The ABA triblock, PNIPAm-P(NIPAm-*co*-AA)-PNIPAm was also tested for gelation to see how it fared relative to the ABC

polymer. PNIPAm-P(NIPAm-*co*-AA)-PNIPAm exhibited mechanical properties similar to PNIPAm-P(NIPAm-co-AA)-PDEAm. At pH 7.4, on heating, the polymer went from a sol to a viscoelastic fluid state at ~45 °C. Thus, substituting one of the end blocks in PNIPAm-P(NIPAm-co-AA)-PNIPAm with PDEAm did not result in improved gelation.

This study suggested that merely having two hydrophobic side blocks does not guarantee gelation of ABA/ABC triblock polymers. From the two systems studied, it can be concluded from the PEP-PEO-PNIPAm study that a micellization step prior to gelation may be critical for obtaining gels at low concentrations. Micellization with one of the end blocks forming the core helps in segregating the A and C blocks. Thus when the other endblock phase separates into hydrophobic domains of its own, the system is able to maximize the number of interdomain linkages.

If the A and C blocks phase separate from solution simultaneously, then segregation of A and C becomes difficult and the probability of A and C mixing increases. In case of PNIPAm-P(NIPAm-*co*-AA)-PDEAm triblock, the sideblocks PNIPAm and PDEAm exhibit LCSTs only a few degrees apart. Moreover, literature reports suggest that PNIPAm and PDEAm form intermolecular H bonds. Thus the amplification of weak repulsive tendencies that often leads to segregation of unlike nonpolar blocks may be replaced by amplified of weak attractions leading to interspersion of the PNIPAm and PDEAm blocks. So, on heating, phase separation of PNIPAm-P(NIPAm-*co*-AA)-PDEAm leads to micelles and aggregates with PNIPAm and PDEAm interacting with one another and collapsing into common hydrophobic domains.

This led to the ABC triblock exhibiting qualitatively similar behaviors behavior as those exhibited by ABA triblocks.

To design efficient triblock gelators based on PNIPAm, the following aspects should be considered:

1. The A block should be highly hydrophobic with a low critical micelle concentration to enable formation of micelles in which the A block is localized in the micelle core
2. The C block can be a thermally responsive polymer, such as PNIPAm
3. The A and C block structures should be studied to ensure that they are not attractive.
4. The B block should be highly hydrophilic

5.2. Future direction

Injectable gels based on stimuli responsive block polymers. Injectable gels can serve as a means of achieving prolonged drug release from polymer matrices while possessing the advantage of being minimally invasive. They also provide a convenient means of drug loading wherein the drug can be mixed with the polymer solution and administered through a syringe needle prior to gelation. Injectable gels can be used for the delivery of both hydrophobic and hydrophilic drugs [207]. They can also be used as tissue engineering scaffolds. Injectable gels, being liquids prior to gelation, can conform to the shape of the implantation site. Gel porosity and mechanical strength can be controlled by polymer composition and molecular weight. Gelation can be made to occur in response to temperature, pH and ionic strength by using stimuli responsive block polymers. Temperature is one of the more widely investigated stimuli as the difference

between room temperature and body temperature can be exploited for biomedical applications [196] .

While there are a number of natural biopolymers such as gelatin, cellulose and carrageenans that form thermoreversible gels, gelation in most of these cases occurs due to lowering of temperature [222]. Amphiphilic block polymers have been widely investigated as inverse thermogels, since they can undergo sol-gel transition with increase in temperature. Their ability to segregate into microscale hydrophobic and hydrophilic domains is crucial to their success as physical gels. A number of triblock polymers based on biocompatible and biodegradable polymers such as poly(ethylene oxide) (PEO), poly(propylene oxide) (PPO), and poly(lactic acid-*co*-glycolic acid) (PLGA) have been tested as thermo gelling injectable systems [223-227]. Such triblocks typically have an ABA architecture with similar endblocks and a chemically different midblock. Gelation in most of these systems is preceded by micellization [228]. The gel state is reached when the micelles undergo close packing with a percolating network mediated through intermicellar entanglements. The critical gelation concentrations for these systems are in the range of 10-25%.

In so far as polymer viscosity is strongly dependent on polymer concentration, such high concentrations may lead to problems with injectability. Lower polymer concentrations are also desirable to reduce the amount of polymer, which is an inactive ingredient, being administered into the body. For these reasons, it is desirable to have injectable gels based on block polymers in which intermicellar linkages set in at relatively low polymer concentrations. There are few studies that have looked at

biocompatible polymers that exhibit such behavior. There are even fewer studies that have looked at ABC triblocks that may lead to gelation at lower polymer concentrations. So there is scope to design better injectable gels based on LCST polymers.

Biocompatible and biodegradable monomers are ultimately required for a triblock to be employed as an injectable gel. One of the end blocks may be a highly hydrophobic polymer such as PCL. A small amount of poly(L-lactide) (PLLA) (< 5 mol%) can be incorporated in PCL to limit its crystallinity and enhance its biodegradability [229]. A hydrophilic polymer such as PEO may be a good candidate to serve as the midblock [230]. For a pH-responsive midblock, poly(2-hydroxymethylacrylate) copolymerized with acrylic acid can be a suitable alternative to PEO. The third end block could be chosen to be a thermoresponsive polymer with an LCST between 25 and 37 °C. A copolymer of 2-(2-methoxyehtoxy)ethyl methacrylate) (MEO_2MA) and oligo(ethylene glycol)ethyl methacrylate (OEGMA) could be used as the thermoresponsive side block [231]. Biodegradability of P(MEO_2MA-*co*-OEGMA) can be enhanced by adding a small fraction of labile ester groups by copolymerizing the PEG analogues with 5,6-benzo-2-methylene-1,3-dioxepane (BMDO) [232]. BMDO has also been reported to improve degradability of PNIPAm [233].

To summarize, the experience garnered in this dissertation work suggests that an ABC triblock with a nonpolar hydrophobic A block, a hydrophilic B block and an inverse thermoresponsive C block would be an ideal candidate to study injectable gels with low critical gel concentration.

Bibliography

1. Kim, J.K., et al., *Functional nanomaterials based on block copolymer self-assembly.* Progress in Polymer Science, 2010. **35**(11): p. 1325-1349.
2. Mijatovic, D., J. Eijkel, and A. Van Den Berg, *Technologies for nanofluidic systems: top-down vs. bottom-up—a review.* Lab on a Chip, 2005. **5**(5): p. 492-500.
3. Lazzari, M., G. Liu, and S. Lecommandoux, *Block copolymers in nanoscience*. 2007: John Wiley & Sons.
4. Darling, S.B., *Directing the self-assembly of block copolymers.* Progress in Polymer Science, 2007. **32**(10): p. 1152-1204.
5. Bates, F.S., *Polymer-Polymer Phase Behavior.* Science, 1991. **251**(4996): p. 898-905.
6. Park, C., J. Yoon, and E.L. Thomas, *Enabling nanotechnology with self assembled block copolymer patterns.* Polymer, 2003. **44**(22): p. 6725-6760.
7. Rodríguez-Hernández, J., et al., *Toward 'smart' nano-objects by self-assembly of block copolymers in solution.* Progress in Polymer Science, 2005. **30**(7): p. 691-724.
8. Matsen, M.W. and F. Bates, *Origins of complex self-assembly in block copolymers.* Macromolecules, 1996. **29**(23): p. 7641-7644.
9. Bates, F.S., et al., *Fluctuations, conformational asymmetry and block copolymer phase behaviour.* Faraday Discuss., 1994. **98**: p. 7-18.
10. Matsen, M.W. and F.S. Bates, *Unifying Weak- and Strong-Segregation Block Copolymer Theories.* Macromolecules, 1996. **29**(4): p. 1091-1098.
11. Malmsten, M. and B. Lindman, *Self-assembly in aqueous block copolymer solutions.* Macromolecules, 1992. **25**(20): p. 5440-5445.
12. Shenhar, R., T.B. Norsten, and V.M. Rotello, *Polymer-Mediated Nanoparticle Assembly: Structural Control and Applications.* Advanced Materials, 2005. **17**(6): p. 657-669.
13. Qiu, Y. and K. Park, *Environment-sensitive hydrogels for drug delivery.* Advanced Drug Delivery Reviews, 2001. **53**(3): p. 321-339.
14. Gil, E.S. and S.M. Hudson, *Stimuli-reponsive polymers and their bioconjugates.* Progress in Polymer Science, 2004. **29**(12): p. 1173-1222.
15. Schmaljohann, D., *Thermo- and pH-responsive polymers in drug delivery.* Advanced Drug Delivery Reviews, 2006. **58**(15): p. 1655-1670.
16. Li, M.-H. and P. Keller, *Stimuli-responsive polymer vesicles.* Soft Matter, 2009. **5**(5): p. 927-937.
17. Chécot, F., et al., *Structure of Polypeptide-Based Diblock Copolymers in Solution: Stimuli-Responsive Vesicles and Micelles.* Langmuir, 2005. **21**(10): p. 4308-4315.
18. Motornov, M., et al., *Stimuli-responsive nanoparticles, nanogels and capsules for integrated multifunctional intelligent systems.* Progress in Polymer Science, 2010. **35**(1–2): p. 174-211.

19. Hoffman, A.S. *"intelligent" polymers in medicine and biotechnology*. in *Macromolecular Symposia*. 1995: Wiley Online Library.
20. Li, D., Q. He, and J. Li, *Smart core/shell nanocomposites: intelligent polymers modified gold nanoparticles.* Advances in colloid and interface science, 2009. **149**(1): p. 28-38.
21. Alarcon, C.D.H., S. Pennadam, and C. Alexander, *Stimuli responsive polymers for biomedical applications.* Chemical Society Reviews, 2005. **34**(3): p. 276-285.
22. Jeong, B. and A. Gutowska, *Lessons from nature: stimuli-responsive polymers and their biomedical applications.* Trends in Biotechnology, 2002. **20**(7): p. 305-311.
23. Galaev, I.Y. and B. Mattiasson, *'Smart' polymers and what they could do in biotechnology and medicine.* Trends in Biotechnology, 1999. **17**(8): p. 335-340.
24. Mendes, P.M., *Stimuli-responsive surfaces for bio-applications.* Chemical Society Reviews, 2008. **37**(11): p. 2512-2529.
25. Ebara, M., et al., *Temperature-Responsive Cell Culture Surfaces Enable "On−Off" Affinity Control between Cell Integrins and RGDS Ligands.* Biomacromolecules, 2004. **5**(2): p. 505-510.
26. Kretlow, J.D., L. Klouda, and A.G. Mikos, *Injectable matrices and scaffolds for drug delivery in tissue engineering.* Advanced Drug Delivery Reviews, 2007. **59**(4): p. 263-273.
27. Furth, M.E., A. Atala, and M.E. Van Dyke, *Smart biomaterials design for tissue engineering and regenerative medicine.* Biomaterials, 2007. **28**(34): p. 5068-5073.
28. Tokarev, I., et al., *Stimuli-Responsive Hydrogel Membranes Coupled with Biocatalytic Processes.* ACS Applied Materials & Interfaces, 2009. **1**(3): p. 532-536.
29. Hyun, J., et al., *Capture and Release of Proteins on the Nanoscale by Stimuli-Responsive Elastin-Like Polypeptide "Switches".* Journal of the American Chemical Society, 2004. **126**(23): p. 7330-7335.
30. Wang, Y., et al., *Nanostructured polymer assemblies formed at interfaces: applications from immobilization and encapsulation to stimuli-responsive release.* Physical Chemistry Chemical Physics, 2011. **13**(11): p. 4782-4801.
31. Gibson, M.I. and R.K. O'Reilly, *To aggregate, or not to aggregate? considerations in the design and application of polymeric thermally-responsive nanoparticles.* Chemical Society Reviews, 2013. **42**(17): p. 7204-7213.
32. Hoogenboom, R., et al., *Solubility and Thermoresponsiveness of PMMA in Alcohol-Water Solvent Mixtures.* Australian Journal of Chemistry, 2010. **63**(8): p. 1173-1178.
33. Glatzel, S., A. Laschewsky, and J.-F. Lutz, *Well-defined uncharged polymers with a sharp UCST in water and in physiological milieu.* Macromolecules, 2010. **44**(2): p. 413-415.
34. Aoki, T., et al., *Adenosine-induced changes of the phase transition of poly (6-(acryloyloxymethyl) uracil) aqueous solution.* Polymer journal, 1999. **31**: p. 1185-1188.

35. Liu, R., M. Fraylich, and B.R. Saunders, *Thermoresponsive copolymers: from fundamental studies to applications.* Colloid Polym Sci, 2009. **287**: p. 627-643.
36. Cho, E.C., J. Lee, and K. Cho, *Role of Bound Water and Hydrophobic Interaction in Phase Transition of Poly(N-isopropylacrylamide) Aqueous Solution.* Macromolecules, 2003. **36**(26): p. 9929-9934.
37. Otake, K., et al., *Thermal analysis of the volume phase transition with N-isopropylacrylamide gels.* Macromolecules, 1990. **23**(1): p. 283-289.
38. Lin, S.-Y., K.-S. Chen, and R.-C. Liang, *Thermal micro ATR/FT-IR spectroscopic system for quantitative study of the molecular structure of poly(N-isopropylacrylamide) in water.* Polymer, 1999. **40**(10): p. 2619-2624.
39. Feil, H., et al., *Effect of comonomer hydrophilicity and ionization on the lower critical solution temperature of N-isopropylacrylamide copolymers.* Macromolecules, 1993. **26**(10): p. 2496-2500.
40. Inomata, H., S. Goto, and S. Saito, *Phase transition of N-substituted acrylamide gels.* Macromolecules, 1990. **23**(22): p. 4887-4888.
41. Laschewsky, A., E.D. Rekaï, and E. Wischerhoff, *Tailoring of Stimuli-Responsive Water Soluble Acrylamide and Methacrylamide Polymers.* Macromolecular Chemistry and Physics, 2001. **202**(2): p. 276-286.
42. Hoffman, A.S., *Stimuli-responsive polymers: Biomedical applications and challenges for clinical translation.* Advanced Drug Delivery Reviews, 2012(0).
43. Friend, D.R., *New oral delivery systems for treatment of inflammatory bowel disease.* Advanced Drug Delivery Reviews, 2005. **57**(2): p. 247-265.
44. Yin, X., A.S. Hoffman, and P.S. Stayton, *Poly(N-isopropylacrylamide-co-propylacrylic acid) Copolymers That Respond Sharply to Temperature and pH.* Biomacromolecules, 2006. **7**(5): p. 1381-1385.
45. Mujumdar, S.K., A.S. Bhalla, and R.A. Siegel, *Novel Hydrogels for Rhythmic Pulsatile Drug Delivery.* Macromolecular Symposia, 2007. **254**(1): p. 338-344.
46. Maeda, Y., H. Yamamoto, and I. Ikeda, *Effects of Ionization of Incorporated Imidazole Groups on the Phase Transitions of Poly(N-isopropylacrylamide), Poly(N,N-diethylacrylamide), and Poly(N-vinylcaprolactam) in Water.* Langmuir, 2001. **17**(22): p. 6855-6859.
47. Maeda, Y., H. Yamamoto, and I. Ikeda, *Effects of ionization on the phase behavior of poly(N-isopropylacrylamide-co-acrylic acid) and poly(N,N-diethylacrylamide-co-acrylic acid) in water.* Colloid and Polymer Science, 2004. **282**(11): p. 1268-1273.
48. Faucheux, N., et al., *Self-assembled monolayers with different terminating groups as model substrates for cell adhesion studies.* Biomaterials, 2004. **25**(14): p. 2721-2730.
49. Zhang, M., T. Desai, and M. Ferrari, *Proteins and cells on PEG immobilized silicon surfaces.* Biomaterials, 1998. **19**(10): p. 953-960.
50. Feng, W., et al., *Adsorption of Fibrinogen and Lysozyme on Silicon Grafted with Poly(2-methacryloyloxyethyl Phosphorylcholine) via Surface-Initiated Atom Transfer Radical Polymerization.* Langmuir, 2005. **21**(13): p. 5980-5987.

51. Hucknall, A., S. Rangarajan, and A. Chilkoti, *In Pursuit of Zero: Polymer Brushes that Resist the Adsorption of Proteins.* Advanced Materials, 2009. **21**(23): p. 2441-2446.
52. Senaratne, W., L. Andruzzi, and C.K. Ober, *Self-Assembled Monolayers and Polymer Brushes in Biotechnology: Current Applications and Future Perspectives.* Biomacromolecules, 2005. **6**(5): p. 2427-2448.
53. Shimizu, T., et al., *Cell sheet engineering for myocardial tissue reconstruction.* Biomaterials, 2003. **24**(13): p. 2309-2316.
54. Kataoka, K., A. Harada, and Y. Nagasaki, *Block copolymer micelles for drug delivery: Design, characterization and biological significance.* Advanced Drug Delivery Reviews, 2012. **64, Supplement**(0): p. 37-48.
55. Blanazs, A., S.P. Armes, and A.J. Ryan, *Self-Assembled Block Copolymer Aggregates: From Micelles to Vesicles and their Biological Applications.* Macromolecular Rapid Communications, 2009. **30**(4-5): p. 267-277.
56. Putnam, D., et al., *Polyhistidine–PEG:DNA nanocomposites for gene delivery.* Biomaterials, 2003. **24**(24): p. 4425-4433.
57. Kataoka, K., et al. *Smart polymeric micelles as nanocarriers for oligonucleotides and siRNA delivery*. in *Nucleic Acids Symposium Series*. 2005: Oxford Univ Press.
58. Li, W. and F.C. Szoka Jr, *Lipid-based nanoparticles for nucleic acid delivery.* Pharmaceutical research, 2007. **24**(3): p. 438-449.
59. Allen, T.M. and P.R. Cullis, *Liposomal drug delivery systems: From concept to clinical applications.* Advanced Drug Delivery Reviews, 2013. **65**(1): p. 36-48.
60. Hoffman, A.S., *The origins and evolution of "controlled" drug delivery systems.* Journal of Controlled Release, 2008. **132**(3): p. 153-163.
61. Rösler, A., G.W.M. Vandermeulen, and H.-A. Klok, *Advanced drug delivery devices via self-assembly of amphiphilic block copolymers.* Advanced Drug Delivery Reviews, 2012. **64, Supplement**(0): p. 270-279.
62. Discher, B.M., et al., *Polymersomes: Tough Vesicles Made from Diblock Copolymers.* Science, 1999. **284**(5417): p. 1143-1146.
63. Katz, J.S., et al., *Modular Synthesis of Biodegradable Diblock Copolymers for Designing Functional Polymersomes.* Journal of the American Chemical Society, 2010. **132**(11): p. 3654-3655.
64. Ahmed, F., et al., *Biodegradable polymersomes loaded with both paclitaxel and doxorubicin permeate and shrink tumors, inducing apoptosis in proportion to accumulated drug.* Journal of Controlled Release, 2006. **116**(2): p. 150-158.
65. Vriezema, D.M., et al., *Positional Assembly of Enzymes in Polymersome Nanoreactors for Cascade Reactions.* Angewandte Chemie International Edition, 2007. **46**(39): p. 7378-7382.
66. Du, J. and R.K. O'Reilly, *Advances and challenges in smart and functional polymer vesicles.* Soft Matter, 2009. **5**(19): p. 3544-3561.
67. Kim, M.S. and D.S. Lee, *Biodegradable and pH-sensitive polymersome with tuning permeable membrane for drug delivery carrier.* Chemical Communications, 2010. **46**(25): p. 4481-4483.

68. Yu, S., et al., *"Breathing" Vesicles.* Journal of the American Chemical Society, 2009. **131**(30): p. 10557-10566.
69. Du, J., et al., *pH-Sensitive Vesicles Based on a Biocompatible Zwitterionic Diblock Copolymer.* Journal of the American Chemical Society, 2005. **127**(51): p. 17982-17983.
70. Rodríguez-Hernández, J. and S. Lecommandoux, *Reversible Inside−Out Micellization of pH-responsive and Water-Soluble Vesicles Based on Polypeptide Diblock Copolymers.* Journal of the American Chemical Society, 2005. **127**(7): p. 2026-2027.
71. Ghoroghchian, P.P., et al., *Bioresorbable vesicles formed through spontaneous self-assembly of amphiphilic poly (ethylene oxide)-block-polycaprolactone.* Macromolecules, 2006. **39**(5): p. 1673-1675.
72. Qin, S., et al., *Temperature-Controlled Assembly and Release from Polymer Vesicles of Poly(ethylene oxide)-block- poly(N-isopropylacrylamide).* Advanced Materials, 2006. **18**(21): p. 2905-2909.
73. Hales, M., et al., *Shell-cross-linked vesicles synthesized from block copolymers of poly (D, L-lactide) and poly (N-isopropyl acrylamide) as thermoresponsive nanocontainers.* Langmuir, 2004. **20**(25): p. 10809-10817.
74. Ahn, S.-k., et al., *Stimuli-responsive polymer gels.* Soft Matter, 2008. **4**(6): p. 1151-1157.
75. Henn, D.M., et al., *Tertiary Amine-Containing Thermo- and pH-Sensitive Hydrophilic ABA Triblock Copolymers: Effect of Different Tertiary Amines on Thermally Induced Sol-Gel Transitions.* Langmuir, 2014.
76. Reinicke, S., et al., *Smart hydrogels based on double responsive triblock terpolymers.* Soft Matter, 2009. **5**(13): p. 2648-2657.
77. Ma, Y., et al., *Synthesis of Biocompatible, Stimuli-Responsive, Physical Gels Based on ABA Triblock Copolymers.* Biomacromolecules, 2003. **4**(4): p. 864-868.
78. Iddon, P.D. and S.P. Armes, *Synthesis of stimulus-responsive block copolymer gelators by atom transfer radical polymerisation.* European Polymer Journal, 2007. **43**(4): p. 1234-1244.
79. Taktak, F.F. and V. Bütün, *Synthesis and physical gels of pH- and thermo-responsive tertiary amine methacrylate based ABA triblock copolymers and drug release studies.* Polymer, 2010. **51**(16): p. 3618-3626.
80. Hillmyer, M., *Block copolymer synthesis.* Current Opinion in Solid State and Materials Science, 1999. **4**(6): p. 559-564.
81. Moad, G., E. Rizzardo, and S.H. Thang, *Living Radical Polymerization by the RAFT Process – A Second Update.* Australian Journal of Chemistry, 2009. **62**(11): p. 1402-1472.
82. Keddie, D.J., *A guide to the synthesis of block copolymers using reversible-addition fragmentation chain transfer (RAFT) polymerization.* Chemical Society Reviews, 2014. **43**(2): p. 496-505.
83. Chong, Y., et al., *A more versatile route to block copolymers and other polymers of complex architecture by living radical polymerization: the RAFT process.* Macromolecules, 1999. **32**(6): p. 2071-2074.

84. Gregory, A. and M.H. Stenzel, *Complex polymer architectures via RAFT polymerization: From fundamental process to extending the scope using click chemistry and nature's building blocks.* Progress in Polymer Science, 2012. **37**(1): p. 38-105.
85. Zhou, C., M.A. Hillmyer, and T.P. Lodge, *Efficient Formation of Multicompartment Hydrogels by Stepwise Self-Assembly of Thermoresponsive ABC Triblock Terpolymers.* Journal of the American Chemical Society, 2012. **134**(25): p. 10365-10368.
86. Balsara, N.P., M. Tirrell, and T.P. Lodge, *Micelle formation of BAB triblock copolymers in solvents that preferentially dissolve the A block.* Macromolecules, 1991. **24**(8): p. 1975-1986.
87. Nath, N. and A. Chilkoti, *Creating "Smart" Surfaces Using Stimuli Responsive Polymers.* Advanced Materials, 2002. **14**(17): p. 1243-1247.
88. Stuart, M.A.C., et al., *Emerging applications of stimuli-responsive polymer materials.* Nature Materials, 2010. **9**(2): p. 101-113.
89. Hosoya, K., et al., *Temperature-Controlled High-Performance Liquid Chromatography Using A Uniformly Sized Temperature-Responsive Polymer-Based Packing Material.* Analytical Chemistry, 1995. **67**(11): p. 1907-1911.
90. Wischerhoff, E., et al., *Smart bioactive surfaces.* Soft Matter, 2010. **6**(4): p. 705-713.
91. Galperin, A., T.J. Long, and B.D. Ratner, *Degradable, Thermo-Sensitive Poly(N-isopropyl acrylamide)-Based Scaffolds with Controlled Porosity for Tissue Engineering Applications.* Biomacromolecules, 2010. **11**(10): p. 2583-2592.
92. Kanazawa, H., et al., *Temperature-Responsive Chromatography Using Poly(N-isopropylacrylamide)-Modified Silica.* Analytical Chemistry, 1996. **68**(1): p. 100-105.
93. Kanazawa, H., et al., *Temperature-Responsive Chromatographic Separation of Amino Acid Phenylthiohydantoins Using Aqueous Media as the Mobile Phase.* Analytical Chemistry, 2000. **72**(24): p. 5961-5966.
94. Kobayashi, J., et al., *Aqueous Chromatography Utilizing pH-/Temperature-Responsive Polymer Stationary Phases To Separate Ionic Bioactive Compounds.* Analytical Chemistry, 2001. **73**(9): p. 2027-2033.
95. Kikuchi, A. and T. Okano, *Intelligent thermoresponsive polymeric stationary phases for aqueous chromatography of biological compounds.* Progress in Polymer Science, 2002. **27**(6): p. 1165-1193.
96. Akiyama, Y., et al., *Ultrathin Poly(N-isopropylacrylamide) Grafted Layer on Polystyrene Surfaces for Cell Adhesion/Detachment Control.* Langmuir, 2004. **20**(13): p. 5506-5511.
97. Xu, F.J., et al., *Surface-Active and Stimuli-Responsive Polymer−Si(100) Hybrids from Surface-Initiated Atom Transfer Radical Polymerization for Control of Cell Adhesion.* Biomacromolecules, 2004. **5**(6): p. 2392-2403.
98. Cole, M.A., et al., *Stimuli-responsive interfaces and systems for the control of protein–surface and cell–surface interactions.* Biomaterials, 2009. **30**(9): p. 1827-1850.

99. Mizutani, A., et al., *Preparation of thermoresponsive polymer brush surfaces and their interaction with cells.* Biomaterials, 2008. **29**(13): p. 2073-2081.
100. Mano, J.F., *Stimuli-Responsive Polymeric Systems for Biomedical Applications.* Advanced Engineering Materials, 2008. **10**(6): p. 515-527.
101. Kim, S. and K.E. Healy, *Synthesis and Characterization of Injectable Poly(N-isopropylacrylamide-co-acrylic acid) Hydrogels with Proteolytically Degradable Cross-Links.* Biomacromolecules, 2003. **4**(5): p. 1214-1223.
102. Nakamura, K., et al., *Uptake and release of budesonide from mucoadhesive, pH-sensitive copolymers and their application to nasal delivery.* Journal of Controlled Release, 1999. **61**(3): p. 329-335.
103. Schild, H.G., *Poly(N-isopropylacrylamide): experiment, theory and application.* Progress in Polymer Science, 1992. **17**(2): p. 163-249.
104. Winnik, F.M., *Fluorescence studies of aqueous solutions of poly(N-isopropylacrylamide) below and above their LCST.* Macromolecules, 1990. **23**(1): p. 233-242.
105. Heskins, M. and J.E. Guillet, *Solution Properties of Poly(N-isopropylacrylamide).* Journal of Macromolecular Science: Part A - Chemistry, 1968. **2**(8): p. 1441-1455.
106. Fujishige, S., K. Kubota, and I. Ando, *Phase transition of aqueous solutions of poly(N-isopropylacrylamide) and poly(N-isopropylmethacrylamide).* The Journal of Physical Chemistry, 1989. **93**(8): p. 3311-3313.
107. Ono, Y. and T. Shikata, *Hydration and Dynamic Behavior of Poly(N-isopropylacrylamide)s in Aqueous Solution: A Sharp Phase Transition at the Lower Critical Solution Temperature.* Journal of the American Chemical Society, 2006. **128**(31): p. 10030-10031.
108. Shibayama, M., M. Morimoto, and S. Nomura, *Phase Separation Induced Mechanical Transition of Poly(N-isopropylacrylamide)/Water Isochore Gels.* Macromolecules, 1994. **27**(18): p. 5060-5066.
109. Kogure, H., et al., *Hydration and dehydration behavior of <i>N</i>-isopropylacrylamide gel particles.* Colloid & Polymer Science, 2005. **283**(11): p. 1163-1171.
110. Maeda, Y., T. Higuchi, and I. Ikeda, *Change in Hydration State during the Coil−Globule Transition of Aqueous Solutions of Poly(N-isopropylacrylamide) as Evidenced by FTIR Spectroscopy†.* Langmuir, 2000. **16**(19): p. 7503-7509.
111. Wei, H., et al., *Thermo-sensitive polymeric micelles based on poly(N-isopropylacrylamide) as drug carriers.* Progress in Polymer Science, 2009. **34**(9): p. 893-910.
112. Vogt, A.P. and B.S. Sumerlin, *Temperature and redox responsive hydrogels from ABA triblock copolymers prepared by RAFT polymerization.* Soft Matter, 2009. **5**(12): p. 2347-2351.
113. Lin, H.-H. and Y.-L. Cheng, *In-Situ Thermoreversible Gelation of Block and Star Copolymers of Poly(ethylene glycol) and Poly(N-isopropylacrylamide) of Varying Architectures.* Macromolecules, 2001. **34**(11): p. 3710-3715.

114. Li, C., et al., *Synthesis and Characterization of Biocompatible Thermo-Responsive Gelators Based on ABA Triblock Copolymers.* Biomacromolecules, 2005. **6**(2): p. 994-999.
115. Angelopoulos, S.A. and C. Tsitsilianis, *Thermo-Reversible Hydrogels Based on Poly(N,N-diethylacrylamide)-block-poly(acrylic acid)-block-poly(N,N-diethylacrylamide) Double Hydrophilic Triblock Copolymer.* Macromolecular Chemistry and Physics, 2006. **207**(23): p. 2188-2194.
116. Kirkland, S.E., et al., *Thermoreversible Hydrogels from RAFT-Synthesized BAB Triblock Copolymers: Steps toward Biomimetic Matrices for Tissue Regeneration†.* Biomacromolecules, 2007. **9**(2): p. 481-486.
117. Bromberg, L.E. and E.S. Ron, *Temperature-responsive gels and thermogelling polymer matrices for protein and peptide delivery.* Advanced Drug Delivery Reviews, 1998. **31**(3): p. 197-221.
118. Li, C., et al., *Synthesis and Characterization of Biocompatible, Thermoresponsive ABC and ABA Triblock Copolymer Gelators.* Langmuir, 2005. **21**(24): p. 11026-11033.
119. Nedelcheva, A.N., et al., *Associative block copolymers comprising poly(N-isopropylacrylamide) and poly(ethylene oxide) end-functionalized with a fluorophilic or hydrophilic group. Synthesis and aqueous solution properties.* Journal of Polymer Science Part A: Polymer Chemistry, 2004. **42**(22): p. 5736-5744.
120. Sugihara, S., S. Kanaoka, and S. Aoshima, *Stimuli-responsive ABC triblock copolymers by sequential living cationic copolymerization: Multistage self-assemblies through micellization to open association.* Journal of Polymer Science Part A: Polymer Chemistry, 2004. **42**(11): p. 2601-2611.
121. Zhou, C., M.A. Hillmyer, and T.P. Lodge, *Micellization and Micellar Aggregation of Poly(ethylene-alt-propylene)-b-poly(ethylene oxide)-b-poly(N-isopropylacrylamide) Triblock Terpolymers in Water.* Macromolecules, 2011. **44**(6): p. 1635-1641.
122. O'Lenick, T.G., X. Jiang, and B. Zhao, *Thermosensitive Aqueous Gels with Tunable Sol−Gel Transition Temperatures from Thermo- and pH-Responsive Hydrophilic ABA Triblock Copolymer.* Langmuir, 2010. **26**(11): p. 8787-8796.
123. Yoshida, R., et al., *Modulating the phase transition temperature and thermosensitivity in N-isopropylacrylamide copolymer gels.* Journal of Biomaterials Science, Polymer Edition, 1995. **6**(6): p. 585-598.
124. Vasilevskaya, V.V., A.R. Khokhlov, and K. Yoshikawa, *Single Polyelectrolyte Molecule in Salt Solution: Effect of Escaped Counter Ions.* Macromol. Theory Sim. , 2000. **9**: p. 600-607.
125. Kang, S.I. and Y.H. Bae, *pH/Temperature-Sensitive Polymer:Poly(N-Isopropylacrylamide-co-Methacryloylated Sulfamethoxypyridazine).* Macromol. Chem. Symp., 2001. **14**: p. 145-155.
126. Charbonneau, C.l., et al., *Controlling the Dynamics of Self-Assembled Triblock Copolymer Networks via the pH.* Macromolecules, 2011. **44**(11): p. 4487-4495.

127. Chen, G. and A.S. Hoffman, *Temperature-induced phase transition behaviors of random vs. graft copolymers of N-isopropylacrylamide and acrylic acid.* Macromolecular Rapid Communications, 1995. **16**(3): p. 175-182.
128. Schilli, C.M., et al., *A New Double-Responsive Block Copolymer Synthesized via RAFT Polymerization: Poly(N-isopropylacrylamide)-block-poly(acrylic acid).* Macromolecules, 2004. **37**(21): p. 7861-7866.
129. Jones, M.S., *Effect of pH on the lower critical solution temperatures of random copolymers of N-isopropylacrylamide and acrylic acid.* European Polymer Journal, 1999. **35**(5): p. 795-801.
130. Yoo, M.K., et al., *Effect of polymer complex formation on the cloud-point of poly(N-isopropyl acrylamide) (PNIPAAm) in the poly(NIPAAm-co-acrylic acid): polyelectrolyte complex between poly(acrylic acid) and poly(allylamine).* Polymer, 1997. **38**(11): p. 2759-2765.
131. Qiu, X., C.M.S. Kwan, and C. Wu, *Laser Light Scattering Study of the Formation and Structure of Poly(N-isopropylacrylamide-co-acrylic acid) Nanoparticles.* Macromolecules, 1997. **30**(20): p. 6090-6094.
132. Bokias, G., G. Staikos, and I. Iliopoulos, *Solution properties and phase behaviour of copolymers of acrylic acid with N-isopropylacrylamide: the importance of the intrachain hydrogen bonding.* Polymer, 2000. **41**(20): p. 7399-7405.
133. Bokias, G., et al., *Influence of Migrating Ionic Groups on the Solubility of Polyelectrolytes: Phase Behavior of Ionic Poly(N-isopropylacrylamide) Copolymers in Water.* Macromolecules, 2000. **33**(26): p. 9757-9763.
134. Snowden, M.J., et al., *Colloidal copolymer microgels of N-isopropylacrylamide and acrylic acid: pH, ionic strength and temperature effects.* Journal of the Chemical Society, Faraday Transactions, 1996. **92**(24): p. 5013-5016.
135. Han, C.K. and Y.H. Bae, *Inverse thermally-reversible gelation of aqueous N-isopropylacrylamide copolymer solutions.* Polymer, 1998. **39**(13): p. 2809-2814.
136. Bae, Y.H., et al., *Extracellular matrix for a rechargeable cell delivery system.* Journal of Controlled Release, 1998. **53**(1–3): p. 249-258.
137. Dong, L.C. and A.S. Hoffman, *A novel approach for preparation of pH-sensitive hydrogels for enteric drug delivery.* Journal of Controlled Release, 1991. **15**(2): p. 141-152.
138. Akamatsu, K. and T. Yamaguchi, *Novel Preparation Method for Obtaining pH-Responsive Core−Shell Microcapsule Reactors.* Industrial & Engineering Chemistry Research, 2006. **46**(1): p. 124-130.
139. Ibrahim, K., B. Lofgren, and J. Seppala, *Synthesis of tertiary-butyl acrylate polymers and preparation of diblock copolymers using atom transfer radical polymerization.* European Polymer Journal, 2003. **39**(10): p. 2005-2010.
140. Lai, J.T., D. Filla, and R. Shea, *Functional polymers from novel carboxyl-terminated trithiocarbonates as highly efficient RAFT agents.* Macromolecules, 2002. **35**(18): p. 6754-6756.
141. Kujawa, P., et al., *Impact of End-Group Association and Main-Chain Hydration on the Thermosensitive Properties of Hydrophobically Modified Telechelic*

Poly(N-isopropylacrylamides) in Water. Macromolecules, 2005. **39**(1): p. 341-348.
142. Mehta, A., et al., *Improved Efficiency and Selectivity in Peptide-Synthesis - Use of Triethylsilane as a Carbocation Scavenger in Deprotection of Tert-Butyl Esters and Tert-Butoxycarbonyl-Protected Sites.* Tetrahedron Letters, 1992. **33**(37): p. 5441-5444.
143. Nicolai, T., et al., *Dynamic behavior of .THETA. solutions of polystyrene investigated by dynamic light scattering.* Macromolecules, 1990. **23**(4): p. 1165-1174.
144. Jakeš, J., *Testing of the constrained regularization method of inverting Laplace transform on simulated very wide quasielastic light scattering autocorrelation functions.* Czechoslovak Journal of Physics, 1988. **38**(12): p. 1305-1316.
145. Harding, S.E., D.B. Sattelle, and V.A. Bloomfield, in *Laser Light Scattering in Biochemistry*. 1992, The Royal Society of Chemistry: Cambridge. p. 81.
146. Schillen, K., W. Brown, and R.M. Johnsen, *Micellar Sphere-to-Rod Transition in an Aqueous Triblock Copolymer System. A Dynamic Light Scattering Study of Translational and Rotational Diffusion.* Macromolecules, 1994. **27**(17): p. 4825-4832.
147. Zheng, S., et al., *Study on micellization of poly(N-isopropylacrylamide-butyl acrylate) macromonomers in aqueous solution.* Journal of Applied Polymer Science, 2010. **118**(2): p. 671-677.
148. Zhang, Q.-S., et al., *Synthesis and characterization of novel, temperature-sensitive microgels based on N-isopropylacrylamide and tert-butyl acrylate.* Journal of Applied Polymer Science, 2007. **103**(5): p. 2962-2967.
149. Osada, Y., *Equilibrium study of polymer–polymer complexation of poly(methacrylic acid) and poly(acrylic acid) with complementary polymers through cooperative hydrogen bonding.* Journal of Polymer Science: Polymer Chemistry Edition, 1979. **17**(11): p. 3485-3498.
150. Maeda, Y., H. Yamamoto, and I. Ikeda, *Effects of ionization on the phase behavior of poly(<i>N</i>-isopropylacrylamide-co-acrylic acid) and poly(<i>N</i>, <i>N</i>-diethylacrylamide-co-acrylic acid) in water.* Colloid & Polymer Science, 2004. **282**(11): p. 1268-1273.
151. Lee, K.K., J.C. Jung, and M.S. Jhon, *The synthesis and thermal phase transition behavior of poly(N-isopropylacrylamide)-b-poly(ethylene oxide).* Polymer Bulletin, 1998. **40**(4): p. 455-460.
152. Virtanen, J., et al., *Aggregation in Aqueous Poly(N-isopropylacrylamide)-block-poly(ethylene oxide) Solutions Studied by Fluorescence Spectroscopy and Light Scattering.* Macromolecules, 2002. **35**(12): p. 4763-4769.
153. Zhang, W., et al., *Thermoresponsive Micellization of Poly(ethylene glycol)-b-poly(N-isopropylacrylamide) in Water.* Macromolecules, 2005. **38**(13): p. 5743-5747.
154. Mueller, K.F., *Thermotropic aqueous gels and solutions of N,N-dimethylacrylamide-acrylate copolymers.* Polymer, 1992. **33**(16): p. 3470-3476.

155. Felber, A.E., M.-H. Dufresne, and J.-C. Leroux, *pH-sensitive vesicles, polymeric micelles, and nanospheres prepared with polycarboxylates.* Advanced Drug Delivery Reviews, 2012. **64**(11): p. 979-992.
156. Ivanov, A.E., et al., *Photosensitive copolymer of N-isopropylacrylamide and methacryloyl derivative of spyrobenzopyran.* Polymer, 2002. **43**(13): p. 3819-3823.
157. Irie, M., *Stimuli-responsive poly(<i>N</i>-isopropylacrylamide). Photo- and chemical-induced phase transitions*
Responsive Gels: Volume Transitions II, K. Dušek, Editor. 1993, Springer Berlin / Heidelberg. p. 49-65.
158. Roy, D., J.N. Cambre, and B.S. Sumerlin, *Triply-responsive boronic acid block copolymers: solution self-assembly induced by changes in temperature, pH, or sugar concentration.* Chemical Communications, 2009(16): p. 2106-2108.
159. Shiomori, K., et al., *Thermoresponsive Properties of Sugar Sensitive Copolymer of N-Isopropylacrylamide and 3-(Acrylamido)phenylboronic Acid.* Macromolecular Chemistry and Physics, 2004. **205**(1): p. 27-34.
160. Hoare, T. and R. Pelton, *Engineering Glucose Swelling Responses in Poly(N-isopropylacrylamide)-Based Microgels.* Macromolecules, 2007. **40**(3): p. 670-678.
161. Lapeyre, V., et al., *Monodispersed Glucose-Responsive Microgels Operating at Physiological Salinity.* Biomacromolecules, 2006. **7**(12): p. 3356-3363.
162. Zhang, Y., Y. Guan, and S. Zhou, *Synthesis and Volume Phase Transitions of Glucose-Sensitive Microgels.* Biomacromolecules, 2006. **7**(11): p. 3196-3201.
163. Wang, D., et al., *Stimuli-Responsive Fluorescent Poly(N-isopropylacrylamide) Microgels Labeled with Phenylboronic Acid Moieties as Multifunctional Ratiometric Probes for Glucose and Temperatures.* Macromolecules, 2011. **44**(7): p. 2282-2290.
164. Roy, D., J.N. Cambre, and B.S. Sumerlin, *Sugar-responsive block copolymers by direct RAFT polymerization of unprotected boronic acid monomers.* Chemical Communications, 2008(21): p. 2477-2479.
165. Roy, D. and B.S. Sumerlin, *Glucose-Sensitivity of Boronic Acid Block Copolymers at Physiological pH.* ACS Macro Letters, 2012. **1**(5): p. 529-532.
166. Brazel, C.S. and N.A. Peppas, *Synthesis and Characterization of Thermo- and Chemomechanically Responsive Poly(N-isopropylacrylamide-co-methacrylic acid) Hydrogels.* Macromolecules, 1995. **28**(24): p. 8016-8020.
167. Hillmyer, M.A. and F.S. Bates, *Synthesis and characterization of model polyalkane-poly(ethylene oxide) block copolymers.* Macromolecules, 1996. **29**(22): p. 6994-7002.
168. Rzayev, J. and M.A. Hillmyer, *Nanochannel array plastics with tailored surface chemistry.* Journal of the American Chemical Society, 2005. **127**(38): p. 13373-13379.
169. Qiu, X.P. and F.M. Winnik, *Facile and efficient one-pot transformation of RAFT polymer end groups via a mild aminolysis/Michael addition sequence.* Macromolecular Rapid Communications, 2006. **27**(19): p. 1648-1653.

170. Nykänen, A., et al., *Phase Behavior and Temperature-Responsive Molecular Filters Based on Self-Assembly of Polystyrene-block-poly(N-isopropylacrylamide)-block-polystyrene.* Macromolecules, 2007. **40**(16): p. 5827-5834.
171. Tokarev, I., M. Orlov, and S. Minko, *Responsive Polyelectrolyte Gel Membranes.* Advanced Materials, 2006. **18**(18): p. 2458-2460.
172. Wandera, D., S.R. Wickramasinghe, and S.M. Husson, *Stimuli-responsive membranes.* Journal of Membrane Science, 2010. **357**(1–2): p. 6-35.
173. Peng, T. and Y.L. Cheng, *PNIPAAm and PMAA co-grafted porous PE membranes: living radical co-grafting mechanism and multi-stimuli responsive permeability.* Polymer, 2001. **42**(5): p. 2091-2100.
174. Tokarev, I. and S. Minko, *Stimuli-Responsive Porous Hydrogels at Interfaces for Molecular Filtration, Separation, Controlled Release, and Gating in Capsules and Membranes.* Advanced Materials, 2010. **22**(31): p. 3446-3462.
175. Schacher, F., M. Ulbricht, and A.H.E. Müller, *Self-Supporting, Double Stimuli-Responsive Porous Membranes From Polystyrene-block-poly(N,N-dimethylaminoethyl methacrylate) Diblock Copolymers.* Advanced Functional Materials, 2009. **19**(7): p. 1040-1045.
176. Zhang, R., et al., *A novel pH- and ionic-strength-sensitive carboxy methyl dextran hydrogel.* Biomaterials, 2005. **26**(22): p. 4677-4683.
177. Hassan, C.M., F.J. Doyle, and N.A. Peppas, *Dynamic Behavior of Glucose-Responsive Poly(methacrylic acid-g-ethylene glycol) Hydrogels.* Macromolecules, 1997. **30**(20): p. 6166-6173.
178. Hoare, T.R. and D.S. Kohane, *Hydrogels in drug delivery: Progress and challenges.* Polymer, 2008. **49**(8): p. 1993-2007.
179. Chaterji, S., I.K. Kwon, and K. Park, *Smart polymeric gels: Redefining the limits of biomedical devices.* Progress in Polymer Science, 2007. **32**(8–9): p. 1083-1122.
180. Aguilar, M.R., et al., *Smart Polymers and Their Applications as Biomaterials*, in *Topics in Tissue Engineering*, N. Ashammakhi, R.L. Reis, and E. Chiellini, Editors. 2007.
181. Maeda, Y., T. Nakamura, and I. Ikeda, *Change in Solvation of Poly(N,N-diethylacrylamide) during Phase Transition in Aqueous Solutions As Observed by IR Spectroscopy.* Macromolecules, 2002. **35**(27): p. 10172-10177.
182. Idziak, I., et al., *Thermosensitivity of Aqueous Solutions of Poly(N,N-diethylacrylamide).* Macromolecules, 1999. **32**(4): p. 1260-1263.
183. Pei, Y., et al., *The effect of pH on the LCST of poly(N-isopropylacrylamide) and poly(N-isopropylacrylamide-co-acrylic acid).* Journal of Biomaterials Science, Polymer Edition, 2004. **15**(5): p. 585-594.
184. Moad, G., E. Rizzardo, and S.H. Thang, *Living Radical Polymerization by the RAFT Process—A First Update.* Australian Journal of Chemistry, 2006. **59**(10): p. 669-692.
185. Chiefari, J., et al., *Living free-radical polymerization by reversible addition-fragmentation chain transfer: the RAFT process.* Macromolecules, 1998. **31**(16): p. 5559-5562.

186. Convertine, A.J., et al., *Facile, Controlled, Room-Temperature RAFT Polymerization of N-Isopropylacrylamide†.* Biomacromolecules, 2004. **5**(4): p. 1177-1180.
187. Ganachaud, F., et al., *Molecular Weight Characterization of Poly(N-isopropylacrylamide) Prepared by Living Free-Radical Polymerization.* Macromolecules, 2000. **33**(18): p. 6738-6745.
188. Ray, B., et al., *RAFT Polymerization of N-Isopropylacrylamide in the Absence and Presence of Y(OTf)3: Simultaneous Control of Molecular Weight and Tacticity.* Macromolecules, 2004. **37**(5): p. 1702-1710.
189. Kotsuchibashi, Y., et al., *Synthesis and characterization of double thermo-responsive block copolymer consisting N-isopropylacrylamide by atom transfer radical polymerization.* Journal of Polymer Science Part A: Polymer Chemistry, 2008. **46**(18): p. 6142-6150.
190. Wei, H., et al., *Self-assembled thermoresponsive micelles of poly(N-isopropylacrylamide-b-methyl methacrylate).* Biomaterials, 2006. **27**(9): p. 2028-2034.
191. Furyk, S., et al., *Effects of end group polarity and molecular weight on the lower critical solution temperature of poly(N-isopropylacrylamide).* Journal of Polymer Science Part A: Polymer Chemistry, 2006. **44**(4): p. 1492-1501.
192. Liu, H.Y. and X.X. Zhu, *Lower critical solution temperatures of N-substituted acrylamide copolymers in aqueous solutions.* Polymer, 1999. **40**(25): p. 6985-6990.
193. Wen, O.H., S.-i. Kuroda, and H. Kubota, *Temperature-responsive character of acrylic acid and N-isopropylacrylamide binary monomers-grafted celluloses.* European Polymer Journal, 2001. **37**(4): p. 807-813.
194. Gupta, P., K. Vermani, and S. Garg, *Hydrogels: from controlled release to pH-responsive drug delivery.* Drug Discovery Today, 2002. **7**(10): p. 569-579.
195. Lee, K.Y. and D.J. Mooney, *Hydrogels for tissue engineering.* Chemical reviews, 2001. **101**(7): p. 1869-1880.
196. Gutowska, A., B. Jeong, and M. Jasionowski, *Injectable gels for tissue engineering.* The Anatomical Record, 2001. **263**(4): p. 342-349.
197. Choi, J., et al., *Regulation of cell proliferation by multi-layered phospholipid polymer hydrogel coatings through controlled release of paclitaxel.* Biomaterials, 2012. **33**(3): p. 954-961.
198. Wang, C., Z. Wang, and X. Zhang, *Amphiphilic Building Blocks for Self-Assembly: From Amphiphiles to Supra-amphiphiles.* Accounts of Chemical Research, 2012. **45**(4): p. 608-618.
199. York, A.W., S.E. Kirkland, and C.L. McCormick, *Advances in the synthesis of amphiphilic block copolymers via RAFT polymerization: Stimuli-responsive drug and gene delivery.* Advanced Drug Delivery Reviews, 2008. **60**(9): p. 1018-1036.
200. Zhang, X. and C. Wang, *Supramolecular amphiphiles.* Chemical Society Reviews, 2011. **40**(1): p. 94-101.
201. Xu, C., et al., *Reversible Stimuli-Responsive Nanostructures Assembled from Amphiphilic Block Copolymers.* Nano Letters, 2006. **6**(2): p. 282-287.

202. Jeong, B., S.W. Kim, and Y.H. Bae, *Thermosensitive sol–gel reversible hydrogels.* Advanced Drug Delivery Reviews, 2002. **54**(1): p. 37-51.
203. Idziak, I., et al., *Thermosensitivity of aqueous solutions of poly (N, N-diethylacrylamide).* Macromolecules, 1999. **32**(4): p. 1260-1263.
204. Tamburic, S. and D.Q.M. Craig, *An investigation into the rheological, dielectric and mucoadhesive properties of poly(acrylic acid) gel systems.* Journal of Controlled Release, 1995. **37**(1–2): p. 59-68.
205. Yamazaki, Y., T. Tada, and S. Kunugi, *Effects of acrylic acid incorporation on the pressure–temperature behavior and the calorimetric properties of poly (N-isopropylacrylamide) in aqueous solutions.* Colloid and Polymer Science, 2000. **278**(1): p. 80-83.
206. Dong, L.-c. and A.S. Hoffman, *A novel approach for preparation of pH-sensitive hydrogels for enteric drug delivery.* Journal of Controlled Release, 1991. **15**(2): p. 141-152.
207. Jeong, B., Y.H. Bae, and S.W. Kim, *Drug release from biodegradable injectable thermosensitive hydrogel of PEG–PLGA–PEG triblock copolymers.* Journal of Controlled Release, 2000. **63**(1): p. 155-163.
208. Li, K., et al., *A long-acting formulation of a polypeptide drug exenatide in treatment of diabetes using an injectable block copolymer hydrogel.* Biomaterials, 2013. **34**(11): p. 2834-2842.
209. Huynh, C.T., M.K. Nguyen, and D.S. Lee, *Injectable Block Copolymer Hydrogels: Achievements and Future Challenges for Biomedical Applications.* Macromolecules, 2011. **44**(17): p. 6629-6636.
210. Censi, R., et al., *Hydrogels for protein delivery in tissue engineering.* Journal of Controlled Release, 2012. **161**(2): p. 680-692.
211. Taribagil, R.R., M.A. Hillmyer, and T.P. Lodge, *Hydrogels from ABA and ABC Triblock Polymers.* Macromolecules, 2010. **43**(12): p. 5396-5404.
212. Drzal, P.L. and K.R. Shull, *Origins of Mechanical Strength and Elasticity in Thermally Reversible, Acrylic Triblock Copolymer Gels.* Macromolecules, 2003. **36**(6): p. 2000-2008.
213. Cao, Y., et al., *Solution Properties of a Thermosensitive Triblock Copolymer of N-Alkyl Substituted Acrylamides.* Langmuir, 2008. **25**(3): p. 1699-1704.
214. Zhou, S., et al., *Light-scattering studies of poly(N-isopropylacrylamide) in tetrahydrofuran and aqueous solution.* Polymer, 1995. **36**(7): p. 1341-1346.
215. Mayo, F.R. and F.M. Lewis, *Copolymerization. I. A basis for comparing the behavior of monomers in copolymerization; the copolymerization of styrene and methyl methacrylate.* Journal of the American Chemical Society, 1944. **66**(9): p. 1594-1601.
216. Koonar, I., et al., *ABC Triblock Terpolymers Exhibiting Both Temperature-and pH-Sensitive Micellar Aggregation and Gelation in Aqueous Solution.* Langmuir, 2012. **28**(51): p. 17785-17794.
217. Winter, H., *Can the gel point of a cross-linking polymer be detected by the G'–G "crossover?* Polymer Engineering & Science, 1987. **27**(22): p. 1698-1702.

218. Te Nijenhuis, K. and H.H. Winter, *Mechanical properties at the gel point of a crystallizing poly(vinyl chloride) solution.* Macromolecules, 1989. **22**(1): p. 411-414.
219. Chambon, F. and H.H. Winter, *Linear Viscoelasticity at the Gel Point of a Crosslinking PDMS with Imbalanced Stoichiometry.* Journal of Rheology (1978-present), 1987. **31**(8): p. 683-697.
220. Plamper, F.A., et al., *Toward Copolymers with Ideal Thermosensitivity: Solution Properties of Linear, Well-Defined Polymers of N-Isopropyl Acrylamide and N,N-Diethyl Acrylamide.* Macromolecules, 2012. **45**(19): p. 8021-8026.
221. Pang, X. and S. Cui, *Single-Chain Mechanics of Poly(N,N-diethylacrylamide) and Poly(N-isopropylacrylamide): Comparative Study Reveals the Effect of Hydrogen Bond Donors.* Langmuir, 2013. **29**(39): p. 12176-12182.
222. Yu, L. and J. Ding, *Injectable hydrogels as unique biomedical materials.* Chemical Society Reviews, 2008. **37**(8): p. 1473-1481.
223. Kim, Y.J., et al., *Controlled release of insulin from injectable biodegradable triblock copolymer.* Pharmaceutical research, 2001. **18**(4): p. 548-550.
224. Jeong, B., Y.H. Bae, and S.W. Kim, *In situ gelation of PEG-PLGA-PEG triblock copolymer aqueous solutions and degradation thereof.* Journal of biomedical materials research, 2000. **50**(2): p. 171-177.
225. Qiao, M., et al., *Injectable biodegradable temperature-responsive PLGA–PEG–PLGA copolymers: Synthesis and effect of copolymer composition on the drug release from the copolymer-based hydrogels.* International Journal of Pharmaceutics, 2005. **294**(1–2): p. 103-112.
226. Ding, C., et al., *Dually Responsive Injectable Hydrogel Prepared by In Situ Cross-Linking of Glycol Chitosan and Benzaldehyde-Capped PEO-PPO-PEO.* Biomacromolecules, 2010. **11**(4): p. 1043-1051.
227. Kissel, T., Y. Li, and F. Unger, *ABA-triblock copolymers from biodegradable polyester A-blocks and hydrophilic poly(ethylene oxide) B-blocks as a candidate for in situ forming hydrogel delivery systems for proteins.* Advanced Drug Delivery Reviews, 2002. **54**(1): p. 99-134.
228. Mortensen, K. and J.S. Pedersen, *Structural study on the micelle formation of poly(ethylene oxide)-poly(propylene oxide)-poly(ethylene oxide) triblock copolymer in aqueous solution.* Macromolecules, 1993. **26**(4): p. 805-812.
229. Kang, Y.M., et al., *A biodegradable, injectable, gel system based on MPEG-b-(PCL-ran-PLLA) diblock copolymers with an adjustable therapeutic window.* Biomaterials, 2010. **31**(9): p. 2453-2460.
230. Allen, C., D. Maysinger, and A. Eisenberg, *Nano-engineering block copolymer aggregates for drug delivery.* Colloids and Surfaces B: Biointerfaces, 1999. **16**(1): p. 3-27.
231. Lutz, J.-F. and A. Hoth, *Preparation of ideal PEG analogues with a tunable thermosensitivity by controlled radical copolymerization of 2-(2-methoxyethoxy) ethyl methacrylate and oligo (ethylene glycol) methacrylate.* Macromolecules, 2006. **39**(2): p. 893-896.

232. Lutz, J.-F., et al., *Biocompatible, thermoresponsive, and biodegradable: simple preparation of "all-in-one" biorelevant polymers.* Macromolecules, 2007. **40**(24): p. 8540-8543.
233. Ren, L. and S. Agarwal, *Synthesis, Characterization, and Properties Evaluation of Poly[(N-isopropylacrylamide)-co-ester]s.* Macromolecular Chemistry and Physics, 2007. **208**(3): p. 245-253.